Universidade do Minho
Escola de Engenharia

Vera Maria Rego da Silva Carvalho

Development of carrier systems for the controlled release of interleukin-10

Setembro de 2010

Development of carrier systems for the controlled release of interleukin-10
Vera Maria Rego da Silva Carvalho
UMinho | 2010

Universidade do Minho
Escola de Engenharia

Vera Maria Rego da Silva Carvalho

Development of carrier systems for the controlled release of interleukin-10

Tese de doutoramento em Engenharia Química e Biológica
Área de conhecimento em Tecnologia Enzimática e Bio-separações

Trabalho efectuado sob a orientação do
Doutor Miguel Gama
Doutora Lucília Domingues
Doutor Manuel Vilanova

Setembro de 2010

Agradecimentos

Sendo que finda esta etapa, gostaria de agradecer a todos que, de uma forma ou outra, contribuíram e ajudaram na sua concretização.

Aos meus orientadores Doutor Miguel, Doutora Lucília e Doutor Manuel. Agradeço a disponibilidade e o apoio científico. Agradeço sobretudo a *paciência*, o *incentivo* e a *confiança* que em mim foi depositada para a realização deste trabalho. A todos os meus amigos e colegas do LTEB e LEMM, de forma especial à Susana (Susi Paula, sabes que sem ti muito ficaria por fazer e por dizer), à Carla e Catarina (Carlota e Gonçinha, as nossas boleias tornaram estes dias/meses/anos mais agradáveis, obrigada pelo apoio nos momentos mais difícies), e Orquídea (Kiducha), não há palavras para explicar como vocês me ajudaram a ultrapassar todas as etapas que culminaram nesta tese… *Muito Obrigada* do fundo do meu coração. À Renata, Fábia, Reinaldo, Paula (Paulinha), Silvia F. e Sílvia P., Dina (uma das nossas mais recentes "aquisições"). E a todos os quais os nomes não referi, muito obrigada por serem exemplos de determinação e trabalho, mas agradeço sobretudo a amizade, companheirismo e o ambiente espectacular de trabalho.
Aos colegas do IBCAS: Pedro Madureira, Alexandra Correia e Luzia Teixeira. Muito obrigada pelo vosso apoio. Sempre que estive no ICBAS senti-me em "casa".

A todos os meus amigos do "3º Andar". Que continuemos a organizar as nossas "expedissons" pelo mundo fora! São amigos como vocês que tornam a minha vida mais feliz.
Digo um obrigada especial à Babi… a minha afilhada/madrinha que muitas das minhas lágrimas enxugou e muita força me deu para continuar… Terás sempre um *lugar especial no meu coração*.

Aos meus pais… Sem vocês nada seria possível… Agradeço o *Amor* incondicional e a *paciência* infindável. Obrigada por me deixarem seguir o meu próprio caminho!

Ao Pedro. Porque és tu! Porque sonhas comigo… Porque desejas sempre mais. E porque tenho a felicidade de partilhar a minha vida contigo.

Finalmente, à Fundação para a Ciência e Tecnologia (FCT), pelo apoio financeiro através da bolsa SFRH/BD/27359/2006 e dos projectos POCTI/BIO/45356/2002, PTDC/BIO/67160/2006.

Que é feito de tudo?
Que fiz eu de mim?
Deixa-me dormir,
Dormir a sorrir
E seja isto o fim
(Fernando Pessoa)

Aos meus pais

Abstract

Development of carrier systems for the controlled release of interleukin-10.

Therapeutic proteins are becoming available for the treatment of a wide range of diseases. A main problem limiting the efficiency of protein therapeutics is the reduced stability and short circulation half-lives after parenteral administration.

Interleukin-10 (IL-10) is an anti-inflammatory cytokine, which active form is a non-covalent homodimer with two intramolecular disulphide bonds essential for its biological activity. Due to its immunoregulatory properties, IL-10 is a promising protein to be used in several clinical applications. So, it is essential to develop delivery systems that enhance the protein bioavailability and selectivity, and that enables a targeted controlled release profile. This is the main focus of the present thesis, taking IL-10 as case study.

The use of Carbohydrate-Binding Modules (CBM) as a tool for protein delivery and functionalization was attempted. Proteins and peptides can be used to functionalize biomaterials used for tissue engineering or other biomedical applications, for instance to reduce inflammation (in case of IL-10) or to enhance cellular adhesion (RGD peptide). A method based on the use of a human chitin-binding module, with affinity for chitin, was tested as an alternative approach to the chemical grafting of bioactive proteins/peptides (Chapter 2) on chitin-based biomaterials. A fusion recombinant protein, containing the RGD sequence fused to a human chitin-binding module, was produced and its ability to enhance fibroblasts adhesion to reacetylated chitosan films was tested. The results show that the recombinant protein inhibits the fibroblasts adhesion and proliferation. It was also concluded that the toxic effect was mainly due to the human-chitin biding module.

Several polymer protein delivery systems have been developed and described in the literature. Among them, nanometer-sized polymer hydrogels (nanogels) have attracted growing interest. By trapping proteins in a hydrated polymer-network, nanogels minimize denaturation, simultaneously allowing a slow, continuous and controlled release, ideally maintaining an effective concentration for the necessary period of time. A mutated form of murine IL-10 (rIL-10) was successfully produced

and its biological activity was confirmed on endotoxin-stimulated bone marrow-derived macrophages (Chapter 3). It was shown that a dextrin nanogel (previously developed) effectively incorporated, stabilized, and enabled the slow release, *in vitro*, of biologically active rIL-10 over time.

The IL-10 delivery system based on dextrin nanogels was further analyzed (Chapter 4). Dextrin nanogels were shown to be biocompatible and, after subcutaneous injection, allowed a stable concentration of rIL-10 for at least 4 hours. Despite the low amount of rIL-10 released from the complex nanogel/rIL-10, the rIL-10 released was biologically active *in vivo*, in the mice.

A composite hydrogel made of oxidized dextrin hydrogel with incorporated dextrin nanogels was developed (Chapter 5). The oxidized dextrin hydrogel presented acceptable mechanical properties, biocompatiblity and biodegradability. Additionally, it allowed for the controlled release of the dextrin nanogels. The dextrin nanogel permitted the incorporation of rIL-10, curcumin and β-galatosidase into the oxidized dextrin hydrogel and allowed for their release over time.

In all assays, rIL-10 showed high instability and it is likely that a different release profile from either dextrin nanogel or oxidized dextrin hydrogel could be achieved using other kind of bioactive molecules. So, further studies with other bioactive and more stable proteins should be attempted in order to evaluate the potential of the dextrin nanogel and oxidized dextrin hydrogel as protein delivery systems. Even though, considering the interesting properties of dextrin, the stabilization of rIL-10 by the dextrin nanogels as well as the controlled release rate achieved with the composite hydrogel, we consider as very promising the described systems for protein delivery applications.

Resumo

Desenvolvimento de sistemas para a libertação controlada de interleucina-10.

As proteínas terapêuticas representam uma nova classe de fármacos para o tratamento de diversas doenças. Um dos principais problemas é a estabilidade reduzida e consequentemente o curto tempo de semi-vida das mesmas, após administração parenteral.

A interleucina 10 (IL-10) é uma citocina anti-inflamatória, cuja forma activa é composta por um homodímero com duas ligações intramoleculares dissulfureto, que são essenciais para a sua actividade biológica. Devido às suas propriedades imunoreguladoras, a IL-10 apresenta grandes potencialidades em diversas aplicações clínicas. Portanto, é essencial o desenvolvimento de sistemas que permitam não só a libertação controlada da proteína mas também aumentem a biodisponibilidade da mesma. Este é o objectivo principal desta tese.

Um domínio de ligação a carbohidratos (CBM) foi usado como ferramenta para veicular proteínas e funcionalizar biomateriais. As proteínas e péptidos podem ser usados para funcionalizar biomateriais, por exemplo exercendo actividade anti-inflamatória (IL-10) ou aumentando a adesão celular (péptido RGD). Um método baseado no uso de domínio de ligação à quitina foi utilizado neste trabalho como alternativa ao enxerto químico de proteínas ou péptidos (Chaper 2) em biomateriais de quitina. Foi produzida e testada a capacidade de uma proteína recombinante de fusão, contendo uma sequência RGD fundida com um domínio humano de ligação a quitina, no aumento da adesão de fibroblastos a filmes de quitosano reacetilado. Os resultados mostram que as proteínas recombinantes afectam negativamente os fibroblastos, inibindo a sua adesão e proliferação. Concluiu-se também que este efeito negativo se deve, essencialmente, ao domínio humano de ligação à quitina.

Diversos sistemas de libertação baseados em polímeros têm sido desenvolvidos e descritos na literatura. Entre eles, os hidrogéis de tamanho nanométrico (nanogéis) têm atraído muito interesse. Incorporando as proteínas numa rede hidratada, os nanogéis minimizam a desnaturação, e simultaneamente permitem uma libertação

lenta, contínua e controlada, mantendo uma concentração efectiva da proteína pelo tempo necessário. Uma forma mutada de IL-10 (rIL-10) de ratinho foi produzida com sucesso e a sua actividade biológica confirmada em macrófagos derivados de medula óssea activados (Chapter 3). Demonstrou-se que um nanogel de dextrino (desenvolvido anteriormente) foi capaz de efectivamente incorporar e estabilizar proteína, possibilitando a libertação controlada, *in vitro*, de rIL-10 biologicamente activa.

Os nanogéis como sistema controlado de libertação de IL-10 foram caracterizados detalhadamente (Chapter 4). Os nanogéis são biocompatíveis e, após injecção subcutânea, permitiram que fosse mantida uma concentração estável de IL-10 pelo menos por 4 horas. Apesar das baixas quantidades de rIL-10 libertada do nanogel, a rIL-10 livre é biologicamente activa *in vivo*, em ratinhos.

Foi também desenvolvido um biomaterial composto por um hidrogel de dextrino oxidado com incorporação de nanogéis de dextrino (Chapter 5). O hidrogel de dextrino oxidado apresenta boas propriedades mecânicas, é biocompatível e biodegradável. Adicionalmente, foi verificada a libertação controlada dos nanogéis de dextrino incorporados. O nanogel permitiu a incorporação no hidrogel de dextrino oxidado de rIL-10, curcumina e β-galatosidase e verificou-se a sua libertação ao longo do tempo.

Em todos os ensaios foi verificada uma elevada instabilidade da rIL-10 e é provável que usando outro tipo de moléculas bioactivas seja possível obter um perfil de libertação diferente, tanto dos nanogéis de dextrino como dos hidrogéis de dextrino oxidado. Portanto, de forma a avaliar as potencialidades dos sistemas descritos para a libertação de proteínas, mais estudos deverão ser feitos com proteínas bioactivas mais estáveis. Considerando as propriedades do dextrino, interessantes do ponto de vista do desenvolvimento de aplicações biomédicas, a estabilização da rIL-10 pelos nanogéis assim como a libertação controlada observada nos hidrogéis compostos, podem classificar-se de muito promissores os sistemas descritos para a libertação de proteínas.

Table of contents

List of figures

List of tables

List of schemes

List of abbreviations and nomenclature

AHD	Adipic acid dihydrazide
ANEP	Anti-neuroexcitation peptide
AntiIL-10R	Purified anti-human CD210
APC	Antigen-presenting cell
Arg	Arginine
Asp	Aspartic acid
β-Gal	β-Galactosidase
BM	Bone marrow
BMDM	Bone marrow derived macrophages
BSA	Bovine serum albumin
CBD	Cellulose-binding domain
CBM	Carbohydrate-binding module
CD	Circular dichroism
cDMEM	DMEM complete medium
cDNA	Complementary DNA
ChBM	Human chitin-binding module
cIL-10	Commercial IL-10
cRPMI	RPMI complete medium
Cryo-SEM	Cryo-scanning electron microscopy
CS	Chitosan
CSF	Colony stimulating factor
CSIF	Cytokine synthesis inhibitory factor
CS-NAC	Chitosan-acetyl-L-cysteine
CyA	Cyclosporin-A
Cys	Cysteine
DA	Degree of acetylation
DDS	Drug delivery system
DLS	Dynamic light scattering
DMA	Dynamic mechanical analysis
DMEC	Dimethylethylchitosan
DMEM	Dulbecco'c modified Eagle medium
DMSO	Dimethyl sulfoxide
DNA	Deoxyribonucleic acid
DO	Degree of oxidation
DRG	Chick dorsal root ganglion neurons
ECM	Extracellular matrix
EDTA	Ethylenediamine tetraacetic acid
ELISA	Enzyme-linked immunosorbent assay

FACS	Fluorescence activated cell sorting
FBS	Fetal bovine serum
FDA	United States Food and Drug Administration
G-CSF	Granulocyte colony stimulating factor
GI	Gastrointestinal
Gly	Glycine
GM-CSF	Granulocyte monocyte colony stimulating factor
HA	Hyaluronic acid
HEMA	Hydroxyethyl methacrylate ester
HEPES	4-(2-hydroxyethyl)-1-piperazineethanesulfonic acid
HGC	Hydrophobically modified glycol chitosan
HisTag	Hexahistidine tag
HIV	Human immunodeficiency virus
Ig	Immunoglobulin
IL	Interleukin
IL-10	Interleukin-10
IL-10R	Interleukin-10 receptor
INF	Interferon
IPTG	Isopropyl-β-D-thiogalactopyranoside
iv	Intravenous
LCCM	L929 cell conditioned medium
LDH	Lactate dehydrogenase
LPS	Lipopolysaccharide
LB	Luria-Bertani medium
MHC	Major histocompatibility complex
MHC-II	Class II major histocompatibility complex
MIP	Macrophage inhibiting protein
MTS	3-(4,5-dimethylthiazol-2-yl)-5-(3-carboxymethoxyphenyl)-2-(4-sulfophenyl)-2H-tetrazolium
MTT	3-[4,5-dimethylthiazol-2-yl]-2,5-diphenyl-tetrazolium bromide
MVA	Vinyl methacrylate
Mw	Molecular weight
MWCO	Molecular weight cut off
NF	Nuclear factor
nm	Nanometers
NMR	Nuclear magnetic resonance
NO	Nitric oxide
NP	Nanoparticle
NK	Natural killer
OD	Optical density
oDex	Oxidized dextrin
ORF	Open reading frame

PBS	Phosphate buffer saline
PCR	Polymerase chain reaction
PdI	Polysdispersity index
PEG	Poly(ethylene glycol)
PGA	Poly(glycolic acid)
γ-PGA	Poly-γ-glutamic acid
PLA	Poly(lactic acid)
PLGA	Poly(lactic acid–glycolic acid
RA	Rheumatoid arthritis
RC	Reacetylated chitosan
RGD	Arg-Gly-Asp
rIL-10	IL-10 C149Y
SBM	Starch-binding module
sc	Subcutaneous
SC_{16}	Alkyl chain
SDS	Sodium dodecyl sulfate
SDS-PAGE	Sodium dodecyl sulfate polyacrylamide gel electrophoresis
tBC	*tert*-butylcarbazate
TEC	Triethylchitosan
TGA	Thermogravimetric analysis
TGF	Transforming growth factor
Th cells	T-helper cells
p-THPP	Mesotetra(hydroxyphenyl)porphyrin
TL	Tail lenght
TMC	Trimethyl chitosan
TMC-Cys	TMC-cysteine
TNF	Tumor necrosis factor
TPP	tripolyphosphate
VA	Vinyl acrylate
VMA	Vinyl methacrylate

Scope and aims

Interleukin-10 (IL-10) is a pleiotropic cytokine that regulates several functions of numerous cell populations, in particular immune cells. Its main role seems to be the containment and eventual termination of inflammatory responses allowing for the elimination of infectious organisms with reduced damage to host tissues. As a result of its immunoregulatory properties, IL-10 has been proposed and used in several clinical applications. Unfortunately, IL-10 (as other cytokines) is expensive to produce on a large scale, is easily denatured and has a short half-life *in vivo*. So it is essential to develop delivery systems that, besides allowing for efficient therapeutics at a minimum dosage, can prevent protein denaturation and maintain an effective protein concentration for the necessary period of time.

The main purpose of this work is to develop carrier systems for the controlled release of proteins, using the case study of IL-10. To achieve this goal we envisioned three paths:

1. To express fusion proteins with a carbohydrate-binding module, specifically a human chitin-binding module (ChBM), namely fusions with the RGD peptide and IL-10, so that chitin-based materials could be functionalized with an anti-inflammatory protein and possibly reduce (or eliminate) a graft inflammatory reaction improving the chitin-based biomaterial biocompatibility;
2. To evaluate the ability of dextrin nanohydrogels (nanogels), previously developed in our laboratory, to incorporate, stabilize and enable the slow release of biologically active IL-10; and
3. To develop a composite material of oxidized dextrin (DexOx) hydrogels with incorporated dextrin nanogels and assess its capacity for IL-10 controlled release.

The first chapter presents a revision of these subjects, namely: cytokines and IL-10; protein delivery systems, hydrogels and nanogels; and finally carbohydrate-binding modules.

Chapter 2 describes the strategies to functionalize chitin-based materials using recombinant proteins containing ChBM. The ChBM was first fused with the adhesion-promoting peptide Arg-Gly-Asp (RGD), expressed in *Escherichia coli* and tested *in vitro* using mouse embryo fibroblast 3T3 cells. The aim of this work was to access the biocompatibility of the ChBM to further obtain a recombinant fusion protein with IL-10. This study has been published in *Molecular Biotechnology* (2008) 40:269-279.

The third chapter describes the preliminary studies on dextrin nanogels as an IL-10 carrier system. The production of a recombinant mutated form of IL-10 (rIL-10) is also described. Pedro Castanheira from the Biomolecular Biotechnology Unit of Biocant made the rIL-10 expression and purification. Tiago Faria from the Department of Chemistry of the Faculty of Sciences and Technology of University of Coimbra performed the circular dichroism assays. These results were published on the *International Journal of Pharmaceutics* (2010) 400:243-242.

In the fourth chapter, further characterization of the dextrin nanogel as an IL-10 carrier is presented. Biocompatibility assays were made and rIL-10 release and bioactivity evaluated *in vivo*, in the mice.

In chapter five, the development, mechanical characterization and biocompatibility of an oxidized dextrin hydrogel is described. The mechanical characterization and biocompatibility studies were performed by Maria Molinos. Also, a bidimensional hydrogel made of oxidized dextrin (oDex or DexOx) and incorporated dextrin nanogel, is described. The hydrogel degradation and the nanogel, rIL-10, curcumin and β-galactosidase release profiles were evaluated.

In the final chapter (chapter 6) a review of the main conclusions and some future perspectives are portrayed.

Chapter 1 | General introduction

Cytokines

The word cytokine is derived from the Greek *cyto,* meaning cell, and *kinin,* meaning hormones. Cytokines are soluble hormone-like proteins that allow for communication between cells and the external environment. It is a wide-ranging term that includes lymphokines, monokines, interleukins (ILs), colony stimulating factors (CSFs), interferons (IFNs), tumor necrosis factors (TNFs) and chemokines.

Cytokines are secreted by white blood cells and a variety of other cells (fibroblasts, endothelial cells, epithelial cells, etc.) in response to inducing stimuli. They serve many functions in the body such as mediating and regulating immunity, inflammation and hematopoiesis, but the largest group of cytokines is involved in immune cell proliferation and differentiation. Although cytokines are produced by many cell populations, the predominant ones are helper T cells (Th) and macrophages.

History

The research in the field of cytokines began in the 1950s [1] with the identification of some factors like the 'endogenous pyrogen' [now also known as interleukin-1 (IL-1)] [2]. In 1957, Alick Isaacs and Jean Lindenmann [3] identified interferon-α as a factor produced upon stimulation of cells by viruses. In fact, the name 'interferon' comes from the capacity of this factor to interfere with the production of new virus particles. In 1966, two groups of scientists working independently, John David and Barry Bloom identified a so–called 'migration inhibiting factor' [4, 5]. The authors showed that a factor released from antigen-activated lymphocytes arrested the migration of macrophages *in vitro*. Soon thereafter, the list of soluble mediators that influence several functions of the immune system, found in the culture supernantants of antigen-activated lymphocytes (termed as 'lymphokines' by

Dudley Dumonde [6]), increased amazingly. In a similar way, active factors derived from macrophages and monocytes came to be known as 'monokines'. TNF was first described in the 1970s as a mediator of lipopolysaccharide (LPS)-induced necrosis of transplantable tumors. It was isolated from the serum of mice treated with bacterial endotoxin, and it had the ability to reproduce the endotoxin effects by inducing hemorrhagic necrosis of sarcomas [7].

By the end of the 1970s, at the Second International Lymphokine Workshop (Ermatingen, Switzerland), an improvised nomenclature committee gathered and proposed a classification for these factors. This classification was not based on the cells that produced the factors or even on their biological activities, instead it was established on their molecular structure. The term 'interleukin' was presented as the collective denomination for these factors, followed by an arabic number according to the chronology of molecular characterization [8].

In the 1980s, CSFs were found to stimulate growth and differentiation of various elements of bone marrow and were named according to the specific elements they support, like Granulocyte CSF (G-CSF), Granulocyte monocyte CSF (GM-CSF) and Erythropoietin. In the late 1980s, researchers isolated signaling molecules, which permitted leukocytes communication with one another to seek out and destroy invading pathogens, called chemokines.

With the emerging recombinant DNA technology, in the 1980s, the genes encoding for many of the identified factors were cloned and soon it was noticeable that a given molecule, besides exerting several activities, was often produced by many cells inside and outside of the immune system, and had the ability to regulate the production of other factors [9]. So 'interleukins', as factors produced by leucocytes and affecting other leucocytes, became obsolete and the term 'cytokines', proposed by Cohen *et al* in 1974 [10], was recalled and adopted as the generic name for lymphokines, monokines, TNFs, INFs, etc. Despite this, the term 'interleukin' was kept to classify newly described cytokines that were molecularly and functionally characterized. Each newly described cytokine has to be submitted to an international

committee. Then, the committee attributes an interleukin number to which the literature devoted to this cytokine has to refer. The 1980s were also the period where cytokine receptors began to be identified, their genes cloned and their expression and function analyzed. Independent studies showed that, even though the several cytokines did not share significant homology, their receptors belong to well-defined categories and known genetic superfamilies, sharing and using similar routes for cell triggering. As a consequence, the biological activities of a given cytokine are dependent not only on its expression, but also on the presence and arrangement of its receptors on the surrounding cells.

Untill 2008, 35 interleukins have been identified and characterized [11]; still, there are many more to be discovered and characterized.

Since 1950s, cytokines became known and used in virtually all fields of biology. Their known association with some diseases, their use as therapeutic factors or as targets for inhibitory molecules, attracted great interest from the pharmaceutical industry.

Properties of cytokines

Cytokines are soluble peptidic factors that mediate interactions between immunocompetent and haematopoeitic cells and between the immune and the neuroendocrine systems [9]. They are produced by activated cells and exercise their biological activities by binding to specific receptors expressed on target cells.

There are three major basic properties of cytokines [1, 9]:

1. Pleiotropism: a single cytokine can act on many different types of cells;
2. Redundancy: similar function can be achieved by different cytokines;
3. Multifunctionality: the same cytokine may be able to regulate several different immune functions.

Table 1.1 shows a list of some cytokines, producing and target cells and major functions.

Table 1.1 - Source, target and physiological role of some cytokines.

Cytokines	Main sources	Target cells	Major functions	References
IL-1 α/β	Macrophages, B cells, dendritic cells.	B cells, NK cells, T cells.	Proliferation and differentiation, pyrogenic, bone marrow (BM) proliferation.	12, 13
IL-2	T cells.	Activated T cell, B cells, NK cells.	Proliferation and activation.	14-16
IL-3	T cells, NK cells.	Stem cells.	Hematopoietic precursor proliferation and differentiation.	17, 18
IL-4	Th cells.	B cells, T cells, macrophages.	Proliferation of B-cells and cytotoxic T cells, enhances class II MHC expression, stimulates IgG and IgE production.	14, 15
IL-5	Th cells.	Eosinophils, B cells.	Proliferation and maturation, stimulates IgA and IgM production.	17, 19
IL-6	Th cells, macrophages, fibroblasts.	Activated B cells, plasma cells.	Differentiation into plasma cells, IgG production.	20-22
IL-7	BM stromal cells, epithelial cells.	Stem cells.	B cell and T cell growth factor.	23, 24
IL-8	Monocytes, T cells.	Neutrophilis, T cells.	Chemotaxis, pro-inflammatory.	25, 26
IL-9	Th cell.	T cell, mast cells.	Growth and proliferation.	27, 28
IL-10	T cells and B cells, macrophages.	T cells, B cell precursors, macrophages.	Inhibits cytokine production and mononuclear cell function, anti-inflammatory.	29, 30
IL-11	BM stromal cells.	B cells.	Differentiation, induces acute phase proteins.	31, 32
IL-12	Monocytes, B cells, T cells.	T cells, NK cells.	Activates NK cells, T cells and macrophages.	33, 34
IL-13	T cells.	B cells, NK cells, monocytes.	IgE switch recombination, B cells proliferation.	35, 36
IL-15	Various cells.	T cells and B cells, NK cells.	Proliferation and activation.	37, 38
IL-18	Various cells.	T cells.	Development and activation.	39, 40
INF-α;	Leukocytes;	Various	Anti-viral, anti-proliferative.	41-43

INF-β	Fibroblasts.	cells.		
INF-γ	T cells.	Various cells.	Anti-viral, macrophage activation, increases neutrophil and monocyte function, MHC-I and-II expression on cells.	44, 45
TNF-α; TNF-β	Macrophages. Monocytes; T cells.	Macrophages. Tumor cells.	Phagocyte cell activaction, endotoxic shock. Tumor cytotoxicity, cachexia.	46 47
G-CSF; GM-CSF	T cells, macrophages, fibroblasts.	Stem cells.	Granulocyte, monocyte, eosinophil production.	17, 48, 49
M-CSF	Fibroblast, endothelium.	Stem cells.	Monocyte production and activation.	50, 51
Erythropoietin	Endothelium.	Stem cells.	Red blood cell production.	52, 53
Transforming growth factor (TGF)-β	T cells, B cells.	Activated T cells, B cells.	Inhibit T cell and B cell proliferation, inhibit hematopoiesis, promotes wound healing.	54, 55

Cytokines as therapeutic agents

Cytokines have been the focus of scientific interest for more than two decades now. As they mediate a variety of physiological processes, including haematopoiesis, immune responses, wound healing and general tissue maintenance, it is not surprising that they are also involved in the pathogenesis and treatment of many diseases. The analysis of their expression had also permitted a better understanding of the pathogenesis of various diseases. By now, some cytokine therapies are already used in the clinical practice, ranging from early exploratory trials to well established therapies [1, 56, 57]. In fact, several cytokines are employed for the treatment of malignant, inflammatory and infectious diseases. Some examples of cytokine-related pathologies are given in Table 1.2. These cytokines are involved in the pathogenesis of the disease or/and act as a therapeutic agent.

Table 1.2 – Some examples of cytokine related pathologies.

Cytokine	Pathology	References
IL-1	Rheumatoid arthritis	58, 59
IL-2	Cancer	57, 60, 61
IL-4	Cancer	57, 62
	Psoriasis	57, 63-65
IL-6	Rheumatoid arthritis	20, 57-59, 66, 67
	Cancer	20, 22, 68
	Autoimmune diseases	20, 67
	Bone diseases	20, 68
IL-7	Cancer	57, 69
IL-10	Rheumatoid arthritis	70-72
	Crohn's disease	70, 71, 73
	Psoriasis	57, 64, 65, 70, 71, 74, 75
	Chronic hepatitis C	70, 71, 76
	Cancer	70, 77
IL-11	Psoriasis	57, 64, 65
IL-12	Cancer	61, 78
IL-13	Asthma	35, 79, 80
IL-15	Rheumatoid arthritis	37, 58, 59, 81
	Cancer	37, 60, 69
IL-18	Rheumatoid arthritis	58, 81
	Diabetes	39, 82
	Bone diseases	39, 83
TNF	Rheumatoid arthritis	41, 46, 58, 59, 84
	Cancer	47, 57
	Psoriasis	57, 65
INF	Cancer	41, 57
	Hepatitis C	43, 85
Erythropoietin	Cancer	53, 86, 87
TGF-β	Cancer	88, 89
	Bone diseases	55, 90

Interleukin-10 (IL-10)

Interleukin-10 (IL-10) was initially characterized as a cytokine synthesis inhibitory factor (CSIF) [91], from concanavalin A-stimulated Th2 cells, that inhibited the production of cytokines by Th1 cells. Immediately after this

initial report, B cells and B cell lymphoma were also found to produce IL-10 [92], and a homologue of IL-10, BCRFI, was discovered from the Epstein-Barr virus genome [93]. Studies soon showed that IL-10 profoundly inhibit a broad spectrum of activated macrophage/monocyte functions, including monokine synthesis, nitric oxide (NO) production, and expression of MHC class II (MHC-II) and of costimulatory molecules.

It was therefore proposed that IL-10 plays a key role in suppressing the host immune system.

IL-10 protein, gene and expression

The human and murine IL-10 genes are encoded by five exons on the respective chromosome 1 [94]. Activation of IL-10 gene expression results in about 2 kb mRNA. IL-10 can be expressed by various cell types (including T and B cells, monocytes, and macrophages), usually in response to an activation stimulus. Its expression is regulated by different mechanisms in different cell types. For example, macrophages, the major source of IL-10, are stimulated to produce IL-10 by several endogenous and exogenous factors such as endotoxins (via Toll-like receptor 4, Nuclear Factor (NF)-κB dependent), TNF-α (via TNF receptor p55, NF-κB dependent), catecholamines, and cAMP-elevating drugs (both via protein kinase A, CREB-1/ATF-1 dependent) [70, 71].

DNA sequence from different species is highly conserved and contains an open reading frame (ORF) encoding for a secreted polypeptide of about 178 amino acids with an N-terminal leader sequence of 18 amino acids, with well conserved domains [70] consistent with a α-helical bundle structure. Figure 1.1 shows the alignment of the amino acid sequence of IL-10 from different species, with reference to secondary structural features and functionally important residues.

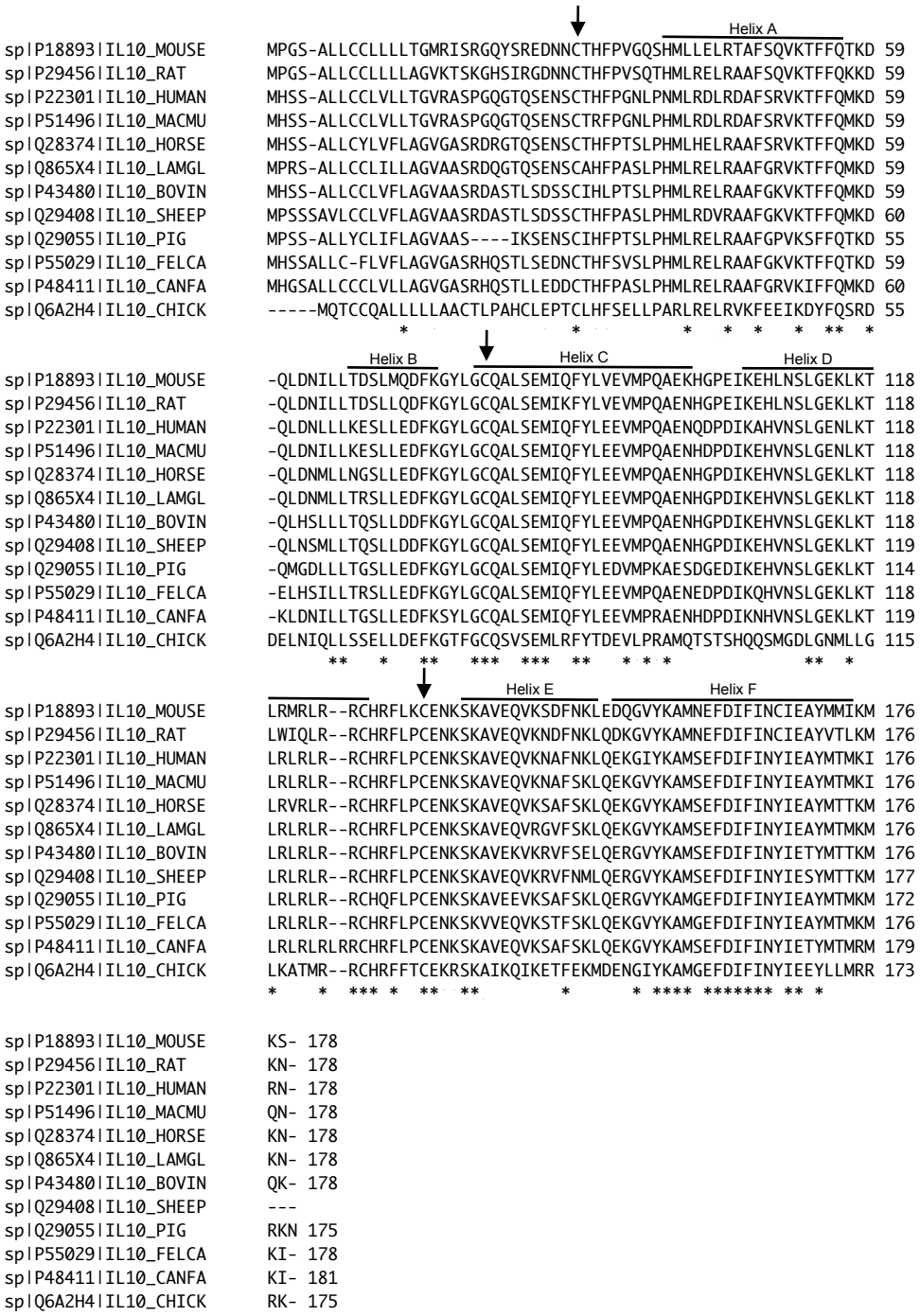

Figure 1.1 – Alignment of IL-10 amino acid sequence from different species. The conserved aminoacids are indicated with asterisks and the conserved cysteins are marked with arrows. The α-helical assignments are based on the structure of human IL-10.

Human IL-10 is composed of two polypeptide chains of 160 amino acids each. The very similar murine IL-10 consists of 157 amino acids and presents a 73% overall sequence identity with the human IL-10 (Figure 1.1). Crystal structure characterization [96-98] revealed that biologically active IL-10 is a non-covalent

symmetric homodimer of two interpenetrating α-helical polypeptide chains, oriented 90º relatively to each other, forming two V shaped domains. Each domain has six α-helix, four (A to D) from one monomer and two (E and F) from the other [96] as pictured in Figure 1.2.

Biophysical characterization of the human and murine IL-10 [99, 100] showed the presence of two disulfide bonds - linking the first to the third and the second to the fourth cysteine residues - essential to the biological activity of the protein [30, 70, 71, 96, 97].

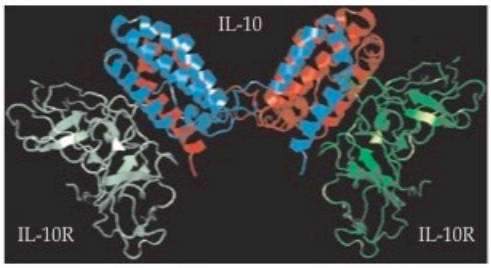

Figure 1.2 – Model structure of the IL-10/IL-10 receptor complex (adapted from Zdanov *et al* [97]).

The IL-10 receptor (IL-10R) and IL-10 signaling

IL-10 pleiotropic activities are conveyed to cells by a high-affinity interaction with its cell surface receptor complex, which is expressed on a variety of cells, especially immune cells.

The IL-10 receptor, composed of at least two subunits (IL-10Rα and IL-10Rβ), is a member of the class 2 cytokine receptor family (or interferon-receptor like group). The interaction of human IL-10R with human IL-10 has already been characterized and seems to be highly complex [101-103] (showed in Figure 1.2).

The receptor subunit α binds IL-10 with the highest affinity and most hemopoietic cells express IL-10Rα. Its expression on T cells is downregulated by activation at both mRNA and protein levels; in contrast, activation of monocytes is related with upregulation of IL-10Rα expression, coherent with IL-10 property as an inhibitor factor of these cells [70, 71].

IL-10Rβ contributes little to IL-10-binding affinity, its main function appears to be the recruitment of a Jak kinase into the signaling complex. IL-10Rβ is

constitutively expressed in most cells and tissues and no evidence was found for significant activation-associated regulation of IL-10Rβ expression in immune cells [70]. So, any stimulus activating IL-10Rα expression should be enough to render most cells receptive to IL-10.

The activation of the IL-10 receptor complex inhibits of the synthesis of several cytokines genes, also hindering several cytokines from inducing their biological activities on their target cells.

The IL-10/IL-10R interaction activates the tyrosine kinases Jak1 and Tyk2, which are associated with the IL-10Rα and IL-10Rβ, respectively [30, 70, 71].

IL-10 controls inflammatory processes by suppressing the production of proinflammatory cytokines, chemokines, adhesion molecules, as well as antigen-presenting and costimulatory molecules in monocytes/macrophages, neutrophils, and T cells [104-110]. NF-κB controls all of these inflammatory proteins, so it was suggested that IL-10 may exert significant part of its anti-inflammatory properties by inhibiting this transcription factor [30, 70, 71].

Immunobiology of IL-10

IL-10 modulates the expression of cytokines, soluble mediators and cell surface molecules in cells of myeloid origin, with significant consequences for their capability to activate and maintain immune and inflammatory responses.

Antigen-presenting cells (APCs) and lymphocytes are the principal targets of IL-10 and the direct consequences on these populations justify the significant immunological impact of IL-10, including the regulation of the Th1/Th2 balance [111]. Th1 cells are known to be essential for effective cellular immunologic reaction against intracellular organisms, whereas Th2 cytokine pattern is especially responsible for effective humoral immunologic mechanisms [111]. IL-10 costimulates the proliferation and differentiation of B cells, which is important for the adequate defense against intestinal parasites, neutralization of bacterial toxins, and local mucosal defense [112]. Moreover, IL-10 suppresses proinflammatory cytokine production and the antigen-

presenting capacity of monocytes/macrophages and dendritic cells [104, 105, 112]. Therefore, IL-10 is a substantial suppressor of cellular immunity [113].

Important effects of IL-10 on immune cells are summarized in Table 1.3 (reviewed by Moore and colleagues in 2001 [70]).

Table 1.3 – Major effects of IL-10 on important immune cell populations.

Cell population	Suppression	Induction	References
Langerhans cells	Antigen presentation.		114
Dendritic cells	CD86 expression, antigen presentation.		113
Monocytes/macrophages	TNF-α, IL-1, IL-6, IL-8, IL-12 production, expression of MCH-II, DC86, CD54, antigen presentation.	IL-1RA production. Soluble TNF receptors.	104-107, 113, 115, 116
Eosinophils	IL-8, GM-CSF liberation.		117
Neutrophils	TNF-α, IL-1, IL-8 production.	IL-1RA production.	118
Mast cells	TNF-α production	Growth. Antigen-induced histamine liberation.	119
T cells	IL-2 and IFN-γ production, mitogen-induced proliferation.		108, 120, 121
NK cells		Citotoxicity.	122
B cells		Growth, IgE synthesis.	123, 124

Summing up, the key physiological roles of IL-10 appear to be the limitation of inflammation, the prevention of uncontrolled and exacerbated immunologic reactions, and the support of the humoral immune responses.

The major physiological roles of IL-10 were confirmed by experimental research in animals, using IL-10 knockout mice [125, 126] and observing the effects of IL-10 in several disease models. Table 1.4 condenses a few effects resulting from IL-10 application in some animal disease models.

Table 1.4 – Some results of IL-10 in animal disease models.

Disease model	Results	References
Inflammation and autoimmune	Prevention of intestinal inflammation, however only successful when IL-10 was administered before disease initiation.	127-129
	Beneficial in the following models of experimental animal models: autoimmune encephalomyelitis; pancreatitis; diabetes mellitus; experimental endotoxemia.	130-133
	Reduced inflammation, cellular infiltrates and joint destruction in various animal models of arthritis	134, 135
Tumor	Depending on the experimental model, IL-10 favors or inhibits the existence and progression of tumors	136-145
Infections	Protection against experimental group B streptococcal arthritis and for helminth infection	70, 146, 147

Numerous studies have been made to investigate the expression of IL-10 under pathophysiological conditions. Both overexpression as well as IL-10 deficiency were found, appearing to have pathophysiological significance. Table 1.5, shows a summary of diseases where IL-10 is abnormally expressed.

Table 1.5 – Examples of some diseases where IL-10 is abnormally expressed.

Disease		Expression	References
Malignant diseases	Melanoma	IL-10 overexpression	148-150
	Carcinoma	IL-10 overexpression	151, 152
	Lymphoma	Increased IL-10 serum levels	153-160
Autoimmune and inflammatory diseases	Systemic lupus erythematosus	Increased IL-10 serum levels	161-163
	Systemic sclerosis	Increased IL-10 serum levels	164
	Psoriasis	Low cutaneous expression	74, 165, 166
Atopic disorders	Atopic dermatitis	IL-10 overexpression	167
	Allergic asthma	IL-10 underproduction	168
Infection diseases		Increased IL-10 release associated with decreased resistance to infections	169-174

IL-10 as a therapeutic agent

The powerful *in vitro* immunomodulating activities of IL-10 and effects observed on animal models of acute and chronic inflammation, autoimmunity, cancer and infections disease, made IL-10 an attractive candidate for therapeutic use. Safety, tolerance, pharmacokinetics, pharmacodynamics, immunological and hematological effects of single and multiple doses of IL-10, administered by intravenous (iv) or subcutaneous (sc) routes, were investigated in Phases I and II clinical trials, performed in several conditions on healthy volunteers and specific patient populations [175-177]. These studies showed that recombinant human IL-10 is well tolerated without serious side effects at doses up to 25 μg/kg; mild to moderate flu-like symptoms were observed in a fraction of recipients at doses up to 100 μg/kg [70, 71].

Prevention of cytokine release in transplant patients and Jarish-Herxheimer reaction.

The effects of IL-10 on systemic production of proinflammatory cytokines in renal transplant patients who received the monoclonal antibody OKT3 as induction therapy were investigated [70, 71, 178]. OKT3 is a powerful T cell-targeting immunosuppressive agent, but it stimulates a dramatic cytokine release by triggering almost all T cells. This results in severe side effects that are particularly related to systemic TNF-α, IL-1β, IL-2, and IFN-γ release. Pretreatment with IL-10 reduced the release of TNF induced by OKT3, but high IL-10 doses may have promoted early sensitization to OKT3 and exerted reversible adverse effects on graft acceptance [70, 71, 178]. By contrast, IL-10 was not successful in altering proinflammatory cytokine production or in modifying physiological changes associated with the Jarisch-Herxheimer reaction, an acute systemic inflammatory response induced by the antibiotic treatment of *Borrelia recurrentis* infection [179].

Therapy of Crohn's disease.

As IL-10 proved to be successful in experimental animals models of intestinal inflammation, it was introduced as a promising anti-inflammatory therapy for Crohn's disease. Indeed, the first successful therapeutic administration was reported in patients treated with IL-10 for steroid-refractory Crohn's disease [180].

Several trials tested multiple IL-10 dosages in patients with mild/moderate or therapy refractory Crohn's disease, as well as in patients undergoing curative ileal or ileocolonic resection, to prevent postoperative occurrence by systemic administration [71, 73, 181, 182]. Despite indications that IL-10 therapy is safe and well tolerated, it did not result in significant higher remission rates or clinical improvement, compared with placebo treatment.

Unfortunately, all clinical results of IL-10 therapy in Crohn's disease were unsatisfactory and it is unlikely that this cytokine will be approved for therapy in this inflammatory bowel disease.

Therapy of rheumatoid arthritis.

Limited efficacy, associated with good safety profile, was observed when IL-10 was administered for 28 days to rheumatoid arthritis (RA) patients [72]. Taken together, the clinical data from RA patients has been rather discouraging, showing only marginal activity of the drug [71].

The role of IL-10 in rheumatoid arthritis is still unclear: on the one hand, there are the known anti-inflammatory properties of IL-10 and the effects observed in various animal models; on the other hand, there are the known correlations between IL-10 and increased autoantibody production, serum factor, and B cell activation in rheumatoid arthritis patients [71]. Despite this, it has to be further determined if IL-10 in combination with other therapies, such as low dose steroid [183] or therapeutic anti-TNF monoclonal antibodies [183] may be beneficial to a significant patient population.

Therapy of psoriasis.

An open label phase II trial on ten psoriasis patients indicated that subcutaneous (sc) IL-10 treatment for seven weeks was well tolerated and

efficacious: significant decreases of psoriatic area and severity index were observed in 9/10 patients [74, 184].

It is likely that IL-10 exerts its antipsoriatic activity by acting on different cell populations, including T cells and APCs, as well as on their mutual interaction. Psoriasis is a T cell-dependent (auto)immune disease, probably initiated by presentation of "psoriasis-related antigens" by specialized cutaneous APCs [71]. IL-10 is able to suppress the antigen-presenting activity of monocytes/macrophages, and the development of dendritic cells, this way inhibiting the presentation of the "psoriasis-related antigens" and consequentially the onset of the disease.

Overall, IL-10 therapy seems to be well tolerated and immunologically effective in psoriasis [74, 111]. Determination of definitive clinical efficacy, however, awaits phase III studies.

Therapy of viral infections – Chronic Hepatitis C and human Immunodeficiency virus (HIV).

Substantial progress has been made in the field of hepatitis C virus since its discovery. However, a major effort must still be made to control hepatitis C virus-related liver disease. The ability of IL-10 to suppress pathology associated with chronic hepatitis C infection has been investigated [76, 185]. IL-10 normalized serum levels of alanine aminotransferase (a marker for hepatic inflammation), improved liver histology and reduced liver fibrosis in over 50% of treated patients [76, 186]. However, IL-10 did not reduce serum chronic hepatitis C RNA levels, indicating that it did not affect viral load, but instead limited pathogen-induced pathology.

IL-10 is a pleiotropic cytokine that regulates several functions of numerous cell populations, in particular immune cells. Its main function seems to be the containment and eventual termination of inflammatory responses, facilitating the elimination of infectious organisms with minimal damage to host tissues. Several studies [70, 71] showed that IL-10, besides mediating suppressive functions, has also stimulatory properties on certain cell populations and for

this reason IL-10 should be considered as immunoregulatory instead of immunosuppressive.

Abnormal IL-10 expression, overexpression or deficiency, appears to have substantial pathophysiological impact. As a result, neutralization of IL-10 or application of IL-10, respectively, could be a promising approach to treat pathologies associated with inadequate IL-10 expression. Effectiveness of IL-10 application as therapeutic agent has already been suggested by several early phase II trials for some immune diseases, as psoriasis. However, other studies with other diseases showed discouraging results.

Protein delivery systems

Therapeutic proteins are becoming available for the treatment of a wide range of diseases, among others cancer, autoimmune diseases and metabolic disorders. A main problem limiting the efficiency of protein therapeutics is the reduced stability and short circulation half-lives after parenteral administration (i.e. intravenous, intramuscular, or subcutaneous) [187]. As a result of the invasive nature, injectable formulations are frequently faced with patient discomfort and noncompliance. In the case of proteins, susceptibility to proteolysis and colloidal instability are additional difficulties. Consequently, a high drug concentration or a high dosing frequency becomes necessary, which may lead to adverse side effects [187-190]. Thus, drug delivery systems (DDS) are urgently needed, for the enhancement of the biopharmaceuticals bioavailability and selectivity, enabling a targeted controlled release profile.

Aiming at achieving an effective protein delivery, carriers such as liposomes, polymer micelles, and micro or nanogels have been developed [187, 190-195]. Among them, nanometer-sized polymer hydrogels (nanogels) have attracted growing interest. By trapping proteins in a hydrated polymer-network, nanogels minimize denaturation, simultaneously allowing a slow, continuous and controlled release of the protein, ideally maintaining an effective

concentration for the necessary period of time [192, 196-198]. Nanocarriers enable localized and specific targeting to their intended tissues or cells, thereby allowing the use of lower drug doses [191].

A model protein delivery system should be able to enhance the protein solubility; allow its controlled and sustained release; improve biodistribution and targeting of the diseased tissue, *in vivo* [199]. In addition, a DDS must not compromise the bioactivity of the protein. On the other hand, binding/trapping must be stable enough as to allow release only at the site of action, in a sustained, controlled way. It is advantageous to formulate DDS with biocompatible and biodegradable materials, so that adverse host responses to DDS are minimized.

Polymers in drug delivery systems

The term *biomaterial* has alternately been used to describe either materials derived from biological sources or used for therapies in the human body [200]. Compared to other types of biomaterial, such as metals and ceramics, polymers have the advantage of being available in different compositions, with a variety of structures and properties. Due to its versatility, polymers are extensively applied in medicine and biotechnology, as well as in the food and cosmetic industries. The use of polymers in medicine is not recent and dates back to the beginning of polymer science. It resulted from the union of several disciplines including the life sciences, medicine, materials science, and engineering. Throughout history there are references to glass eyes and wooden and gold-filled teeth [201], nylon sutures were reported in the early 1940s and reviews on the use of polymers like nylon, Dacron polyester and polyvinyl chloride in surgery, began to appear in important medical journals of the time [200]. These materials are still important in clinical medicine as they are essential components of permanent prosthetic devices such as hip implants, artificial lenses, large diameter vascular grafts, catheters, etc., and these biomaterials are permanently been explored to optimize their stability and performance *in vivo*. Other examples include poly(methyl methacrylate)

bone cement; poly(glycolic acid) degradable sutures; poly(glycolic-co-lactic acid) bone screws; poly(vinyl siloxane) dental impression materials; poly(ethylene glycol) (PEG) is often used to extend the circulation half-life of some drugs; and poly(hydroxyethyl methacrylate) is used to make soft contact lenses [201].

Although the initial uses of polymers in surgery centered essentially on replacements for connective tissues, major advances in sciences, like molecular cell biology and DNA recombinant technology, resulted in the use of these biomaterials for other biomedical applications. These include surgical devices, implants and supporting materials, DDS using different routes of administration and design, carriers of immobilized enzymes and cells, biosensors, components of diagnostic assays, bioadhesives, ocular devices, materials for orthopedic applications, striated and cardiac muscle regeneration, heart valve regeneration, and tendon reconstruction, just to state a few [201, 202].

Nowadays, polymers are extensively used in DDS and as scaffolds for tissue engineering.

Tissue engineering is an interdisciplinary field that aims at regenerating new biological tissue for replacing diseased or destroyed tissues. Tissues or organs can theoretically be engineered using different strategies, but the most appealing approach is the combination of the patient's cells with polymer scaffolds. In this approach, cells are isolated from a specific tissue of the patient and harvested *in vitro.* Then, the cells are incorporated into polymer scaffolds that behave as analogues of the natural extracellular matrices found in tissues. The ideal scaffold is a three-dimensional, highly porous structure with interconnected porosity. It must serve as template for the tissue growth, as a delivery vehicle for transplanted cells, and as drug carrier, activating specific cellular functions resulting in the regeneration of tissues [203-205]. Tissues like artery, bladder, skin, cartilage, bone, ligament and tendon were already engineered using this approach and are now or near clinical use [206-212].

Several natural or synthetic polymers have been used as scaffolds in tissue engineering. Naturally occurring scaffold polymers are composed of

polypeptides, polysaccharides, nucleic acids, hydroxyapatites, or their composites; synthetic polymers used include aliphatic polyesters as poly(glycolic acid) (PGA), poly(lactic acid) (PLA), and copolymers of these materials [201, 206, 213, 214].

Advances in polymer science have led to the development of a wide variety of DDS. Controlled drug delivery applications include both sustained (over days/months/years) delivery and targeted (for example to a tumor) delivery on a one-time or sustained basis [200]. Two key factors stimulated the development of DDS: proteins as potential pharmaceutics, and the demonstration that a sustained released of active proteins from polymer matrices was possible. Controlled delivery devices are generally diffusion-based systems used to release drugs intended either for the systemic circulation or for a localized action. A classic polymeric drug delivery system is the implantable contraceptive Norplant™, composed by a silicone rubber (polydimethylsiloxane) tube filled with a steroid dispersion [200]. The drug release, controlled by the permeability of the steroid in the tube wall, remains fairly constant over several years after an initial transient.

The choice and design of a polymer for DDS is a demanding task due to the natural diversity of structures and compels a comprehensive knowledge of the surface and bulk properties of the polymer providing the desired chemical, interfacial, mechanical and biological properties. The selection of a polymer is dependent not only on its physico-chemical properties, but also on the need for extensive biochemical characterization and specific preclinical tests to insure its safety [215]. In 1999, Angelova and Hunkeler [202] proposed a comprehensive flow chart and table for rational selection of polymers for various biomedical applications.

Surface properties, such as hydrophilicity, lubricity, smoothness and surface energy, influence the biocompatibility, including hemocompatibility, also affecting the physical properties, hence the durability, permeability and degradability [202, 215]. The surface properties also determine the water sorption capacity of the polymers and can be improved by chemical (oxidation and hydrolysis), physical (polymerization or grafting of water soluble polymers)

and biological (incorporation of biologically active molecules) means to increase their biocompatibility.

Polymeric biomaterial development should also be based on the optimization of the bulk polymer structure through the synthesis of new polymer compositions with improved activity and stability [202]. As the bulk structure of the polymer influences its mechanical and physical properties, microstructural design and chemical composition can be used to adapt the biomaterial to its applications. Structural properties of the matrix, namely its micro-morphology and pore size determine its mass transport properties. For non-biodegradable matrices, drug release is in most cases diffusion-controlled and peptide drugs can only be released through the pores and channels created by the dissolved drug phase [215].

Considering biodegradable polymers, it is crucial to recognize that degradation is a chemical process, whereas erosion is a physical phenomenon dependent on dissolution and diffusion processes. Depending on the chemical structure of the polymer backbone, erosion can occur by either surface or bulk erosion. Surface erosion takes place when the rate of erosion exceeds the rate of water permeation into the bulk of the polymer. Poly(anhydrides) [216] are an example of a biomaterial that undergoes surface erosion mediated degradation. Bulk erosion occurs when water molecules permeate into the bulk of the matrix at a faster rate than erosion, resulting in a complex degradation/erosion kinetics. Most of the biodegradable polymers used in drug delivery undergo bulk erosion [215]. Polyesters are an example of biomaterial that undergoes bulk erosion [217]. Hydrogels made of dextrin functionalized with hydroxyethyl methacrylate ester (HEMA) [218], hydrogels formed from acrylate modified poly(vinyl alcohol) [219] and hydrogels made from oxidized dextran [220], also show bulk erosion. However, the use of nanogels or microparticle formulations possessing rather large surface areas results in bulk- and surface-eroding materials that present similar erosion kinetics. Further, the erosion process can be manipulated by modifying the surface area of the DDS or by including hydrophobic monomer units in the polymer.

Table 1.6 gives a representative list of polymers that have been used for drug delivery applications [202, 215].

Natural polymers are usually biodegradable and offer excellent biocompatibility, although they can have batch to batch variation due to difficulties in purification. On the other hand, synthetic polymers are available in a wide variety of compositions with readily adjustable properties [202].

Table 1.6 – Representative list of polymers used in DDS.

Classification	Polymer	References
Natural polymers		
Protein-base polymers	Collagen, albumin, gelatin.	221-224
Polysaccharides	Agarose, alginate, carrageenen, hyalutonic acid, dextran and its derivatives, chitosan and its derivatives, ciclodextrins	224-229
Synthetic polymers		
Biodegradable		
Polyesters	Poly(lactic acid), poly(glycolic acid), poly(hydroxy butyrate), poly(ε-caprolactone), poly(β-malic acid), poly(diaxanones).	229-231
Polyanhydrides	Poly(sebacic acid), poly(adipic acid), poly(terphthalic acid) and various copolymers.	232, 233
Polyamides	Poly(imino carbonates), polyamino acids.	215
Phosphorous-based polymers	Polyphosphates, polyphophonates, polyphosphazenes.	202, 215, 224, 234
Others	Poly(cyano acrylates), polyurethanes, polyortho esters, polydihydropyrans, polyacetals.	215, 235
Non-biodegradable		
Cellulose derivatives	Carboxymethyl cellulose, ethyl cellulose, cellulose acetate propionate, hydroxypropyl methylcellulose.	215, 236
Silicones	Polydimethylsiloxane, colloidal silica.	237, 238
Acrylic polymers	Polymethacrylates, poly(methyl methacrylate), poly hydro(ethylmethacrylate).	224, 239
Others	Polyvivyl pyrrolidone, ethyl vinyl acetate, poloxamers, poloxamines.	215, 224

Dextrin

Polymer therapeutics, such as polymeric drugs, polymer-drug and polymer-protein conjugates, and non-viral vectors for gene delivery are attracting

much attention and finding increasing clinical use [187, 192, 215]. Both synthetic and natural polymers have been used as drug carriers. However, the majority of polymers used in clinical applications are still non-biodegradable synthetic polymers as poly(ethyleneglycol) (PEG) [240-242] and N-(2-hydroxypropyl)methacrylamine (HPMA) [243-245]. Although tolerated by man, the main chain of these polymers are not biodegradable, thus, to ensure renal elimination and to exclude the risk of progressive buildup after repeated administration, only polymers with a molecular weight below the renal threshold (~40 KDa) may be used. Natural polymers, such as dextran and poly(aminoacids), are often considered biodegradable but frequently even low levels of chemical modification (for example, to aid in drug attachment) can lead to the generation of non-degradable sub-products [246]. Furthermore, many natural polymers can be immunogenic and cannot be administered frequently.

Dextrin derives from starch by partial thermal degradation under acidic conditions or enzymatic hydrolysis. The treatment causes the breakdown of starch molecules and results in smaller and less complex molecules. The structure of dextrin, shown in Figure 1.3, is similar to the one of amylopectin.

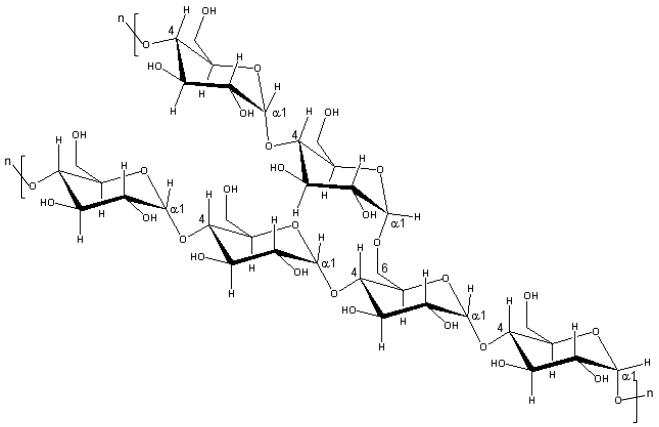

Figure 1.3 – Dextrin molecular structure.

Dextrin is a α-1,4 poly(glucose) polymer with minimal branching (it has less than 5% α-1,6 links). Icodextrin (a polydisperse dextrin), applied in routine clinical use as a peritoneal dialysis solution [247], has been developed as a

carrier solution for intraperitoneal administration of 5-fluorouracil [248]. The proven clinical tolerability and the fact that dextrin is degraded by amylases [247], makes this polymer attractive for development as a drug carrier.

Polymer-based hydrogels and nanogels

A large number of polymers have been developed for controlled and targeted delivery. These polymers, from natural or synthetic sources, can be manipulated to produce specific delivery system as hydrogels, microcapsules, or nanogels (or hydrogel nanoparticles) depending on various requirements like biocompatibility, high loading capacity, extend circulation time, and ability to accumulate in targeted pathological sites [192, 249].

Hydrogels.

Hydrogels are three-dimensional, cross-linked networks of water-soluble polymers that can be prepared from virtually any water-soluble polymer, encompassing a variety of chemical compositions and bulk physical characteristics [250]. In addition, hydrogels can be formulated in a wide range of physical forms, as slabs, microparticles, nanoparticles (nanogels), coatings, and films. As a consequence, they are usually used in clinical practice and experimental medicine in diverse applications [250], including tissue engineering and regenerative medicine [206], diagnostics [251], cellular immobilization [252], and as barrier materials to regulate biological adhesions [253].

Hydrogels are polymer networks swollen with a large amount of water, which normally represents more than 50% of the total weight. On the macroscopic scale hydrogels are solids: they have definite shapes and do not flow; nevertheless, they also behave like solutions on the molecular scale: the transport of water-soluble molecules is characterized by diffusion constants reflecting the size and shape of the diffusing molecules as well as the porosity and tortuosity of the hydrogel [254]. Hydrogels can be achieved through chemical or physical cross-linking of polymers (Scheme 1.1), its properties

depending on the chemical composition, cross-linking density, and hydrophobicity [224, 255].

Scheme 1.1 – Schematic representation of hydrogel formation. Cross-linked network is created by physical associations, ionic bonds, or covalent bonds. Adapted from Lee and Yuk, 2007 [224] and Varghese and Elisseeff, 2006 [255].

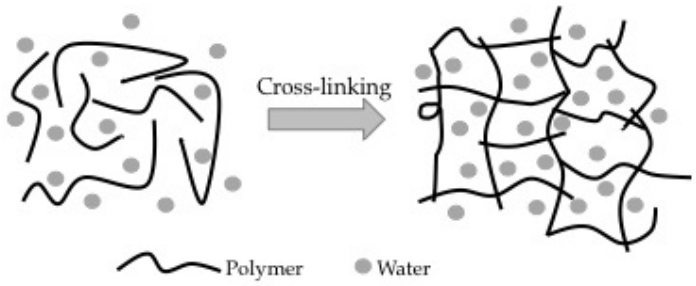

The hydrogel distinctive physical properties have generated particular interest concerning its potential for drug delivery applications. Their highly porous structure can easily be adjusted by controlling the density of cross-links in the gel matrix and the affinity of the hydrogels for the aqueous environment in which they are swollen [250]. Drugs can be loaded into the highly porous gel matrix and subsequently released at a rate dependent on the diffusion coefficient of the small molecule or macromolecules through the gel network.

Hydrogels are commonly considered as highly biocompatible [206, 224, 250, 256], owing to the high water content, and also to the physiochemical similarity with the native extracellular matrix.

The degradation of hydrogels, and therefore the time scale and the drug release kinetics, can be altered via enzymatic or hydrolytic pathways, or environmental switches, such as pH and temperature. Hydrogels are also relatively deformable and can match the shape of the surface to which they are applied. Also, the muco- or bioadhesive properties of some hydrogels can be favorable to promote their immobilization to the site of application.

In spite of their many favorable properties, hydrogels also have some limitations. The low tensile strength limits their use in load-bearing applications and, as a consequence, the premature dissolution or flow away

of the hydrogel from the targeted local site can occur. Concerning drug delivery, the most important drawback of hydrogels relates to the quantity and homogeneity of drug loading, which may be limited, especially in the case of hydrophobic drugs; on the other hand, the high water content and large pores frequently result in relatively rapid drug release. The hydrogel employment, on the clinical context, can also be a problem: although some hydrogels are sufficiently deformable to be injectable, many are not, requiring surgical implantation.

When considering hydrogels as a delivery system, some aspects should be considered [206, 224, 250]:

- The hydrogel loading capacity (amount of drug that can be mixed or grafted into the system);
- The homogenous dispersion of the drug, which can influence the release kinetics;
- The drug binding affinity. This defines how tightly the drug binds to the hydrogel; it should be sufficiently low to permit the drug release but high enough to prevent immediate and uncontrolled release;
- The release kinetics of the loaded drug;
- The long-term stability. The loaded drug must maintain its structure and activity over a prolonged period of time;
- The economical viability. The materials used must be easy to manufacture and handle, and also be cost competitive.

Noteworthy advances have been made in improving the properties of hydrogels used for drug delivery. The diversity of release kinetics using hydrogel-based delivery vehicles has also been expanded. Nevertheless, some issues remain to improve its clinical applicability for drug delivery. A critical future challenge for protein delivery is how polymers can be tailored to effectively deliver the drugs, in response to signals generated in the body.

Nanogels.

In general, nanometric carriers comprise sub-micro particles with size below 1000 nanometers (nm) exhibiting various morphologies, such as nanospheres, nanocapsules, nanomicelles, nanoliposomes, nanodrugs, etc [257-259].

Nanometer-sized polymer hydrogels (nanogels), with properties of both nanoparticles and hydrogels, have attracted growing attention due to the increasing development of nanotechnology.

Nanogel drug delivery systems have outstanding advantages [257, 258, 260]: ability to pass through the smallest capillary vessels and avoid rapid uptake by phagocytes so that clearance from the blood stream is greatly reduced; penetration in cells and tissue gaps to arrive at target organs such as liver, spleen, lung, spinal cord and lymph; potential for controlled release, due to the biodegradability, pH, ion and/or temperature sensibility of materials; improved therapeutic potential for drugs, due to reduced toxic side effects; potential for administration through various routes, including oral, pulmonary nasal, parenteral, ocular; etc.

Nanogels can be used to deliver hydrophilic and hydrophobic drugs, proteins, vaccines, biomacromolecules, etc. They can also be designed to target different sites and organs, such as the lymphatic system, brain, arterial walls, lung, liver, spleen, or made for long-term systemic circulation. As a result, depending on the physicochemical properties of the drug and the preferred delivery route, it is possible to choose the best polymer and method of preparation to achieve an efficient encapsulation. For example, drugs can be entrapped in the polymer matrix, encapsulated in the core, surrounded by a shell-like polymer membrane, chemically conjugated to the polymer, or bound to the particle surface by adsorption [261]. According to their structural characteristics, the nanogels are mainly prepared by covalent cross-linking, ionic cross-linking, polyelectrolyte complexation, and self-assembly of hydrophobically modified polysaccharides.

Presently, the advances on nanogel drug delivery systems focus on: the selection and combination of carrier materials to obtain suitable drug release rates; the surface modification to improve the targeting ability; the

optimization of the formulation for clinical application and industrial production; the investigation of *in vivo* dynamic processes to disclose the interaction of nanogels with blood and targeting tissues and organs, etc [257].

Among nanosized systems, nanogels have been tested as carriers for proteins, peptides and oligosaccharides. Usually, proteins and vaccines are delivered via parenteral routes, due to their low bioavailability and/or poor immunogenicity when administered via non-parenteral routes [262]. In recent years, substantial progresses have been made on the use of non-invasive routes, such as mucosal (oral, nasal, pulmonary and colon) and transdermal, for the delivery of proteins and vaccines, yielding better patient compliance [262-265]. Some examples of specific studies on the use of nanogels for protein delivery are described ahead.

The oral route is considered the most convenient and comfortable means of drug administration, because of its non-invasive nature. It reduces the risk of infection, and do not require trained personnel. Drug molecules may cross the intestinal epithelium by transcellular or paracellular pathways. However, the bioavailability of orally administered proteins is usually poor, because of the hostile gastric and intestinal environments, and also the limited gastrointestinal (GI) mucosal permeability. The intestinal epithelium is a major barrier to the absorption of hydrophilic macromolecules, because they cannot diffuse across the lipid bilayer of the cell membranes, given the large molecular weight (Mw) and hydrophilicity [266, 267]. One possible way to improve the GI uptake of proteins and peptides is the encapsulation in micro/nanogels that, besides protecting from degradation in the GI tract, improve the transportation into the systemic circulation. Lin *et al* [268] reported the production, by ionic gelation, of nanogels composed of chitosan (CS) and poly-γ-glutamic acid (γ-PGA) for oral insulin delivery. The characterization of CS nanogels at distinct pH values, simulating the environments of the GI tract, was investigated and the stability and functionality of CS nanogels *in vitro*, using Caco-2 cell monolayers, and *in vivo*, in a rat model were studied. The authors observed that the CS nanogels could transiently and reversibly open the tight junctions between Caco-2 cells, thus enhancing the paracellular

permeability. In a further development, Sonaje *et al* [269] prepared self-assembled nanogels, by mixing γ-PGA with CS in the presence of $MgSO_4$ and tripolyphosphate (TPP). The introduction of $MgSO_4$ in the preparation of CS nanogels improved the stability in a broader pH range. The *in vitro* results showed that the mucoadhesive properties of CS nanogels are affected by the pH and additionally, the transport of insulin across Caco-2 cell monolayers is pH-dependent: with increasing pH, the amount of insulin transported decreased significantly, due to the lower positive surface charge of the nanogel, hence lower mucoadhesive and absorption enhancement ability. In addition, oral administration of insulin-loaded nanogels demonstrated a significant hypoglycemic action for at least 10 hours, in diabetic rats.

The nasal mucosa is an attractive route for the delivery of drugs because it has a relatively large absorptive surface and low proteolytic activity [264, 270-274]. Importantly, nasally administered drugs can induce both local and systemic immune responses. However, most proteins are not well absorbed from the nasal cavity when administered as simple solutions. The major factors limiting the absorption of nasally administered proteins are the poor ability to cross the nasal epithelia, and the mucociliary clearance, which rapidly removes protein solutions from the absorption site [264, 265, 270]. Mucoadhesive, hydrophilic nanogels have received much attention to overcome these obstacles and deliver protein antigens via the nasal route, because they strongly attach the mucosa increasing mucin viscosity [265, 270, 272, 273]. By this means, mucoadhesive nanogels are able to decrease the nasal mucociliary clearance rate and thus increase the residence time of the formulation in the nasal cavity [264, 270]. Amidi and colleagues [275] prepared and characterized protein loaded trimethyl chitosan (TMC) nanogels as a nasal delivery system. It was observed that TMC nanogels have a high loading efficiency (fraction of protein loaded) and capacity (amount of protein loaded per NPs dry weight) up to 50% (w/w). The integrity of the entrapped ovalbumin (the model protein) was preserved and release studies showed that more than 70% of the protein remained associated with the nanogel for at least 3h of incubation in PBS (pH 7.4), at 37ºC. *In vivo* uptake studies indicated the transport of the

protein across the nasal mucosa. Other authors tested CS nanogels as a nasal delivery system for insulin. Zhang *et al* [276] used polyethylene glycol-grafted CS-NPs to improve the systemic absorption of insulin, following nasal administration. Intranasal administration of the nanogels in rabbits enhanced the absorption of insulin to a greater extent than the free protein. The nasal delivery of insulin using chitosan-acetyl-L-cysteine (CS-NAC) nanogels was proposed by Wang *et al* [277]. These authors observed that intranasal administration of CS-NAC nanogels in rats enhanced the absorption of insulin by the nasal mucosa, as compared with unmodified CS nanogels and control free insulin solution.

Mucosal vaccine strategies have emerged as a viable and attractive alternative to parenteral immunization. Advantages associated with mucosal vaccination are numerous: easy and low cost of administration, patient compliance, avoidance of the hepatic first pass metabolism and ability to induce mucosal as well as systemic immunity. Furthermore, the immune response generated at one mucosal site is able to induce a strong immune response at distal mucosal surfaces [278]. Westerink *et al* [279] examined the effect of mucosal administration of tetanus toxoid in the presence of a non-ionic copolymer, Pluronic® F127 with CS or lysophosphatidylcholine, on the systemic and mucosal immune response. The results suggest that the two components of F127/CS appear to exert an additive or synergistic effect on the immune response.

Pulmonary drug delivery for both local and systemic treatments has many advantages over other delivery routes. The lungs have a large surface area (43 to 102 m^2) [280]. In addition, mucociliary clearance is slower at the alveoli of the lungs than in the airways. Furthermore, the epithelium is thinner and more permeable, making possible the systemic absorption of peptides and proteins. Indeed, a number of high Mw drugs were demonstrated to be absorbed successfully through the lungs [280-282]. The successful delivery of the inhaled particles depends mostly on their size and density, and hence, on the aerodynamic diameter. Grenha *et al* [283] reported the preparation and characterization of dry powders containing protein-loaded TPP-CS nanogels,

using aerosol excipients. Bovine insulin was chosen as model protein, with mannitol and lactose as excipients. These nanogels showed a good protein loading capacity, providing the *in vitro* release of 75–80% insulin within 15 min, and could be easily recovered from microspheres after contact with an aqueous medium, with no significant changes in their size and zeta potential values. Therefore, protein-loaded CS nanogels could be successfully incorporated into microspheres with adequate characteristics as to reach the deep lung; in contact with the aqueous environment, the microspheres were able to release the nanogels and then the therapeutic macromolecule.

Colon targeted drug delivery is useful in improving the absorption of peptide drugs via the GI tract. Site specific drug delivery to the colon is of special interest for drugs instable in the upper part of the GI tract, because of the peptidase activity in the small intestine. The colon is thought to have lower enzymatic activity than other regions of the GI, hence a greater absorption efficiency in this region would be expected, as long as the proteins/peptides are released locally [284]. Bayat *et al* [285] developed a nanoparticulate system using two new quarternized derivatives of CS, triethylchitosan (TEC) and dimethylethylchitosan (DMEC), for insulin colon delivery. The three kinds of nanogels showed a positive charge that could facilitate insulin uptake, allowing a low bursting effect and a steady release of insulin *in vitro*. DMEC NPs and TEC nanogels had smaller particle size, higher insulin loading capacity and improved transport and absorption of insulin in GI tract, as compared with CS nanogels. The blood glucose lowering effect of TEC nanogels and DMEC nanogels, after injection into ascending colon, was superior to that obtained with free insulin or CS nanogels. This study indicated that nanogels prepared from quaternized derivatives of CS might be a promising vehicle of administration of proteins and peptides via colon absorption.

The advantages of the nanogels as delivery systems include simplicity of formulation with the drugs, high loading capacity and stability of the resulting complex in dispersion. These systems allow immobilization of

biologically charged drugs, low molecular mass hydrophobes and biopolymers, as well as plasmid DNA and small globular proteins. Furthermore, nanogels can be chemically modified to incorporate various ligands, for example to improve stability, for targeted drug delivery. The *in vitro* studies suggest that nanogels can be applied for efficient delivery of biopharmaceuticals in cells as well as for augmenting drug delivery across cellular barriers, although some issues, including the *in vivo* biodistribution and intracellular trafficking, are still waiting for a more comprehensive characterization.

Carbohydrate-binding modules

By creating fusion proteins containing carbohydrate-binding modules (CBMs) and a bioactive protein, it is possible to functionalize a carbohydrate-based material without complex reactions and cross-linking processes with low yields and frequently unsuccessful.

A CMB is defined as a contiguous amino acid sequence within a carbohydrate-active enzyme with a discreet fold having carbohydrate-binding activity [286]. Usually, these carbohydrate-active enzymes (glycoside hydrolases) are modular proteins constituted by a catalytic module and by one or more non-catalytic polysaccharide-recognizing modules, the CBMs. Historically, CBMs were termed cellulose-binding domains (CBDs), because the first examples of these protein domains bound crystalline cellulose as their primary ligand [287]. Several CBMs have been characterized experimentally, and many hundred putative CBMs can be further identified on the basis of amino acid similarity. CBMs are divided into families according to its amino acid similarity. Currently, 59 CBM families are described in the Carbohydrate-Active EnZymes (CAZy) database (http://www.cazy.org/). In 2004, Boraston *et al* [287] published a comprehensive and detailed review on the structure and binding modes of the CBMs.

Usually, CMBs are present in glycoside hydrolases that degrade insoluble polysaccharides and are recognized as an essential component of several of these enzymes. CBMs have three general roles with respect to the function of their associated catalytic modules [287-290]:

- Proximity effect. The CMBs promote the association of the enzyme with the substrate, securing a prolonged contact and effectively increasing its concentration.
- Substrate targeting function. It has already been demonstrated that CBMs have specific substrate affinity, distinguishing different crystalline, amorphous, soluble and non-soluble polysaccharides.
- Microcrystallite disruptive function. The crystalline polysaccharides are disrupted by the CBMs leading to an increase in substrate access.

Carbohydrate recognition by proteins, mainly hydrolases, has crucial importance in numerous fundamental biological processes such as cell-cell communication, cellular adhesion, pathogen-host interaction events, or protein trafficking. Despite CBMs role in several biological processes, CBMs are used in various biotechnological applications that include: the improvement of fibers in textile [291, 292] and paper [293, 294] industry; as tags in recombinant proteins for solubilization and purification [295-299]; as probes for protein-carbohydrate interaction and microarrays [300-302], and in the modification of physical and chemical properties of composite materials.

Significant advances have been made in the improvement of biomaterials so that they are able to interact specifically with their biological environment. The chemical, physical and biochemical characteristics of an implant surface are very important for the design of biomedical devices since the first interaction between an implant at the biological environment takes place at the interface. Biological recognition of materials can be enhanced by different mechanisms [256]: by incorporating and controlling the spatial distribution of biomimetic adhesion sites that can be used to promote cell adhesion and migration on or within bioactive materials; by incorporating specific proteins (as growth factors) that potentiate cell survival, promote cell proliferation, or

control cellular phenotype; or, in addition, by incorporating DNA into bioactive materials.

The incorporation of adhesion-promoting peptides, such as the Arg-Gly-Asp (RGD) peptide, into a biomaterial surface has been extensively reviewed [256, 303, 304] and CMBs were already described as a tool to adsorb bioactive peptides to carbohydrate-based materials [305-307], such as cellulose blood vessels [308].

Human chitin-binding module

Chitiosan (poly[β-(1-4)-2-amino-2-deoxy-D-glucopyranose]) is a water soluble polycationic co-polymer of N-glucosamine and N-acetyl-glucosamine, that occurs naturally or is obtained by the partial N-deacetylation of chitin (Scheme 1.2) [309]. Chitosan is biodegradable, non-toxic to animals, soluble in acidic solutions, available in various forms and much more tractable than chitin. As a result, chitosan presents characteristics that make it attractable for numerous biotechnology and biomedical applications.

Scheme 1.2 – Chitin deacetylation to chitosan. The deacetylation can be enzymatic (chitin deacetylases) or chemical (NaOH).

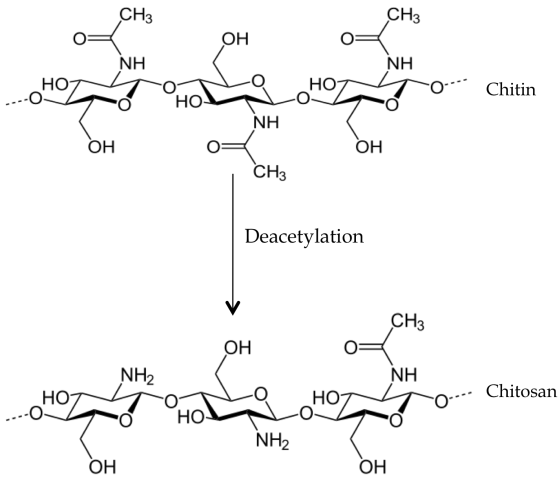

In the biomedical and pharmaceutical fields, chitosan has been applied into the treatment of large burns; the preparation of artificial skin; surgical sutures; contact lenses; blood dialysis membranes and artificial blood vessels; as antitumor, blood anticoagulant, antigastritis, haemostatic,

hypocholesterolaemic and antithrombogenic agents; in drug and gene-delivery systems; and in dental therapy [309-314].

Family 18 of glycosyl hydrolases comprises enzymes that degrade chitin (chitinases) from several species, including bacteria, fungi, insects, and plants. Although chitin has not been found in mammals, a human homologue to fungal, bacterial or plant chitinases was identified and cloned [315, 316]. The human chitinase is produced by activated macrophages where its cDNA is the sixth most common transcript found [317] and it is dramatically elevated in serum from patients with Gaucher disease [318], an inherited lysosomal storage disorder. The physiological purpose for a mammalian chitinase is still unclear however, chitin is an integral component of fungal cell walls, and also the human chitinase is expressed in activated macrophages so, a defensive function against chitinous human pathogens has been suggested for the enzyme.

Comparison of the predicted protein sequence of the chitinase ORF with chitinases from other species showed that the protein is composed by two distinct domains (Figure 1.4) [315, 317]: the catalytic domain, contained within the N-terminal 75% of the protein; and a chitin-binding domain in the C-terminus. Consistent with the hypothesis that this C-terminal is a chitin-binding domain, in 1997, Renkema *et al* [319], described a C-terminally truncated form of the human chitinase that can hydrolyze chitin but is unable to bind to it. The 72 C-terminal aminoacids mediate the binding to chitin and together form a functional and structurally independent domain in the human chitinase.

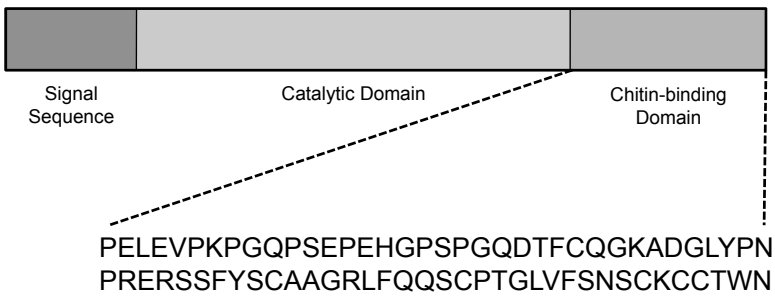

Figure 1.4 – Proposed domain structure of human chitinase [317]. The sequence of the C-terminal 72 aminoacids is presented.

In addition to its strong affinity for chitin, the chitin-binding domain is largely specific for chitin and little or no binding occurs to cellulose, mannan, or xylan [317], this suggests that the binding domain is tightly constrained to a specific ligand composition and conformation.

Many carbohydrate-binding domains of proteins that metabolize polysaccharides are rich in cysteine residues and interestingly, Tjoelker *et al* [317] showed that the six cysteine residues present in the C-terminal half of the protein are essential for the chitin binding activity of the domain. The indispensability of all cysteines implies that each one may be engaged in disulfide bond formation.

The human chitin-binding domain belongs to the carbohydrate-binding module family 14 (CAZy classification). This family is constituted by binding modules of approximately 70 aminoacid residues that are found attached to a number of chitinase catalytic domains.

Besides their use in the biotechnology areas, CBMs are now seen as useful tools for the biomedical field. Using recombinant DNA technology, it is possible to fuse these highly specific CBMs with biologically active agents to functionalize carbohydrate-based biomaterials. For example, RGD peptides can be immobilized on the surface of the biomaterials, improving cell adhesion spreading and proliferation; or, on the other hand, grafting an anti-inflammatory molecule, as IL-10, it is conceivable that it may to diminish an implant inflammatory reaction, overall improving a biomaterial biocompatibility.

References

(1) Tayal, V.; Kalra, B. S., *Eur J Pharmacol* **2008,** 579, (1-3), 1-12.

(2) Bennett, I. L., Jr.; Beeson, P. B., *J Exp Med* **1953,** 98, (5), 493-508.

(3) Isaacs, A.; Lindenmann, J., *Proc R Soc Lond B Biol Sci* **1957,** 147, (927), 258-67.

(4) Bloom, B. R.; Bennett, B., *Science* **1966,** 153, (731), 80-2.

(5) David, J. R., *Proc Natl Acad Sci U S A* **1966,** 56, (1), 72-7.

(6) Dumonde, D. C.; Wolstencroft, R. A.; Panayi, G. S.; Matthew, M.; Morley, J.; Howson, W. T., *Nature* **1969,** 224, (5214), 38-42.

(7) Carswell, E. A.; Old, L. J.; Kassel, R. L.; Green, S.; Fiore, N.; Williamson, B., *Proc Natl Acad Sci U S A* **1975,** 72, (9), 3666-70.

(8) Aarden, L. A.; Brunner, T. K.; Cerottini, J. C.; Dayer, J. M.; Deweck, A. L.; Dinarello, C. A.; Disabato, G.; Farrar, J. J.; Gery, I.; Gillis, S.; Handschumacher, R. E.; Henney, C. S.; Hoffmann, M. K.; Koopman, W. J.; Krane, S. M.; Lachman, L. B.; Lefkowits, I.; Mishell, R. I.; Mizel, S. B.; Oppenheim, J. J.; Paetkau, V.; Plate, J.; Rollinghoff, M.; Rosenstreich, D.; Rosenthal, A. S.; Rosenwasser, L. J.; Schimpl, A.; Shin, H. S.; Simon, P. L.; Smith, K. A.; Wagner, H.; Watson, J. D.; Wecker, E.; Wood, D. D., *Mol Immunol* **1980,** 17, (5), 641-643.

(9) Fridman, W. H.; Tartour, E., *Mol Aspects Med* **1997,** 18, (1), 3-90.

(10) Cohen, S.; Bigazzi, P. E.; Yoshida, T., *Cell Immunol* **1974,** 12, (1), 150-9.

(11) Niedbala, W.; Wei, X. Q.; Cai, B.; Hueber, A. J.; Leung, B. P.; McInnes, I. B.; Liew, F. Y., *Eur J Immunol* **2007,** 37, (11), 3021-9.

(12) Dinarello, C. A., *Cytokine Growth Factor Rev* **1997,** 8, (4), 253-65.

(13) Rosenwasser, L. J., *J Allergy Clin Immunol* **1998,** 102, (3), 344-50.

(14) Or, R.; Renz, H.; Terada, N.; Gelfand, E. W., *Clin Immunol Immunopathol* **1992,** 64, (3), 210-7.

(15) Augustine, J. A.; Schlager, J. W.; Abraham, R. T., *Biochim Biophys Acta* **1990,** 1052, (2), 313-22.

(16) Gaffen, S. L.; Liu, K. D., *Cytokine* **2004,** 28, (3), 109-23.

(17) Lopez, A. F.; Elliott, M. J.; Woodcock, J.; Vadas, M. A., *Immunol Today* **1992,** 13, (12), 495-500.

(18) Schmitt, E.; Huls, C.; Nagel, B.; Rude, E., *Cytokine* **1990,** 2, (6), 407-15.

(19) McKenzie, A. N.; Sanderson, C. J., *Chem Immunol* **1992,** 51, 135-52.

(20) Stein, B.; Sutherland, M. S. K., *Drug Discov Today* **1998,** 3, (5), 202-213.

(21) Hirano, T.; Akira, S.; Taga, T.; Kishimoto, T., *Immunol Today* **1990,** 11, (12), 443-9.

(22) Kammuller, M. E., *Toxicology* **1995,** 105, (1), 91-107.

(23) Suda, T.; Zlotnik, A., *Adv Neuroimmunol* **1992,** 2, (2), 99-108.

(24) Hofmeister, R.; Khaled, A. R.; Benbernou, N.; Rajnavolgyi, E.; Muegge, K.; Durum, S. K., *Cytokine Growth Factor Rev* **1999,** 10, (1), 41-60.

(25) Mire-Sluis, A. R.; Gaines Das, R.; Thorpe, R., *J Immunol Methods* **1997,** 200, (1-2), 1-16.

(26) Schroder, J. M., *Adv Neuroimmunol* **1992,** 2, (2), 109-124.

(27) Matsuzawa, S.; Sakashita, K.; Kinoshita, T.; Ito, S.; Yamashita, T.; Koike, K., *J Immunol* **2003,** 170, (7), 3461-7.

(28) White, B.; Leon, F.; White, W.; Robbie, G., *Clin Ther* **2009,** 31, (4), 728-40.

(29) Fickenscher, H.; Hor, S.; Kupers, H.; Knappe, A.; Wittmann, S.; Sticht, H., *Trends Immunol* **2002,** 23, (2), 89-96.

(30) Pestka, S.; Krause, C. D.; Sarkar, D.; Walter, M. R.; Shi, Y.; Fisher, P. B., *Annu Rev Immunol* **2004,** 22, 929-79.

(31) Tenney, R.; Turnbull, J. R.; Stansfield, K. A.; Pekala, P. H., *Adv Enzyme Regul* **2003,** 43, 153-66.

(32) Tafuri, A.; Lemoli, R. M.; Petrucci, M. T.; Ricciardi, M. R.; Fogli, M.; Bonsi, L.; Ariola, C.; Strippoli, P.; Gregorj, C.; Petti, M. C.; Tura, S.; Mandelli, F.; Bagnara, G. P., *Exp Hematol* **1999,** 27, (8), 1255-63.

(33) Biron, C. A.; Gazzinelli, R. T., *Curr Opin Immunol* **1995,** 7, (4), 485-96.

(34) Watford, W. T.; Moriguchi, M.; Morinobu, A.; O'Shea, J. J., *Cytokine Growth Factor Rev* **2003,** 14, (5), 361-8.

(35) Kasaian, M. T.; Miller, D. K., *Biochem Pharmacol* **2008,** 76, (2), 147-155.

(36) McKenzie, A. N.; Culpepper, J. A.; de Waal Malefyt, R.; Briere, F.; Punnonen, J.; Aversa, G.; Sato, A.; Dang, W.; Cocks, B. G.; Menon, S.; et al., *Proc Natl Acad Sci U S A* **1993,** 90, (8), 3735-9.

(37) Budagian, V.; Bulanova, E.; Paus, R.; Bulfone-Paus, S., *Cytokine Growth Factor Rev* **2006,** 17, (4), 259-80.

(38) Tagaya, Y.; Bamford, R. N.; DeFilippis, A. P.; Waldmann, T. A., *Immunity* **1996,** 4, (4), 329-36.

(39) Gillespie, M. T.; Horwood, N. J., *Cytokine Growth Factor Rev* **1998,** 9, (2), 109-16.

(40) McInnes, I. B.; Gracie, J. A.; Leung, B. P.; Wei, X. Q.; Liew, F. Y., *Immunol Today* **2000,** 21, (7), 312-5.

(41) Belardelli, F.; Gresser, I., *Immunol Today* **1996,** 17, (8), 369-372.

(42) Biron, C. A., *Immunity* **2001,** 14, (6), 661-664.

(43) Chevaliez, S.; Pawlotsky, J. M., *Adv Drug Deliv Rev* **2007,** 59, (12), 1222-41.

(44) Muhl, H.; Pfeilschifter, J., *Int Immunopharmacol* **2003,** 3, (9), 1247-1255.

(45) Shtrichman, R.; Samuel, C. E., *Curr Opin Microbiol* **2001,** 4, (3), 251-259.

(46) Tracey, D.; Klareskog, L.; Sasso, E. H.; Salfeld, J. G.; Tak, P. P., *Pharmacol Ther* **2008,** 117, (2), 244-79.

(47) Mocellin, S.; Rossi, C. R.; Pilati, P.; Nitti, D., *Cytokine Growth Factor Rev* **2005,** 16, (1), 35-53.

(48) Elliott, M. J.; Vadas, M. A.; Eglinton, J. M.; Park, L. S.; To, L. B.; Cleland, L. G.; Clark, S. C.; Lopez, A. F., *Blood* **1989,** 74, (7), 2349-59.

(49) Bratton, D. L.; Hamid, Q.; Boguniewicz, M.; Doherty, D. E.; Kailey, J. M.; Leung, D. Y., *J Clin Invest* **1995,** 95, (1), 211-8.

(50) Flanagan, A. M.; Lader, C. S., *Curr Opin Hematol* **1998,** 5, (3), 181-5.

(51) Barreda, D. R.; Hanington, P. C.; Belosevic, M., *Dev Comp Immunol* **2004,** 28, (5), 509-54.

(52) Fisher, J. W., *Exp Biol Med (Maywood)* **2003,** 228, (1), 1-14.

(53) Szenajch, J.; Wcislo, G.; Jeong, J. Y.; Szczylik, C.; Feldman, L., *Biochim Biophys Acta* **2010**.

(54) Massague, J., *Annu Rev Cell Biol* **1990,** 6, 597-641.

(55) Grimaud, E.; Heymann, D.; Redini, F., *Cytokine Growth Factor Rev* **2002,** 13, (3), 241-57.

(56) Asadullah, K.; Volk, H. D.; Sterry, W., *Trends Immunol* **2002,** 23, (1), 47-53.

(57) Asadullah, K.; Sterry, W.; Trefzer, U., *Exp Dermatol* **2002,** 11, (2), 97-106.

(58) Chang, J.; Kavanaugh, A., *Pathophysiology* **2005,** 12, (3), 217-25.

(59) Senolt, L.; Vencovsky, J.; Pavelka, K.; Ospelt, C.; Gay, S., *Autoimmun Rev* **2009,** 9, (2), 102-7.

(60) Fehniger, T. A.; Cooper, M. A.; Caligiuri, M. A., *Cytokine Growth Factor Rev* **2002,** 13, (2), 169-83.

(61) Parmiani, G.; Rivoltini, L.; Andreola, G.; Carrabba, M., *Immunol Lett* **2000,** 74, (1), 41-4.

(62) Landi, S.; Bottari, F.; Gemignani, F.; Gioia-Patricola, L.; Guino, E.; Osorio, A.; de Oca, J.; Capella, G.; Canzian, F.; Moreno, V., *Eur J Cancer* **2007,** 43, (4), 762-8.

(63) Martin, R., *Trends Pharmacol Sci* **2003,** 24, (12), 613-6.

(64) Tzu, J.; Mamelak, A.; Sauder, D. N., *Clinical and Applied Immunology Reviews* **2006,** 6, (2), 99-130.

(65) Pietrzak, A. T.; Zalewska, A.; Chodorowska, G.; Krasowska, D.; Michalak-Stoma, A.; Nockowski, P.; Osemlak, P.; Paszkowski, T.; Rolinski, J. M., *Clin Chim Acta* **2008,** 394, (1-2), 7-21.

(66) Jazayeri, J. A.; Carroll, G. J.; Vernallis, A. B., *Int Immunopharmacol* **2010,** 10, (1), 1-8.

(67) Ishihara, K.; Hirano, T., *Cytokine Growth Factor Rev* **2002,** 13, (4-5), 357-68.

(68) Blanchard, F.; Duplomb, L.; Baud'huin, M.; Brounais, B., *Cytokine Growth Factor Rev* **2009,** 20, (1), 19-28.

(69) Alpdogan, O.; van den Brink, M. R., *Trends Immunol* **2005,** 26, (1), 56-64.

(70) Moore, K. W.; de Waal Malefyt, R.; Coffman, R. L.; O'Garra, A., *Annu Rev Immunol* **2001,** 19, 683-765.

(71) Asadullah, K.; Sterry, W.; Volk, H. D., *Pharmacol Rev* **2003,** 55, (2), 241-69.

(72) Keystone, E.; Wherry, J.; Grint, P., *Rheum Dis Clin North Am* **1998,** 24, (3), 629-39.

(73) Schreiber, S.; Fedorak, R. N.; Nielsen, O. H.; Wild, G.; Williams, C. N.; Nikolaus, S.; Jacyna, M.; Lashner, B. A.; Gangl, A.; Rutgeerts, P.; Isaacs, K.; van Deventer, S. J.;

Koningsberger, J. C.; Cohard, M.; LeBeaut, A.; Hanauer, S. B., *Gastroenterology* **2000,** 119, (6), 1461-72.

(74) Asadullah, K.; Sterry, W.; Stephanek, K.; Jasulaitis, D.; Leupold, M.; Audring, H.; Volk, H. D.; Docke, W. D., *J Clin Invest* **1998,** 101, (4), 783-94.

(75) McInnes, I. B.; Illei, G. G.; Danning, C. L.; Yarboro, C. H.; Crane, M.; Kuroiwa, T.; Schlimgen, R.; Lee, E.; Foster, B.; Flemming, D.; Prussin, C.; Fleisher, T. A.; Boumpas, D. T., *J Immunol* **2001,** 167, (7), 4075-82.

(76) Nelson, D. R.; Lauwers, G. Y.; Lau, J. Y.; Davis, G. L., *Gastroenterology* **2000,** 118, (4), 655-60.

(77) Mocellin, S.; Panelli, M. C.; Wang, E.; Nagorsen, D.; Marincola, F. M., *Trends Immunol* **2003,** 24, (1), 36-43.

(78) Melero, I.; Mazzolini, G.; Narvaiza, I.; Qian, C.; Chen, L.; Prieto, J., *Trends Immunol* **2001,** 22, (3), 113-5.

(79) Cohn, L.; Ray, A., *Pharmacol Ther* **2000,** 88, (2), 187-96.

(80) Leath, T. M.; Singla, M.; Peters, S. P., *Drug Discov Today* **2005,** 10, (23-24), 1647-55.

(81) Bessis, N.; Boissier, M. C., *Joint Bone Spine* **2001,** 68, (6), 477-81.

(82) Altinova, A. E.; Yetkin, I.; Akbay, E.; Bukan, N.; Arslan, M., *Cytokine* **2008,** 42, (2), 217-21.

(83) Inoue, H.; Hiraoka, K.; Hoshino, T.; Okamoto, M.; Iwanaga, T.; Zenmyo, M.; Shoda, T.; Aizawa, H.; Nagata, K., *Bone* **2008,** 42, (6), 1102-10.

(84) Feldmann, M.; Maini, R. N., *Joint Bone Spine* **2002,** 69, (1), 12-8.

(85) Mangia, A.; Leandro, G.; Helbling, B.; Renner, E. L.; Tabone, M.; Sidoli, L.; Caronia, S.; Foster, G. R.; Zeuzem, S.; Berg, T.; Di Marco, V.; Cino, N.; Andriulli, A., *J Hepatol* **2004,** 40, (3), 478-83.

(86) Sigounas, G.; Sallah, S.; Sigounas, V. Y., *Cancer Lett* **2004,** 214, (2), 171-9.

(87) Osterborg, A.; Aapro, M.; Cornes, P.; Haselbeck, A.; Hayward, C. R.; Jelkmann, W., *Eur J Cancer* **2007,** 43, (3), 510-9.

(88) Pinkas, J.; Teicher, B. A., *Biochem Pharmacol* **2006,** 72, (5), 523-9.

(89) Pardali, K.; Moustakas, A., *Biochim Biophys Acta* **2007,** 1775, (1), 21-62.

(90) Blaney Davidson, E. N.; van der Kraan, P. M.; van den Berg, W. B., *Osteoarthritis Cartilage* **2007,** 15, (6), 597-604.

(91) Fiorentino, D. F.; Bond, M. W.; Mosmann, T. R., *J Exp Med* **1989,** 170, (6), 2081-95.

(92) O'Garra, A.; Stapleton, G.; Dhar, V.; Pearce, M.; Schumacher, J.; Rugo, H.; Barbis, D.; Stall, A.; Cupp, J.; Moore, K.; et al., *Int Immunol* **1990,** 2, (9), 821-32.

(93) Moore, K. W.; Vieira, P.; Fiorentino, D. F.; Trounstine, M. L.; Khan, T. A.; Mosmann, T. R., *Science* **1990,** 248, (4960), 1230-4.

(94) Kim, J. M.; Brannan, C. I.; Copeland, N. G.; Jenkins, N. A.; Khan, T. A.; Moore, K. W., *J Immunol* **1992,** 148, (11), 3618-23.

(95) Rothwell, L.; Young, J. R.; Zoorob, R.; Whittaker, C. A.; Hesketh, P.; Archer, A.; Smith, A. L.; Kaiser, P., *J Immunol* **2004,** 173, (4), 2675-82.

(96) Zdanov, A.; Schalk-Hihi, C.; Gustchina, A.; Tsang, M.; Weatherbee, J.; Wlodawer, A., *Structure* **1995,** 3, (6), 591-601.

(97) Zdanov, A.; Schalk-Hihi, C.; Wlodawer, A., *Protein Sci* **1996,** 5, (10), 1955-62.

(98) Walter, M. R.; Nagabhushan, T. L., *Biochemistry* **1995,** 34, (38), 12118-25.

(99) Windsor, W. T.; Syto, R.; Tsarbopoulos, A.; Zhang, R.; Durkin, J.; Baldwin, S.; Paliwal, S.; Mui, P. W.; Pramanik, B.; Trotta, P. P.; et al., *Biochemistry* **1993,** 32, (34), 8807-15.

(100) Bondoc, L. L., Jr.; Varnerin, J. P.; Tang, J. C., *Anal Biochem* **1997,** 246, (2), 234-8.

(101) Ho, A. S.; Liu, Y.; Khan, T. A.; Hsu, D. H.; Bazan, J. F.; Moore, K. W., *Proc Natl Acad Sci U S A* **1993,** 90, (23), 11267-71.

(102) Reineke, U.; Sabat, R.; Volk, H. D.; Schneider-Mergener, J., *Protein Sci* **1998,** 7, (4), 951-60.

(103) Tan, J. C.; Indelicato, S. R.; Narula, S. K.; Zavodny, P. J.; Chou, C. C., *Journal of Biological Chemistry* **1993,** 268, (28), 21053-21059.

(104) Malefyt, R. D.; Abrams, J.; Bennett, B.; Figdor, C. G.; Devries, J. E., *Journal of Experimental Medicine* **1991,** 174, (5), 1209-1220.

(105) Fiorentino, D. F.; Zlotnik, A.; Mosmann, T. R.; Howard, M.; O'Garra, A., *J Immunol* **1991,** 147, (11), 3815-22.

(106) Gazzinelli, R. T.; Oswald, I. P.; James, S. L.; Sher, A., *J Immunol* **1992,** 148, (6), 1792-6.

(107) Bogdan, C.; Vodovotz, Y.; Nathan, C., *J Exp Med* **1991,** 174, (6), 1549-55.

(108) Groux, H.; Bigler, M.; de Vries, J. E.; Roncarolo, M. G., *J Immunol* **1998,** 160, (7), 3188-93.

(109) Willems, F.; Marchant, A.; Delville, J. P.; Gerard, C.; Delvaux, A.; Velu, T.; de Boer, M.; Goldman, M., *Eur J Immunol* **1994,** 24, (4), 1007-9.

(110) Creery, W. D.; DiazMitoma, F.; Filion, L.; Kumar, A., *European Journal of Immunology* **1996,** 26, (6), 1273-1277.

(111) Asadullah, K.; Sabat, R.; Wiese, A.; Docke, W. D.; Volk, H. D.; Sterry, W., *Arch Dermatol Res* **1999,** 291, (12), 628-36.

(112) Romagnani, S., *J Clin Immunol* **1995,** 15, (3), 121-9.

(113) Malefyt, R. D.; Yssel, H.; Roncarolo, M. G.; Spits, H.; Devries, J. E., *Current Opinion in Immunology* **1992,** 4, (3), 314-320.

(114) Peguet-Navarro, J.; Moulon, C.; Caux, C.; Dalbiez-Gauthier, C.; Banchereau, J.; Schmitt, D., *Eur J Immunol* **1994,** 24, (4), 884-91.

(115) Qiu, H. B.; Chen, D. C.; Pan, J. Q.; Liu, D. W.; Ma, S., *Zhongguo Yao Li Xue Bao* **1999,** 20, (3), 271-5.

(116) Armstrong, L.; Jordan, N.; Millar, A., *Thorax* **1996,** 51, (2), 143-9.

(117) Takanaski, S.; Nonaka, R.; Xing, Z.; O'Byrne, P.; Dolovich, J.; Jordana, M., *J Exp Med* **1994,** 180, (2), 711-5.

(118) Cassatella, M. A.; Meda, L.; Gasperini, S.; Calzetti, F.; Bonora, S., *J Exp Med* **1994,** 179, (5), 1695-9.

(119) Thompson-Snipes, L.; Dhar, V.; Bond, M. W.; Mosmann, T. R.; Moore, K. W.; Rennick, D. M., *J Exp Med* **1991,** 173, (2), 507-10.

(120) Malefyt, R. D.; Yssel, H.; Devries, J. E., *Journal of Immunology* **1993,** 150, (11), 4754-4765.

(121) Malefyt, R. D.; Haanen, J.; Spits, H.; Roncarolo, M. G.; Tevelde, A.; Figdor, C.; Johnson, K.; Kastelein, R.; Yssel, H.; Devries, J. E., *Journal of Experimental Medicine* **1991,** 174, (4), 915-924.

(122) Carson, W. E.; Lindemann, M. J.; Baiocchi, R.; Linett, M.; Tan, J. C.; Chou, C. C.; Narula, S.; Caligiuri, M. A., *Blood* **1995,** 85, (12), 3577-85.

(123) Rousset, F.; Garcia, E.; Defrance, T.; Peronne, C.; Vezzio, N.; Hsu, D. H.; Kastelein, R.; Moore, K. W.; Banchereau, J., *Proc Natl Acad Sci U S A* **1992,** 89, (5), 1890-3.

(124) Defrance, T.; Vanbervliet, B.; Briere, F.; Durand, I.; Rousset, F.; Banchereau, J., *J Exp Med* **1992,** 175, (3), 671-82.

(125) Kuhn, R.; Lohler, J.; Rennick, D.; Rajewsky, K.; Muller, W., *Cell* **1993,** 75, (2), 263-74.

(126) Rennick, D. M.; Fort, M. M., *Am J Physiol-Gastr L* **2000,** 278, (6), G829-G833.

(127) Barbara, G.; Xing, Z.; Hogaboam, C. M.; Gauldie, J.; Collins, S. M., *Gut* **2000,** 46, (3), 344-9.

(128) Herfarth, H. H.; Mohanty, S. P.; Rath, H. C.; Tonkonogy, S.; Sartor, R. B., *Gut* **1996,** 39, (6), 836-45.

(129) Powrie, F.; Leach, M. W.; Mauze, S.; Caddle, L. B.; Coffman, R. L., *Int Immunol* **1993,** 5, (11), 1461-71.

(130) Rott, O.; Fleischer, B.; Cash, E., *Eur J Immunol* **1994,** 24, (6), 1434-40.

(131) Van Laethem, J. L.; Marchant, A.; Delvaux, A.; Goldman, M.; Robberecht, P.; Velu, T.; Deviere, J., *Gastroenterology* **1995,** 108, (6), 1917-22.

(132) Pennline, K. J.; Roque-Gaffney, E.; Monahan, M., *Clin Immunol Immunopathol* **1994,** 71, (2), 169-75.

(133) Gerard, C.; Bruyns, C.; Marchant, A.; Abramowicz, D.; Vandenabeele, P.; Delvaux, A.; Fiers, W.; Goldman, M.; Velu, T., *J Exp Med* **1993,** 177, (2), 547-50.

(134) Persson, S.; Mikulowska, A.; Narula, S.; O'Garra, A.; Holmdahl, R., *Scand J Immunol* **1996,** 44, (6), 607-14.

(135) Tanaka, Y.; Otsuka, T.; Hotokebuchi, T.; Miyahara, H.; Nakashima, H.; Kuga, S.; Nemoto, Y.; Niiro, H.; Niho, Y., *Inflamm Res* **1996,** 45, (6), 283-8.

(136) Matsuda, M.; Salazar, F.; Petersson, M.; Masucci, G.; Hansson, J.; Pisa, P.; Zhang, Q. J.; Masucci, M. G.; Kiessling, R., *J Exp Med* **1994,** 180, (6), 2371-6.

(137) Salazar-Onfray, F.; Charo, J.; Petersson, M.; Freland, S.; Noffz, G.; Qin, Z.; Blankenstein, T.; Ljunggren, H. G.; Kiessling, R., *J Immunol* **1997,** 159, (7), 3195-202.

(138) Salazar-Onfray, F.; Petersson, M.; Franksson, L.; Matsuda, M.; Blankenstein, T.; Karre, K.; Kiessling, R., *J Immunol* **1995,** 154, (12), 6291-8.

(139) Hagenbaugh, A.; Sharma, S.; Dubinett, S. M.; Wei, S. H.; Aranda, R.; Cheroutre, H.; Fowell, D. J.; Binder, S.; Tsao, B.; Locksley, R. M.; Moore, K. W.; Kronenberg, M., *J Exp Med* **1997,** 185, (12), 2101-10.

(140) Kundu, N.; Dorsey, R.; Jackson, M. J.; Guiterrez, P.; Wilson, K.; Fu, S.; Ramanujam, K.; Thomas, E.; Fulton, A. M., *Int J Cancer* **1998,** 76, (5), 713-9.

(141) Stearns, M. E.; Garcia, F. U.; Fudge, K.; Rhim, J.; Wang, M., *Clin Cancer Res* **1999,** 5, (3), 711-20.

(142) Huang, S.; Ullrich, S. E.; Bar-Eli, M., *J Interferon Cytokine Res* **1999,** 19, (7), 697-703.

(143) Huang, S.; Xie, K.; Bucana, C. D.; Ullrich, S. E.; Bar-Eli, M., *Clin Cancer Res* **1996,** 2, (12), 1969-79.

(144) Gerard, C. M.; Bruyns, C.; Delvaux, A.; Baudson, N.; Dargent, J. L.; Goldman, M.; Velu, T., *Hum Gene Ther* **1996,** 7, (1), 23-31.

(145) Kundu, N.; Fulton, A. M., *Cell Immunol* **1997,** 180, (1), 55-61.

(146) Puliti, M.; von Hunolstein, C.; Verwaerde, C.; Bistoni, F.; Orefici, G.; Tissi, L., *Infection and Immunity* **2002,** 70, (6), 2862-2868.

(147) Schopf, L. R.; Hoffmann, K. F.; Cheever, A. W.; Urban, J. F.; Wynn, T. A., *Journal of Immunology* **2002,** 168, (5), 2383-2392.

(148) Dummer, W.; Bastian, B. C.; Ernst, N.; Schanzle, C.; Schwaaf, A.; Brocker, E. B., *Int J Cancer* **1996,** 66, (5), 607-10.

(149) Kruger-Krasagakes, S.; Krasagakis, K.; Garbe, C.; Schmitt, E.; Huls, C.; Blankenstein, T.; Diamantstein, T., *Br J Cancer* **1994,** 70, (6), 1182-5.

(150) Yue, F. Y.; Dummer, R.; Geertsen, R.; Hofbauer, G.; Laine, E.; Manolio, S.; Burg, G., *Int J Cancer* **1997,** 71, (4), 630-7.

(151) Kim, J.; Modlin, R. L.; Moy, R. L.; Dubinett, S. M.; McHugh, T.; Nickoloff, B. J.; Uyemura, K., *J Immunol* **1995,** 155, (4), 2240-7.

(152) Smith, D. R.; Kunkel, S. L.; Burdick, M. D.; Wilke, C. A.; Orringer, M. B.; Whyte, R. I.; Strieter, R. M., *Am J Pathol* **1994,** 145, (1), 18-25.

(153) Blay, J. Y.; Burdin, N.; Rousset, F.; Lenoir, G.; Biron, P.; Philip, T.; Banchereau, J.; Favrot, M. C., *Blood* **1993,** 82, (7), 2169-74.

(154) Stasi, R.; Zinzani, L.; Galieni, P.; Lauta, V. M.; Damasio, E.; Dispensa, E.; Dammacco, F.; Tura, S.; Papa, G., *Cancer* **1994,** 74, (6), 1792-800.

(155) Cortes, J.; Kurzrock, R., *Leuk Lymphoma* **1997,** 26, (3-4), 251-9.

(156) Cortes, J. E.; Talpaz, M.; Cabanillas, F.; Seymour, J. F.; Kurzrock, R., *Blood* **1995,** 85, (9), 2516-20.

(157) Bohlen, H.; Kessler, M.; Sextro, M.; Diehl, V.; Tesch, H., *Ann Hematol* **2000,** 79, (3), 110-3.

(158) Vassilakopoulos, T. P.; Nadali, G.; Angelopoulou, M. K.; Siakantaris, M. P.; Dimopoulou, M. N.; Kontopidou, F. N.; Rassidakis, G. Z.; Doussis-Anagnostopoulou, I. A.; Hatzioannou, M.; Vaiopoulos, G.; Kittas, C.; Sarris, A. H.; Pizzolo, G.; Pangalis, G. A., *Haematologica* **2001,** 86, (3), 274-81.

(159) Fayad, L.; Keating, M. J.; Reuben, J. M.; O'Brien, S.; Lee, B. N.; Lerner, S.; Kurzrock, R., *Blood* **2001,** 97, (1), 256-63.

(160) Asadullah, K.; Gellrich, S.; Haeussler-Quade, A.; Friedrich, M.; Docke, W. D.; Jahn, S.; Sterry, W., *Exp Dermatol* **2000,** 9, (1), 71-6.

(161) Llorente, L.; Garcia-Padilla, C.; Richaud-Patin, Y.; Wijdenes, J.; Cardiel, M.; Alcocer-Varela, J.; Alarcon-Segovia, D.; Galanaud, P.; Emilie, D., *Arthritis and Rheumatism* **1998,** 41, (9), S109-S109.

(162) Llorente, L.; Zou, W. P.; Levy, Y.; Richaudpatin, Y.; Wijdenes, J.; Alcocervarela, J.; Morelfourrier, B.; Brouet, J. C.; Alarconsegovia, D.; Galanaud, P.; Emilie, D., *Journal of Experimental Medicine* **1995,** 181, (3), 839-844.

(163) Park, Y. B.; Lee, S. K.; Kim, D. S.; Lee, J.; Lee, C. H.; Song, C. H., *Clin Exp Rheumatol* **1998,** 16, (3), 283-288.

(164) Hasegawa, M.; Fujimoto, M.; Kikuchi, K.; Takehara, K., *J Rheumatol* **1997,** 24, (2), 328-32.

(165) Mussi, A.; Bonifati, C.; Carducci, M.; Viola, M.; Tomaselli, R.; Sacerdoti, G.; Fazio, M.; Ameglio, F., *J Biol Regul Homeost Agents* **1994,** 8, (4), 117-20.

(166) Nickoloff, B. J.; Fivenson, D. P.; Kunkel, S. L.; Strieter, R. M.; Turka, L. A., *Clin Immunol Immunopathol* **1994,** 73, (1), 63-8.

(167) Asadullah, K.; Docke, W. D.; Haeussler, A.; Sterry, W.; Volk, H. D., *J Invest Dermatol* **1996,** 107, (6), 833-7.

(168) Chung, F., *Mediat Inflamm* **2001,** 10, (2), 51-59.

(169) Lyons, A.; Kelly, J. L.; Rodrick, M. L.; Mannick, J. A.; Lederer, J. A., *Ann Surg* **1997,** 226, (4), 450-8; discussion 458-60.

(170) van Dissel, J. T.; van Langevelde, P.; Westendorp, R. G.; Kwappenberg, K.; Frolich, M., *Lancet* **1998,** 351, (9107), 950-3.

(171) Opal, S. M.; Huber, C. E., *Curr Opin Infect Dis* **2000,** 13, (3), 221-226.

(172) Volk, H. D.; Reinke, P.; Docke, W. D., *Chem Immunol* **2000,** 74, 162-77.

(173) Muehlstedt, S. G.; Lyte, M.; Rodriguez, J. L., *Shock* **2002,** 17, (6), 443-50.

(174) Spies, C. D.; Kern, H.; Schroder, T.; Sander, M.; Sepold, H.; Lang, P.; Stangl, K.; Behrens, S.; Sinha, P.; Schaffartzik, W.; Wernecke, K. D.; Kox, W. J.; Jain, U., *Anesth Analg* **2002,** 95, (1), 9-18, table of contents.

(175) Chernoff, A. E.; Granowitz, E. V.; Shapiro, L.; Vannier, E.; Lonnemann, G.; Angel, J. B.; Kennedy, J. S.; Rabson, A. R.; Wolff, S. M.; Dinarello, C. A., *J Immunol* **1995,** 154, (10), 5492-9.

(176) Huhn, R. D.; Radwanski, E.; O'Connell, S. M.; Sturgill, M. G.; Clarke, L.; Cody, R. P.; Affrime, M. B.; Cutler, D. L., *Blood* **1996,** 87, (2), 699-705.

(177) Huhn, R. D.; Radwanski, E.; Gallo, J.; Affrime, M. B.; Sabo, R.; Gonyo, G.; Monge, A.; Cutler, D. L., *Clin Pharmacol Ther* **1997,** 62, (2), 171-80.

(178) Wissing, K. M.; Morelon, E.; Legendre, C.; De Pauw, L.; LeBeaut, A.; Grint, P.; Maniscalki, M.; Ickx, B.; Vereerstraeten, P.; Chatenoud, L.; Kreis, H.; Goldman, M.; Abramowicz, D., *Transplantation* **1997,** 64, (7), 999-1006.

(179) Cooper, P. J.; Fekade, D.; Remick, D. G.; Grint, P.; Wherry, J.; Griffin, G. E., *J Infect Dis* **2000,** 181, (1), 203-9.

(180) van Deventer, S. J.; Elson, C. O.; Fedorak, R. N., *Gastroenterology* **1997,** 113, (2), 383-9.

(181) Colombel, J. F.; Rutgeerts, P.; Malchow, H.; Jacyna, M.; Nielsen, O. H.; Rask-Madsen, J.; Van Deventer, S.; Ferguson, A.; Desreumaux, P.; Forbes, A.; Geboes, K.; Melani, L.; Cohard, M., *Gut* **2001,** 49, (1), 42-6.

(182) Fedorak, R. N.; Gangl, A.; Elson, C. O.; Rutgeerts, P.; Schreiber, S.; Wild, G.; Hanauer, S. B.; Kilian, A.; Cohard, M.; LeBeaut, A.; Feagan, B., *Gastroenterology* **2000,** 119, (6), 1473-82.

(183) Maini, R. N.; Taylor, P. C., *Annu Rev Med* **2000,** 51, 207-29.

(184) Asadullah, K.; Docke, W. D.; Ebeling, M.; Friedrich, M.; Belbe, G.; Audring, H.; Volk, H. D.; Sterry, W., *Arch Dermatol* **1999,** 135, (2), 187-92.

(185) McHutchison, J. G.; Giannelli, G.; Nyberg, L.; Blatt, L. M.; Waite, K.; Mischkot, P.; Pianko, S.; Conrad, A.; Grint, P., *J Interferon Cytokine Res* **1999,** 19, (11), 1265-70.

(186) Dharancy, S.; Canva, V.; Gambiez, L.; Paris, J. C.; Desreumaux, P., *Gastroenterology* **2000,** 119, (5), 1411-2.

(187) Haag, R.; Kratz, F., *Angew Chem Int Ed Engl* **2006,** 45, (8), 1198-215.

(188) Schellekens, H., *Nat Rev Drug Discov* **2002,** 1, (6), 457-62.

(189) Schellekens, H., *Clin Ther* **2002,** 24, (11), 1720-40; discussion 1719.

(190) Nair, L. S.; Laurencin, C. T., *Adv Biochem Eng Biot* **2006,** 102, 47-90.

(191) Devalapally, H.; Chakilam, A.; Amiji, M. M., *J Pharm Sci* **2007,** 96, (10), 2547-65.

(192) Kim, S.; Kim, J. H.; Jeon, O.; Kwon, I. C.; Park, K., *Eur J Pharm Biopharm* **2009,** 71, (3), 420-30.

(193) Lukyanov, A. N.; Torchilin, V. P., *Adv Drug Deliv Rev* **2004,** 56, (9), 1273-89.

(194) Branco, M. C.; Schneider, J. P., *Acta Biomater* **2009,** 5, (3), 817-31.

(195) Nayak, S.; Lyon, L. A., *Angew Chem Int Ed Engl* **2005,** 44, (47), 7686-708.

(196) Murthy, N.; Thng, Y. X.; Schuck, S.; Xu, M. C.; Frechet, J. M., *J Am Chem Soc* **2002,** 124, (42), 12398-9.

(197) Murthy, N.; Xu, M.; Schuck, S.; Kunisawa, J.; Shastri, N.; Frechet, J. M., *Proc Natl Acad Sci U S A* **2003,** 100, (9), 4995-5000.

(198) Leonard, M.; De Boisseson, M. R.; Hubert, P.; Dalencon, F.; Dellacherie, E., *J Control Release* **2004,** 98, (3), 395-405.

(199) Tan, M. L.; Choong, P. F.; Dass, C. R., *Peptides* **2010,** 31, (1), 184-93.

(200) Griffith, L. G., *Acta Mater* **2000,** 48, (1), 263-277.

(201) Seal, B. L.; Otero, T. C.; Panitch, A., *Mat Sci Eng R* **2001,** 34, (4-5), 147-230.

(202) Angelova, N.; Hunkeler, D., *Trends Biotechnol* **1999,** 17, (10), 409-21.

(203) Murphy, W. L.; Mooney, D. J., *J Periodontal Res* **1999,** 34, (7), 413-419.

(204) Thanos, C. G.; Emerich, D. F., *Recent Pat Drug Deliv Formul* **2008,** 2, (1), 19-24.

(205) Marler, J. J.; Upton, J.; Langer, R.; Vacanti, J. P., *Adv Drug Deliver Rev* **1998,** 33, (1-2), 165-182.

(206) Lee, K. Y.; Mooney, D. J., *Chem Rev* **2001,** 101, (7), 1869-1879.

(207) Niklason, L. E., *Science* **1999,** 286, (5444), 1493-1494.

(208) Niklason, L. E.; Gao, J.; Abbott, W. M.; Hirschi, K. K.; Houser, S.; Marini, R.; Langer, R., *Science* **1999,** 284, (5413), 489-493.

(209) Oberpenning, F.; Meng, J.; Yoo, J. J.; Atala, A., *Nat Biotechnol* **1999,** 17, (2), 149-155.

(210) Pomahac, B.; Svensjo, T.; Yao, F.; Brown, H.; Eriksson, E., *Crit Rev Oral Biol M* **1998,** 9, (3), 333-344.

(211) Zhang, R. Y.; Ma, P. X., *Journal of Biomedical Materials Research* **1999,** 44, (4), 446-455.

(212) Lin, V. S.; Lee, M. C.; O'Neal, S.; McKean, J.; Sung, K. L. P., *Tissue Eng* **1999,** 5, (5), 443-451.

(213) Rosso, F.; Marino, G.; Giordano, A.; Barbarisi, M.; Parmeggiani, D.; Barbarisi, A., *J Cell Physiol* **2005,** 203, (3), 465-470.

(214) Peppas, N. A.; Bures, P.; Leobandung, W.; Ichikawa, H., *Eur J Pharm Biopharm* **2000,** 50, (1), 27-46.

(215) Pillai, O.; Panchagnula, R., *Curr Opin Chem Biol* **2001,** 5, (4), 447-451.

(216) Muggli, D. S.; Burkoth, A. K.; Anseth, K. S., *Journal of Biomedical Materials Research* **1999,** 46, (2), 271-278.

(217) Dang, W. B.; Daviau, T.; Ying, P.; Zhao, Y.; Nowotnik, D.; Clow, C. S.; Tyler, B.; Brem, H., *Journal of Controlled Release* **1996,** 42, (1), 83-92.

(218) Carvalho, J.; Moreira, S.; Maia, J.; Gama, F. M., *Journal of Biomedical Materials Research Part A* **2010,** 93A, (1), 389-399.

(219) Martens, P.; Holland, T.; Anseth, K. S., *Polymer* **2002,** 43, (23), 6093-6100.

(220) Maia, J.; Ferreira, L.; Carvalho, R.; Ramos, M. A.; Gil, M. H., *Polymer* **2005,** 46, (23), 9604-9614.

(221) Takezawa, T.; Takeuchi, T.; Nitani, A.; Takayama, Y.; Kino-Oka, M.; Taya, M.; Enosawa, S., *J Biotechnol* **2007,** 131, (1), 76-83.

(222) Kratz, F., *Journal of Controlled Release* **2008,** 132, (3), 171-183.

(223) Olsen, D.; Yang, C.; Bodo, M.; Chang, R.; Leigh, S.; Baez, J.; Carmichael, D.; Perala, M.; Hamalainen, E. R.; Jarvinen, M.; Polarek, J., *Adv Drug Deliv Rev* **2003,** 55, (12), 1547-67.

(224) Lee, K. Y.; Yuk, S. H., *Prog Polym Sci* **2007,** 32, (7), 669-697.

(225) Li, J.; Loh, X. J., *Adv Drug Deliv Rev* **2008,** 60, (9), 1000-17.

(226) Mehvar, R., *J Control Release* **2000,** 69, (1), 1-25.

(227) George, M.; Abraham, T. E., *J Control Release* **2006,** 114, (1), 1-14.

(228) Dev, A.; Mohan, J. C.; Sreeja, V.; Tamura, H.; Patzke, G. R.; Hussain, F.; Weyeneth, S.; Nair, S. V.; Jayakumar, R., *Carbohyd Polym* **2010,** 79, (4), 1073-1079.

(229) Sahoo, S.; Sasmal, A.; Nanda, R.; Phani, A. R.; Nayak, P. L., *Carbohyd Polym* **2010,** 79, (1), 106-113.

(230) Dailey, L. A.; Wittmar, M.; Kissel, T., *Journal of Controlled Release* **2005,** 101, (1-3), 137-149.

(231) Wischke, C.; Schwendeman, S. P., *International Journal of Pharmaceutics* **2008,** 364, (2), 298-327.

(232) Kumar, N.; Langer, R. S.; Domb, A. J., *Adv Drug Deliv Rev* **2002,** 54, (7), 889-910.

(233) Modi, S.; Jain, J. P.; Domb, A. J.; Kumar, N., *Eur J Pharm Biopharm* **2006,** 64, (3), 277-86.

(234) Lakshmi, S.; Katti, D. S.; Laurencin, C. T., *Adv Drug Deliv Rev* **2003,** 55, (4), 467-82.

(235) Huynh, T. T. N.; Padois, K.; Sonvico, F.; Rossi, A.; Zani, F.; Pirot, F.; Doury, J.; Falson, F., *European Journal of Pharmaceutics and Biopharmaceutics* **2010,** 74, (2), 255-264.

(236) Siepmann, J.; Peppas, N. A., *Adv Drug Deliv Rev* **2001,** 48, (2-3), 139-57.

(237) Prokopowicz, M., *Acta Biomater* **2009,** 5, (1), 193-207.

(238) Slowing, II; Vivero-Escoto, J. L.; Wu, C. W.; Lin, V. S., *Adv Drug Deliv Rev* **2008,** 60, (11), 1278-88.

(239) Wu, J. Y.; Liu, S. Q.; Heng, P. W.; Yang, Y. Y., *J Control Release* **2005,** 102, (2), 361-72.

(240) Pasut, G.; Veronese, F. M., *Adv Drug Deliv Rev* **2009,** 61, (13), 1177-88.

(241) Greenwald, R. B., *Journal of Controlled Release* **2001,** 74, (1-3), 159-171.

(242) Pasut, G.; Sergi, M.; Veronese, F. M., *Adv Drug Deliver Rev* **2008,** 60, (1), 69-78.

(243) Lammers, T., *Adv Drug Deliv Rev* **2010,** 62, (2), 203-30.

(244) Liu, X. M.; Miller, S. C.; Wang, D., *Adv Drug Deliv Rev* **2010,** 62, (2), 258-71.

(245) Duncan, R.; Vicent, M. J., *Adv Drug Deliver Rev* **2010,** 62, (2), 272-282.

(246) Hreczuk-Hirst, D.; Chicco, D.; German, L.; Duncan, R., *International Journal of Pharmaceutics* **2001,** 230, (1-2), 57-66.

(247) Frampton, J. E.; Plosker, G. L., *Drugs* **2003,** 63, (19), 2079-105.

(248) Hosie, K. B.; Kerr, D. J.; Gilbert, J. A.; Downes, M.; Lakin, G.; Pemberton, G.; Timms, K.; Young, A.; Stanley, A., *Eur J Surg Oncol* **2003,** 29, (3), 254-60.

(249) Torchilin, V. P., *Pharm Res* **2007,** 24, (1), 1-16.

(250) Hoare, T. R.; Kohane, D. S., *Polymer* **2008,** 49, (8), 1993-2007.

(251) van der Linden, H. J.; Herber, S.; Olthuis, W.; Bergveld, P., *Analyst* **2003,** 128, (4), 325-331.

(252) Jen, A. C.; Wake, M. C.; Mikos, A. G., *Biotechnol Bioeng* **1996,** 50, (4), 357-364.

(253) Bennett, S. L.; Melanson, D. A.; Torchiana, D. F.; Wiseman, D. M.; Sawhney, A. S., *J Cardiac Surg* **2003,** 18, (6), 494-499.

(254) Tanaka, Y.; Gong, J. P.; Osada, Y., *Prog Polym Sci* **2005,** 30, (1), 1-9.

(255) Varghese, S.; Elisseeff, J. H., *Adv Polym Sci* **2006**, 95-144.

(256) Sakiyama-Elbert, S. E.; Hubbell, J. A., *Ann Rev Mater Res* **2001,** 31, 183-201.

(257) Liu, Z.; Jiao, Y.; Wang, Y.; Zhou, C.; Zhang, Z., *Adv Drug Deliv Rev* **2008,** 60, (15), 1650-62.

(258) Jung, T.; Kamm, W.; Breitenbach, A.; Kaiserling, E.; Xiao, J. X.; Kissel, T., *Eur J Pharm Biopharm* **2000,** 50, (1), 147-60.

(259) Pinto Reis, C.; Neufeld, R. J.; Ribeiro, A. J.; Veiga, F., *Nanomedicine* **2006,** 2, (1), 8-21.

(260) Conçalves, C.; Pereira, P.; Gama, M., *Materials* **2010,** 3, 1420-1460.

(261) Hans, M. L.; Lowman, A. M., *Curr Opin Solid St M* **2002,** 6, (4), 319-327.

(262) Giudice, E. L.; Campbell, J. D., *Adv Drug Deliv Rev* **2006,** 58, (1), 68-89.

(263) Alpar, H. O.; Somavarapu, S.; Atuah, K. N.; Bramwell, V. W., *Adv Drug Deliv Rev* **2005,** 57, (3), 411-30.

(264) Soane, R. J.; Frier, M.; Perkins, A. C.; Jones, N. S.; Davis, S. S.; Illum, L., *Int J Pharm* **1999,** 178, (1), 55-65.

(265) Illum, L., *J Control Release* **2003,** 87, (1-3), 187-98.

(266) Norris, D. A.; Puri, N.; Sinko, P. J., *Adv Drug Deliv Rev* **1998,** 34, (2-3), 135-154.

(267) Lee, Y.; Nam, J. H.; Shin, H. C.; Byun, Y., *Circulation* **2001,** 104, (25), 3116-20.

(268) Lin, Y., Chen, CT., Liang, HF., Kulkarni, A. R., Lee, PW., Chen, CH., Sung, HW, *Nanotechnology* **2007,** 18, 105102-105113.

(269) Sonaje, K.; Lin, Y.-H.; Juang, J.-H.; Wey, S.-P.; Chen, C.-T.; H-W., S., *Biomaterials* **2009,** 30, 2329-2339.

(270) Soane, R. J.; Hinchcliffe, M.; Davis, S. S.; Illum, L., *Int J Pharm* **2001,** 217, (1-2), 183-91.

(271) Davis, S. S., *Adv Drug Deliv Rev* **2001,** 51, (1-3), 21-42.

(272) Illum, L.; Farraj, N. F.; Davis, S. S., *Pharm Res* **1994,** 11, (8), 1186-9.

(273) Illum, L.; Jabbal-Gill, I.; Hinchcliffe, M.; Fisher, A. N.; Davis, S. S., *Adv Drug Deliv Rev* **2001,** 51, (1-3), 81-96.

(274) Almeida, A. J.; Alpar, H. O., *J Drug Target* **1996,** 3, (6), 455-67.

(275) Amidi, M.; Romeijn, S. G.; Borchard, G.; Junginger, H. E.; Hennink, W. E.; Jiskoot, W., *J Control Release* **2006,** 111, (1-2), 107-16.

(276) Zhang, X.; Zhang, H.; Wu, Z.; Wang, Z.; Niu, H.; Li, C., *Eur J Pharm Biopharm* **2008,** 68, (3), 526-34.

(277) Wang, X.; Zheng, C.; Wu, Z.; Teng, D.; Zhang, X.; Wang, Z.; Li, C., *J Biomed Mater Res Part B: Appl Biomater B* **2009,** 88, 150-161.

(278) Miller, C. J.; McChesney, M.; Moore, P. F., *Lab Invest* **1992,** 67, (5), 628-34.

(279) Westerink, M. A.; Smithson, S. L.; Srivastava, N.; Blonder, J.; Coeshott, C.; Rosenthal, G. J., *Vaccine* **2001,** 20, (5-6), 711-23.

(280) Kohler, D., *Lung* **1990,** 168 Suppl, 677-84.

(281) Yamamoto, A., *Yakugaku Zasshi* **2001,** 121, (12), 929-48.

(282) Garcia-Contreras, L.; Morcol, T.; Bell, S. J.; Hickey, A. J., *AAPS PharmSci* **2003,** 5, (2), E9.

(283) Grenha, A.; Seijo, B.; Remunan-Lopez, C., *Eur J Pharm Sci* **2005,** 25, (4-5), 427-37.

(284) Asghar, L. F.; Chandran, S., *J Pharm Pharm Sci* **2006,** 9, (3), 327-38.

(285) Bayat, A.; Dorkoosh, F. A.; Dehpour, A. R.; Moezi, L.; Larijani, B.; Junginger, H. E.; Rafiee-Tehrani, M., *Int J Pharm* **2008,** 356, (1-2), 259-66.

(286) Shoseyov, O.; Shani, Z.; Levy, I., *Microbiol Mol Biol R* **2006,** 70, (2), 283-+.

(287) Boraston, A. B.; Bolam, D. N.; Gilbert, H. J.; Davies, G. J., *Biochem J* **2004,** 382, 769-781.

(288) Bolam, D. N.; Ciruela, A.; McQueen-Mason, S.; Simpson, P.; Williamson, M. P.; Rixon, J. E.; Boraston, A.; Hazlewood, G. P.; Gilbert, H. J., *Biochem J* **1998,** 331 (Pt 3), 775-81.

(289) Eriksson, J.; Malmsten, M.; Tiberg, F.; Callisen, T. H.; Damhus, T.; Johansen, K. S., *J Colloid Interf Sci* **2005,** 285, (1), 94-99.

(290) Henshaw, J.; Horne-Bitschy, A.; van Bueren, A. L.; Money, V. A.; Bolam, D. N.; Czjzek, M.; Ekborg, N. A.; Weiner, R. M.; Hutcheson, S. W.; Davies, G. J.; Boraston, A. B.; Gilbert, H. J., *J Biol Chem* **2006,** 281, (25), 17099-107.

(291) Cavaco-Paulo, A.; Morgado, J.; Andreaus, J.; Kilburn, D., *Enzyme Microb Tech* **1999,** 25, (8-9), 639-643.

(292) Fukuda, T.; Kato-Murai, M.; Kuroda, K.; Ueda, M.; Suye, S. I., *Appl Microbiol Biot* **2008,** 77, (6), 1225-1232.

(293) Levy, I.; Nussinovitch, A.; Shpigel, E.; Shoseyov, O., *Cellulose* **2002,** 9, (1), 91-98.

(294) Machado, J.; Araujo, A.; Pinto, R.; Gama, F. M., *Cellulose* **2009,** 16, (5), 817-824.

(295) Guerreiro, C. I.; Fontes, C. M.; Gama, M.; Domingues, L., *Protein Expr Purif* **2008,** 59, (1), 161-8.

(296) Kavoosi, M.; Creagh, A. L.; Kilburn, D. G.; Haynes, C. A., *Biotechnol Bioeng* **2007,** 98, (3), 599-610.

(297) Kavoosi, M.; Sanaie, N.; Dismer, F.; Hubbuch, J.; Kilburn, D. G.; Haynes, C. A., *J Chromatogr A* **2007,** 1160, (1-2), 137-149.

(298) Xu, Y.; Foong, F. C., *Journal of Biotechnology* **2008,** 135, (4), 319-325.

(299) Ramos, R.; Domingues, L.; Gama, M., *Protein Expr Purif* **2010,** 71, (1), 1-7.

(300) Filonova, L.; Gunnarsson, L. C.; Daniel, G.; Ohlin, M., *BMC Plant Biol* **2007,** 7, 54.

(301) Filonova, L.; Kallas, A. M.; Greffe, L.; Johansson, G.; Teeri, T. T.; Daniel, G., *Biomacromolecules* **2007,** 8, (1), 91-97.

(302) Ofir, K.; Berdichevsky, Y.; Benhar, I.; Azriel-Rosenfeld, R.; Larned, R.; Barak, Y.; Bayer, E. A.; Morag, E., *Proteomics* **2005,** 5, (7), 1806-1814.

(303) Yamada, K. M., *Journal of Biological Chemistry* **1991,** 266, (20), 12809-12812.

(304) Hubbell, J. A., *Curr Opin Biotech* **1999,** 10, (2), 123-129.

(305) Andrade, F. K.; Moreira, S. M.; Domingues, L.; Gama, F. M., *J Biomed Mater Res A* **2008,** 92, (1), 9-17.

(306) Hsu, S. H.; Chu, W. P.; Lin, Y. S.; Chiang, Y. L.; Chen, D. C.; Tsai, C. L., *J Biotechnol* **2004,** 111, (2), 143-54.

(307) Wang, T. W.; Wu, H. C.; Huang, Y. C.; Sun, J. S.; Lin, F. H., *J Biomed Mater Res B Appl Biomater* **2006,** 79, (2), 379-87.

(308) Andrade, F. K.; Costa, R.; Domingues, L.; Soares, R.; Gama, M., *Acta Biomater* **2010**.

(309) Tsigos, I.; Martinou, A.; Kafetzopoulos, D.; Bouriotis, V., *Trends Biotechnol* **2000,** 18, (7), 305-12.

(310) De Campos, A. M.; Sanchez, A.; Alonso, M. J., *International Journal of Pharmaceutics* **2001,** 224, (1-2), 159-168.

(311) Dodane, V.; Vilivalam, V. D., *Pharm Sci Technol To* **1998,** 1, (6), 246-253.

(312) Felt, O.; Buri, P.; Gurny, R., *Drug Dev Ind Pharm* **1998,** 24, (11), 979-993.

(313) Madihally, S. V.; Matthew, H. W. T., *Biomaterials* **1999,** 20, (12), 1133-1142.

(314) Koide, S. S., *Nutr Res* **1998,** 18, (6), 1091-1101.

(315) Boot, R. G.; Renkema, G. H.; Strijland, A.; Vanzonneveld, A. J.; Aerts, J. M. F. G., *Journal of Biological Chemistry* **1995,** 270, (44), 26252-26256.

(316) Renkema, G. H.; Boot, R. G.; Muijsers, A. O.; Donkerkoopman, W. E.; Aerts, J. M. F. G., *Journal of Biological Chemistry* **1995,** 270, (5), 2198-2202.

(317) Tjoelker, L. W.; Gosting, L.; Frey, S.; Hunter, C. L.; Le Trong, H.; Steiner, B.; Brammer, H.; Gray, P. M., *Journal of Biological Chemistry* **2000,** 275, (1), 514-520.

(318) Hollak, C. E. M.; Vanweely, S.; Vanoers, M. H. J.; Aerts, J. M. F. G., *Journal of Clinical Investigation* **1994,** 93, (3), 1288-1292.

(319) Renkema, G. H.; Boot, R. G.; Strijland, A.; DonkerKoopman, W. E.; vandenBerg, M.; Muijsers, A. O.; Aerts, J. M. F. G., *Eur J Biochem* **1997,** 244, (2), 279-285.

Chapter 2 | Development of strategies to functionalize chitin-based materials using a human chitin-binding module

Adapted from: *Molecular Biotechnology* (2008) **40**:269-279.

Biomaterials used for tissue engineering applications must provide a structural support for the tissue development and also actively interact with cells, promoting adhesion, proliferation and differentiation. To achieve this goal, adhesion molecules may be used, such as the tripeptide Arg-Gly-Asp (RGD). A method based on the use of a Carbohydrate-Binding Module, with affinity for chitin, was tested as an alternative approach to the chemical grafting of bioactive peptides. This approach would simultaneously allow the production of recombinant peptides (alternatively to peptide synthesis) and provide a simple way for the specific and strong adsorption of the peptides to the biomaterial.

A fusion recombinant protein, containing the RGD sequence fused to a human chitin-binding module (ChBM), was expressed in E. coli. The adhesion of fibroblasts to reacetylated chitosan (RC) films was the model system selected to analyse the properties of the obtained proteins. Thus, the evaluation of cell attachment and proliferation on polystyrene surfaces and reacetylated chitosan films, coated with the recombinant proteins, was performed using mouse embryo fibroblasts 3T3. The results show that the recombinant proteins affect negatively fibroblasts anchorage to the materials surface, inhibiting its adhesion and proliferation. We also conclude that this negative effect is fundamentally due to the human chitin-binding domain.

Introduction

Chitosan is a polycationic biopolymer obtained by the N-deacetylation of chitin [1]. This polymer exhibits a number of characteristics that makes it attractive for different applications, namely on the pharmaceutical industry [2-10]. Due to its biocompatibility, biodegradability and potential for formulation as flakes, membranes, sponges, fibres, gels or particles, it is considered as a very interesting polymer also for biomedical applications.

In the biomedical and pharmaceutical fields, chitosan has been used in the preparation of artificial skin, surgical sutures, contact lenses, blood dialysis membranes and artificial blood vessels, as antitumor, blood anticoagulant, antigastritis, haemostatic, hypocholesterolaemic and antithrombogenic agents, in drug- and gene-delivery systems and in dental therapy [1, 3, 6-9]. It also stimulates the immune system of the host against viral and bacterial infections [10].

The control of the physical, chemical and biochemical properties of an implant surface is one of the most important issues in the design of biomedical devices, since the first interaction between a foreign body (implant) and the biological environment occurs at the interface. Surfaces that mimic the natural extracellular matrix (ECM) are of great interest for tissue engineering and regenerative medicine [11, 12].

Several strategies may be employed to improve the cell adhesion, proliferation and differentiation on biomaterials, such as the reduction of unspecific protein adsorption, or the immobilization of adhesion molecules to ensure controlled interaction between cells and synthetic substrates [13-17]. Adhesion motifs are present in ECM molecules such as laminin, vitronectin and fibronectin. These proteins regulate the adhesion, migration and growth of cells by binding to integrin receptors located on the outer cellular membranes [18, 19].

The peptide Arg-Gly-Asp (RGD) was found to be the major functional amino acid sequence responsible for cellular adhesion. This sequence can be used to elicit specific cellular responses [20]. It has been extensively demonstrated that RGD sequence improves cell adhesion, spreading and proliferation in different materials [20-24].

The immobilization of fibronectin or RGD to the surface of a material can be achieved by different techniques [20] but most of these include complex chemical reactions and crosslinking processes, with low yields and often not successful [20, 25, 26]. An alternative method was developed, through the creation of fusion proteins containing carbohydrate-binding modules, to immobilize RGD on polysaccharide surfaces [21, 22]. In this work, the RGD peptide was fused with a human chitin-binding module by recombinant DNA technology.

A protein with homology to fungal, bacterial or plant chitinases has been identified in humans. This enzyme, later identified as a chitotriosidase, is expressed by macrophages and its activity is dramatically elevated in patients with Gaucher disease [27, 28]. The human chitin-binding module (ChBM) is comprised by the 72 C-terminal amino acids of the human chitinase [29].

In this study we examine: (1) the production of two active fusion proteins containing RGD and/or a human chitin-binding module (RGDChBM and ChBM, respectively); (2) the effect of ChBM and RGDChBM on cellular adhesion to polystyrene plate (selected as a model surface, where the recombinant proteins were allowed to adsorb); (3) the effect of the recombinant fusion proteins on fibroblasts cultures; and (4) the effect of the proteins on fibroblasts adhesion to reacetylated chitosan films.

Experimental

Reagents

All reagents used were of laboratory grade and purchased from Sigma-Aldrich (USA), unless stated otherwise.

Construction of the expression plasmids

The DNA encoding for the chitin-binding module of the human chitinase (ChBM) was synthesised by GenScript Corporation (USA) with optimized codons for bacterial expression.

The genic fusion RGDChBM was obtained by PCR using as template the DNA encoding for the ChBM. Briefly, the RGDChBM sequence was amplified using the forward primer 5'-CTT CCA TGG CC**A GAG GTG AT**C CGG AAC TGG AAG TGC C-3' (*Nco*I restriction site is underlined and RGD sequence is in bold) and the reverse primer 5'-CCA CTC GAG GTT CCA GGT GCA GCA TTT G-3' (the *Xho*I restrition site is underlined). The PCR was performed as follows: preheating at 98ºC for 30 seconds; 40 amplification cycles at 98ºC for 10 seconds, 70ºC for 30 seconds and 72ºC for 10 seconds; and a final elongation period of 10 minutes at 72ºC, using Phusion DNA Polymerase from Finnzymes (Finland) in a My Cycler™ Thermal Cycler (Bio-Rad, USA).

The PCR amplified product RGDChBM was digested with *Nco*I (Roche Diagnostics GmbH, Germany) and *Xho*I (Roche Diagnostics GmbH, Germany) and then cloned, using T4 DNA ligase (Promega, USA), into the *Nco*I and *Xho*I restriction sites of the expression vector pET25b(+) (Novagen, USA), yielding the recombinant expression vector pET25RGDChBM. The synthesised sequence encoding for the ChBM was also cloned in pET25b(+) vector using *Nco*I and *Xho*I restriction sites, yielding the pET25ChBM recombinant expression vector. The nucleotide sequences of the recombinant constructs were analyzed by dideoxy nucleotide sequencing to ensure the lack of errors.

Expression and purification of the recombinant proteins

Escherichia coli strain Tuner(DE3) (Novagen, USA), transformed with the recombinant expression vectors, was grown at 37ºC in minimal medium M9 supplemented with 100 μg/mL ampicillin to an $O.D._{260\ nm}$ of 0.4. Isopropyl-β-

D-thiogalactopyranoside (IPTG) was then added to a final concentration of 0.1 mM. The cells were harvested after 16 hours incubation at 30ºC by centrifugation (10 minutes at 10000 g) and the cell pellet was resuspended in buffer A (20 mM Tris-HCl, 500 mM NaCl, pH7.4 and 1 mM phenylmethylsulfonylfluoride). The cells were disrupted by sonication (Branson Sonifier; duty cycle 50%; output 5) on ice and the insoluble debris removed by centrifugation (30 minutes, 10000 g, 4ºC). Purification was made by immobilized metal ion affinity chromatography, using a HiTrap™ Chelating HP 5 mL column (GE Healthcare, UK), following the manufacturer instructions. For that purpose, imidazole was added to the soluble fraction of the lysate, to a final concentration of 40 mM, and the pH was adjusted to 7.4. After purification, proteins were dialysed against buffer A, filtered through a 0.22 μm Millipore membrane (to sterilize the proteins) and stored and conserved at -20ºC, until use. Concentration of the two proteins was estimated from the absorbance at 280 nm (ε_{ChBM} = 10345 M^{-1} cm^{-1} and $\varepsilon_{RGDChBM}$ =10345 M^{-1} cm^{-1}).

Proteins were analyzed by SDS-PAGE, using 15% (w/v) acrylamide gels. Staining was carried out with 0.05% (w/v) Coomassie brilliant blue.

ChBM and RGDChBM affinity assays

To evaluate the carbohydrate-binding activity of ChBM and RGDChBM, solid-phase binding assays were done using chitin or chitosan. These affinity assays were performed mixing 0.5 mL purified protein (0.5 mg/mL) with 100 mg of chitin or chitosan, followed by 2 hours incubation at 4ºC. Then, the mixture was centrifuged (10000 g, 10 minutes, 4ºC), the proteins in the supernantant (not bound to the polysaccharide) were collected and the proteins bound unspecifically were washed out with buffer A. The elution of the proteins bound specifically to chitin or chitosan was made using buffer A with 1% sodium dodecyl sulfate (SDS). Proteins that did not bind to chitin or chitosan were analyzed by 15% (w/v) SDS-PAGE acrylamide gel stained with 0.05% (w/v) Coomassie brilliant blue.

Cell cultivation and viability evaluation

Mouse embryo fibroblasts 3T3 (ATCC CCL-164) were grown in Dulbecco's modified Eagle's media (Sigma-Aldrich, USA) supplemented with 10% newborn calf serum (Invitrogen, UK) and 1 μg/mL penicillin/streptavidin (DMEM complete medium) at 37ºC in a 95% humidified air containing 5% CO_2. At confluency, 3T3 fibroblasts were harvested with 0.05% (w/v) trypsin-EDTA (Sigma-Aldrich, USA) and subcultivated in the same medium.

The viability of the 3T3 fibroblast cells was determined using 3-[4,5-dimethylthiazol-2-yl]-2,5-diphenyl tetrazolium bromide (MTT) assay (Sigma-Aldrich, USA). The MTT assay accurately measure the activity of living cells via mitochondrial dehydrogenase activity. Mitochondrial dehydrogenases of viable cells cleave the tetrazolium ring, yielding purple MTT formazon crystals that can be dissolved in DMSO, resulting in a purple solution that is spectrophotometrically measured. The increase in cell number results in an increase in absorbance. After 5 hours of MTT incubation with cells, the light absorbance at 570 nm was measured by an ELISA 96-well plate reader.

Effect of the recombinant fusion proteins on the adhesion of fibroblasts on polystyrene plates

The recombinant proteins were added to the wells (0.05 μg/well) of a 96-well polystyrene plate (Orange Scientific, Belgium) and left adsorbing overnight to the polystyrene, at 4ºC. Then, the unbound proteins were collected in order to estimate, by absorbance at 280 nm, the amount of proteins bound to the polystyrene wells. Finally, the wells were washed twice with PBS sterile solution. Fibroblasts were seeded in DMEM medium, with or without newborn calf serum, at a density of 2.5 x 10^3 cells/well or 5 x 10^3 cells/well, respectively and incubated at 37ºC, 5% CO_2. After one hour incubation, the wells were washed twice with sterile PBS solution to remove free cells and DMEM complete medium was added.

Light microscope observations and MTT assay were carried out at 1, 5, 24 and 48 hours after the cells seeding and the results compared to assays carried out with cells adherent to wells without adsorbed proteins.

In order to compare the effect of ChBM and RGDChBM on fibroblast adhesion to polystyrene wells to the effect of other RGD fused recombinant proteins, we tested four more recombinant proteins developed in our laboratory. Andrade *et al* [30] produced a fusion protein with RGD and a cellulose-binding module (RGDCBM) and Moreira *et al* [31] created a fusion protein with RGD and a starch-binding module (RGDSBM). The three carbohydrate-binding modules (ChBM, CBM and SBM) and the three RGD fusion proteins (RGDChBM, RGDCBM and RGDSBM), were tested as described above.

Cytocompatibility tests

To evaluate the direct cytotoxicity of the recombinant proteins towards fibroblasts, 4 x 10^3 cells/well were seeded in a 96-well polystyrene plate (Orange Scientific, Belgium) and incubated at 37ºC, 5% CO_2. After 5 hours, the wells were washed twice with sterile PBS solution, to remove floating cells, and the medium was replaced. Then, the MTT test was carried out to quantify the cells adherent to the wells. At that time, 0.02 mL sterilized protein solution (0.5 mg/mL) or buffer A was added to the wells and the cells incubated 37ºC, 5% CO_2. Cell proliferation and viability was followed by regular light microscope observations and by the MTT test. The results were compared to a control prepared with the same cell culture without the addition of proteins.

Live and Dead assay

After the first hour of cell adhesion, a test was performed to verify whether the cells were alive or dead. The LIVE/DEAD® Viability/Cytotoxicity Kit for mammalian cells (Invitrogen, UK) was used to determine cell viability. This

kit provides two-color fluorescence cell viability assay, based on the simultaneous determination of live and dead cells with two probes that measure intracellular esterase activity and plasma membrane integrity. In a few words, the proteins (1 mg/well) were let to absorb to the wells of a 6-well polystyrene plate (Orange Scientific, Belgium) overnight at 4ºC. After the unbound proteins were collected and the wells washed, the fibroblasts were seeded, 2 x 10^4 cells/well, in DMEM medium without serum and incubated at 37ºC, 5% CO_2, for one hour. Then, 100 μL of a solution of 2 μM calcein AM and 4 μM ethidium homodimer-1, in sterile PBS, were added to the wells, incubated for 30 to 45 minutes at 37ºC, 5% CO_2 and visualized in a fluorescence microscope with or without the culture medium, to see the condition of the cells attached to the polystyrene wells.

Effect of the recombinant proteins on the adhesion of fibroblasts on reacetylated chitosan films

Reacetylated chitosan (RC) films were obtained as follows: briefly, a 1 % chitosan (from crab shells, purchased from Sigma-Aldrich (USA)) solution in 0.2 mM acetic acid was made. The resulting solution was autoclaved (20 minutes, 121ºC, 1 atm) and 50 μL was added to each well of a 96-well polystyrene plate (Orange Scientific, Belgium). The plate was air-dried at room temperature. To obtain reacetylated films, 10 μL of acetic anhydride was added and further air-dried. The wells were then washed successively with PBS sterile solution.

The adhesion of fibroblasts on RC films was accessed as described previously for the polystyrene plates. Succinctly, proteins were let adsorbing to plates coated with RC films overnight, at 4ºC. Then, the unbound proteins were collected and the wells washed twice with PBS sterile solution. Fibroblasts, 5 x 10^3 cells/well, were seeded in DMEM without serum. After one hour incubation at 37ºC, 5% CO_2, non-adherent cells were washed and DMEM complete medium was added.

Light microscope observations and MTT assay were carried out at 1, 5, 24 and 48 hours after the cells were seeded and the results compared to cells adherent to control wells (wells without proteins and wells coated with RC films without proteins).

Results

Production of the recombinant proteins

The sequence encoding for the human chitin-binding module was used to obtain the genic fusion encoding for RGDChBM, by PCR. The two nucleotide sequences, ChBM and RGDChBM, were inserted in the *Nco*I and *Xho*I restriction sites of the expression vector pET25b(+). The pET25b(+) expression vector has a T7*lac* promotor and expresses a C-terminal hexa histidine tag fused with the recombinant proteins, allowing purification by immobilized metal ion affinity chromatography. It also contains a pelB leader sequence that targets the recombinant proteins produced to the periplasmic space. This pelB leader sequence is usually cleaved after the proteins are exported to the perisplasmic space. Figure 2.1 shows the amino acid sequences and relevant features of the two recombinant proteins produced.

As shown in Figure 2.2A, the two proteins were successfully expressed in *E. coli* Tuner(DE3), in the soluble fraction (Figure 2.2A-lanes 1), and almost completely purified from the *E. coli* contaminant proteins (Figure 2.2A-lanes 3). The bands seen in lane 3 (Figure 2.2A) correspond to the processed fusion protein RGDChBM (where the pelB leader sequence was cleaved) and to the unprocessed protein (where the pelB leader sequence was not cleaved), with a higher molecular weight. About 0.5 mg of the recombinant proteins were obtained from 1 liter of *E. coli* cultured in M9 minimal medium.

A

Met Ala Pro Glu Leu Glu Val Pro Lys Pro Gly Gln Pro Ser Glu Pro Glu His Gly

Pro Ser Pro Gly Gln Asp Thr Phe Cys Gln Gly Lys Ala Asp Gly Leu Tyr Pro Asn

Pro Arg Glu Arg Glu Arg Ser Ser Phe Tyr Ser Cys Ala Ala Gly Arg Leu Phe Gln

Gln Ser Cys Pro Thr Gly Leu Val Phe Ser Asn Ser Cys Lys Cys Cys Thr Trp Asn

Leu Glu Ile Lys Arg Ala Ser Gln Pro Glu Leu Ala Pro Glu Asp Pro Glu Asp Val

Glu **His His His His His His**

B

Met Ala **Arg Gly Asp** Pro Glu Leu Glu Val Pro Lys Pro Gly Gln Pro Ser Glu Pro

Glu His Gly Pro Ser Pro Gly Gln Asp Thr Phe Cys Gln Gly Lys Ala Asp Gly Leu

Tyr Pro Asn Pro Arg Glu Arg Glu Arg Ser Ser Phe Tyr Ser Cys Ala Ala Gly Arg

Leu Phe Gln Gln Ser Cys Pro Thr Gly Leu Val Phe Ser Asn Ser Cys Lys Cys Cys

Thr Trp Asn Leu Glu Ile Lys Arg Ala Ser Gln Pro Glu Leu Ala Pro Glu Asp Pro

Glu Asp Val Glu **His His His His His His**

Figure 2.1 – Amino acid sequence and relevant characteristics of (A) ChBM and (B) RGDChBM. Underlined are represented the 72 amino acids comprising the human chitin-binding module. In bold, the 6 histidine tag used for purification. Underlined and in bold is represented the RGD sequence.

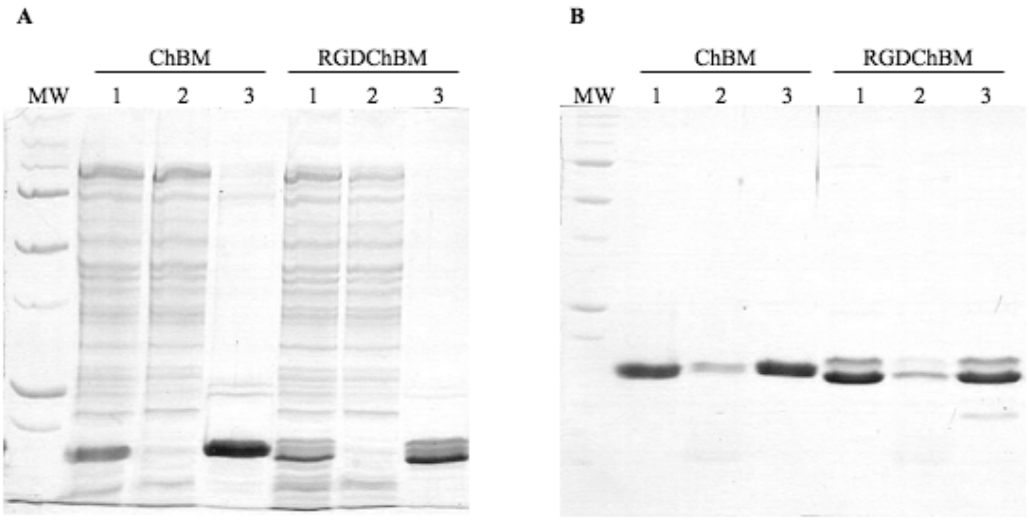

Figure 2.2 - (A) Protein expression and purification analysis by SDS-PAGE. MW – Molecular weight marker (250 kDa, 150 kDa, 100 kDa, 75 kDa, 50 kDa, 37 kDa, 25 kDa, 20 kDa, 15 kDa) from Bio-Rad (USA); 1 – Protein soluble lysate; 2 – Flowthrough fraction from HisTrapTM HP 5 mL column; 3 – Protein eluted with 300 mM Imidazole. (B) Binding activity and carbohydrate binding specificity of the recombinant proteins analysis by SDS-PAGE. MW – Molecular weight marker (250 kDa, 150 kDa, 100 kDa, 75 kDa, 50 kDa, 37 kDa, 25 kDa, 20 kDa, 15 kDa) from Bio-Rad (USA); 1 – Soluble protein before carbohydrate absorption; 2 – Protein fraction after adsorption to chitin; 3 – Protein fraction after adsorption to chitosan. The samples analyzed on lanes 2 and 3 are the supernantants (with non-adsorbed protein) obtained in the adsorption assays carried out respectively with chitin and chitosan.

Figure 2.2B shows the results of the affinity assays analyzed by SDS-PAGE. As it can be seen, there is almost no binding of the proteins to chitosan (Figure

2.2B-lanes 3) while the recombinant fusion proteins binds strongly to chitin (Figure 2.2B-lanes 2), indicating that the human chitin-binding module is functional, maintaining its affinity and specificity towards chitin.

Effect of the recombinant proteins on the adhesion of fibroblasts on polystyrene plates

Proteins were left adsorbing to polystyrene wells overnight, at 4ºC. The binding module used has specific affinity for chitin, but about 15% of the recombinant proteins absorbed (non-specifically) to the polystyrene wells. Although the final goal of the work is the binding of RGD peptides to partially reacetylated chitosan-made materials, polystyrene was used as a model material to analyze the interaction of the proteins with fibroblasts (selected as model animal cells). Although realizing there are major differences in the two assays (ChBMs adsorb strongly, specifically and with a specific orientation to chitin, as opposed to what happens in polystyrene), cell culture plates offer a convenient and simple way to observe the adsorption and morphology of cells. In Figure 2.3A, we can see light microscopy photographs of fibroblasts 1, 5, 24 and 48 hours after the cells were seeded, in DMEM complete medium. In Figure 2.3B and Figure 2.3C, the MTT absorbance results are shown for the assays with (Figure 2.3B) or without (Figure 2.3C) serum in the culture medium.

As it can be seen, the fibroblasts culture in control wells (without bound proteins or with Buffer A), with or without serum, behaves normally: the cells adhere one hour after seeding and proliferate, reaching confluency after 48 hours. In the wells coated with the recombinant proteins, the initial value of attached cells is very low as compared to the control and cells do not proliferate (as evaluated by the MTT assay), especially in the medium without serum (Figure 3.3C) where the absorbance values are lower. We can also see that the few adhered cells are still round, indicating a delay in adhesion and spreading.

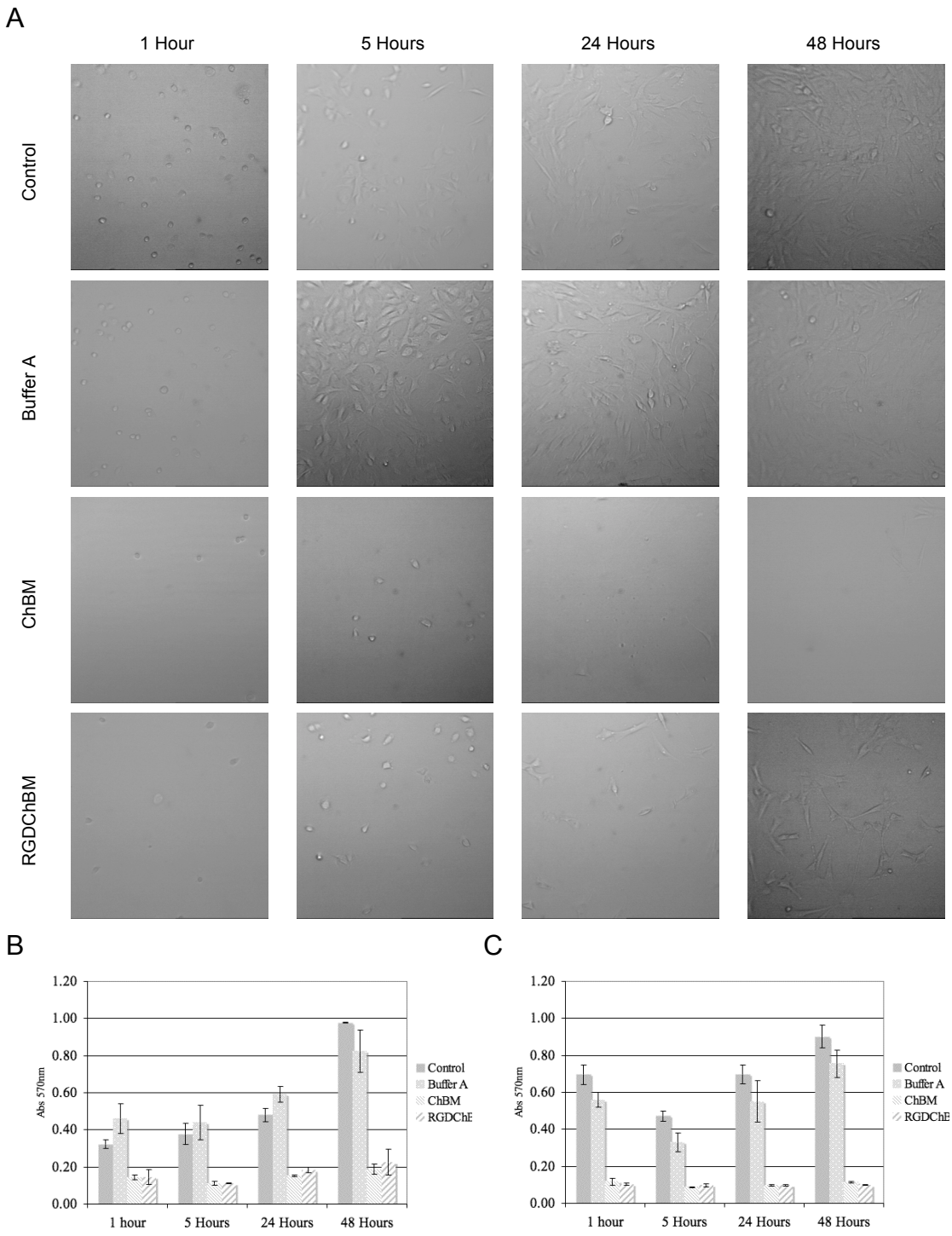

Figure 2.3 – Effect of the recombinant proteins coated on polystyrene wells. (A) Light microscope photographs 1 hour, 5 hours, 24 hours and 48 hours after cells were seeded, in DMEM complete medium, on polystyrene wells coated or not with the two recombinant proteins, ChBM, RGDChBM or with buffer A. MTT assay results after cell seeding, in (B) DMEM complete medium or in (C) DMEM without serum, on wells coated or not with ChBM, RGDChBM or buffer A.

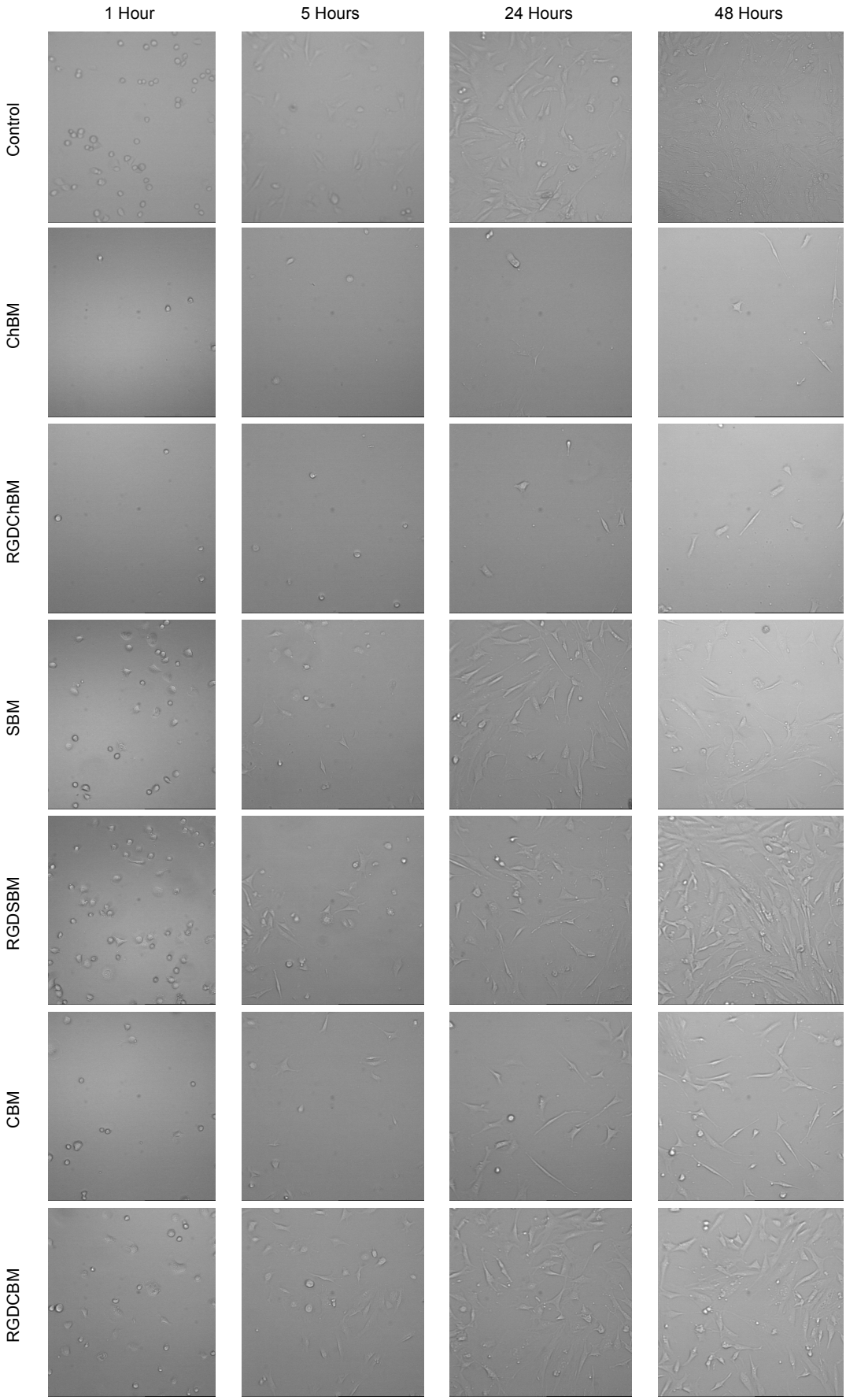

Figure 2.4 – Light microscope photographs 1 hour, 5 hours, 24 hours and 48 hours after cells were seeded, in DMEM complete medium, on polystyrene wells coated with the six recombinant proteins, ChBM, SBM, CBM, RGDChBM, RGDSBM and RGDCBM.

In Figure 2.4 we can see light microcopy photographs of fibroblasts seeded, in complete medium, on wells coated with the six different recombinant proteins ChBM, CBM, SBM, RGDChBM, RGDCBM and RGDSBM. The images clearly show that RGDSBM and RGDCBM improve cell adhesion and, on the contrary, the protein RGDChBM inhibits cell adhesion. Concerning the carbohydrate-binding modules (with no RGD bound), we can see that SBM and CBM neither improve nor hinder cell adhesion, taking as reference the effect of polystyrene plates on the fibroblasts adhesion. On the contrary, the ChBM does not allow the attachment of the cells.

Cytocompatibility tests

Considering the poor adhesion of fibroblasts on the polystyrene surface, we decided to analyze the cytotoxicity of the recombinant proteins under study. Figure 2.5A shows light microscopy photographs of fibroblasts 24, 48 hours and 6 days after the proteins were added to the cell cultures. In Figure 2.5B, the corresponding MTT assay results are presented.

As it can be observed, in the control wells, fibroblasts proliferated normally and neither cell death nor growth disorders were noticed; the cells have the typical fibroblast morphology, they are flattened and spread. After 48 hours, the cultures reached confluency, as expected.

In the wells where the proteins were added, the cells appear morphologically normal but there is a progressive decrease in the cell number, as compared to the controls. In the first 72 hours there is an increase of cell density (as measured by the MTT assay) almost comparable to the control, but, after 6 days, the number of cells is considerably lower than on the control. Although this effect is observed with both recombinant proteins, it seems that RGDChBM has a less negative effect on the cells.

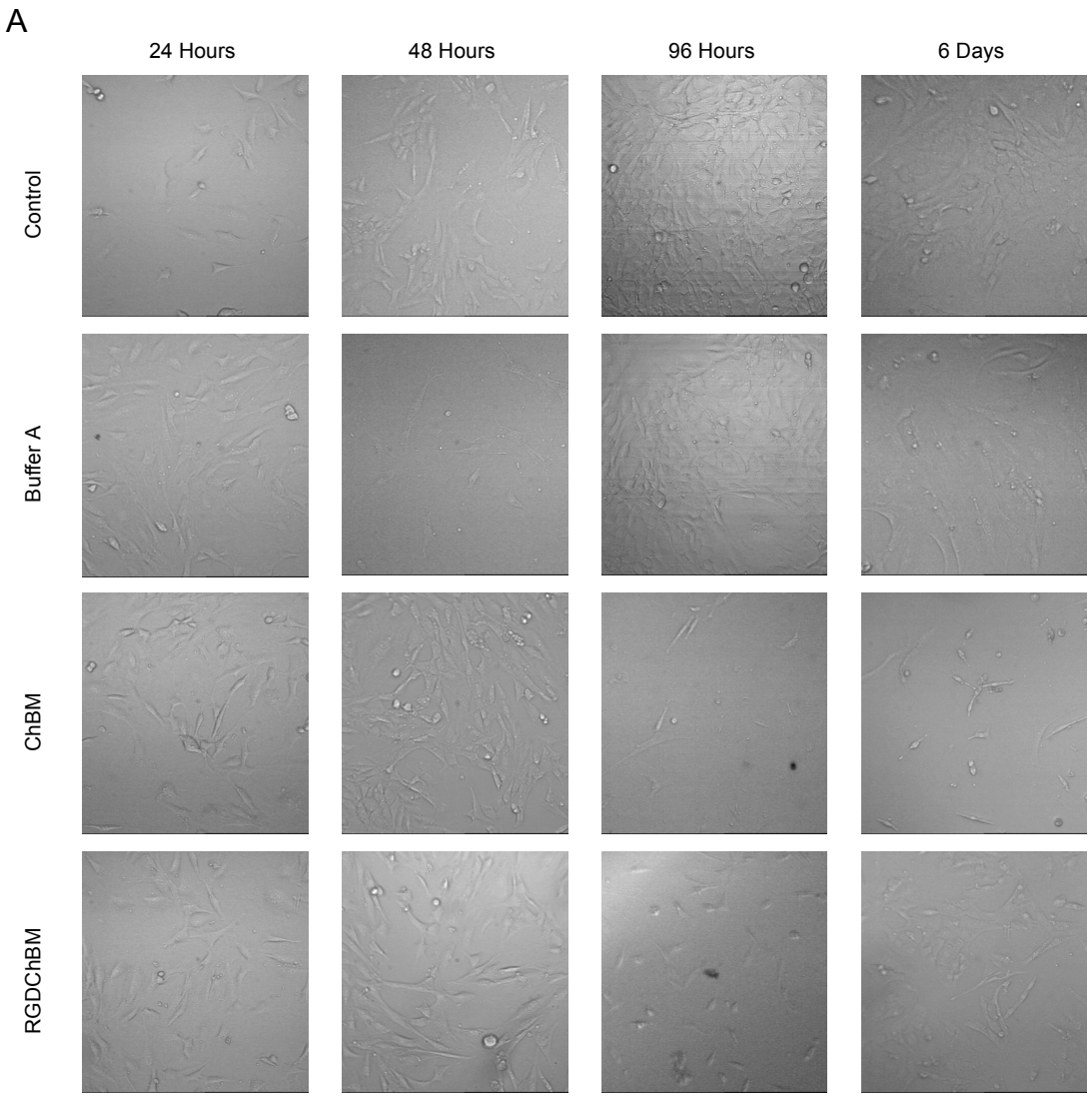

Figure 2.5 – Effect of the recombinant proteins on cultured fibroblasts. (A) Light microscope photographs 24 hours, 48 hours, 96 hours and 6 days after the recombinant proteins were added. (B) MTT absorbance results.

Live and Dead assay

In order to estimate the viability of the cells during the initial stage of the interaction with the proteins (first hour of adhesion), we performed the Live and Dead assay.

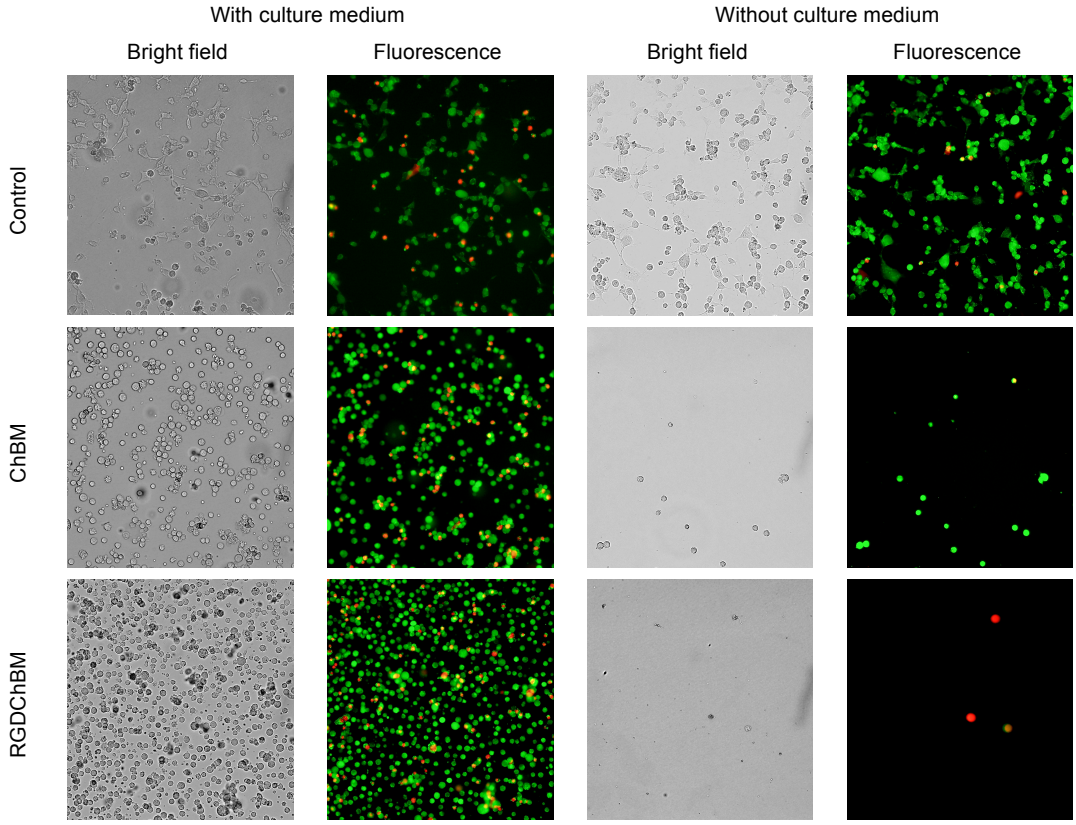

Figure 2.6 - Bright field and fluorescence photographs of fibroblasts with and without culture medium stained with LIVE/DEAD® Viability/Cytotoxicity Kit for mammalian cells. Live cells are stained in green and dead cells are stained in red.

In Figure 2.6, bright field and fluorescence images of the cells, in the presence and absence of culture medium, are shown. The presence of the culture medium is relevant to distinguish between cells in suspension and cells actually adhered to the wells. It can be seen that, in control wells (not coated with proteins) there is almost no alteration in the number of cells before and after the culture medium was discarded. Thus, the cells started adhering and spreading and the number of living cells (stained in green) is far superior to the number of dead cells (stained in red). In the wells coated with ChBM and

RGDChBM, the situation is rather different: a large number of round, not attached, cells can be observed; when the culture medium is discarded, most of these cells are also removed. It can also be noticed that some of the cells that remain adherent to the coated wells are turning red, meaning they are dying.

Effect of the recombinant fusion proteins on the adhesion of fibroblasts on reacetylated chitosan films

To evaluate the effects of the recombinant proteins on the adhesion of fibroblasts to reacetylated chitosan (RC) films, proteins were left adsorbing overnight at 4ºC. Polystyrene wells and RC films without adhered proteins were used as controls in these assays. Figure 2.7 presents the MTT absorbance values.

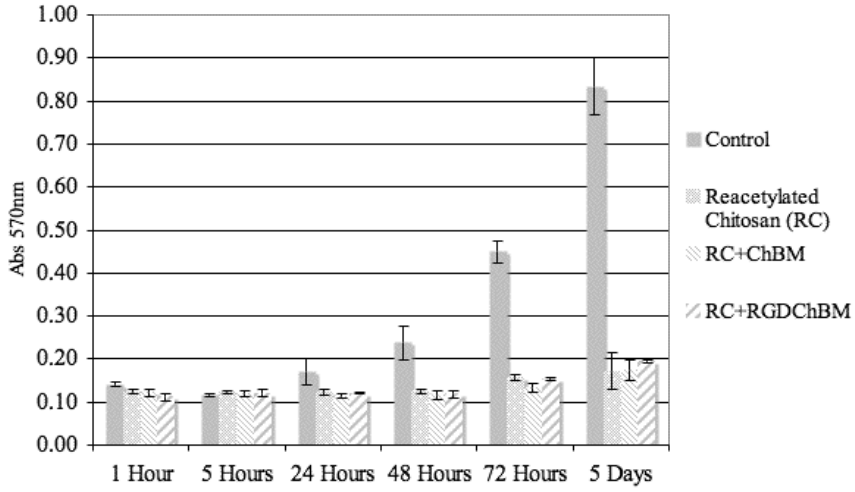

Figure 2.7 - MTT assay results after fibroblast seeding, in DMEM without serum, on wells coated with chitosan films, reacetylated chitosan (RC) films, RC films with linked ChBM and RC with linked RGDChBM.

In the first 24 hours, similar absorbance values were obtained in the different wells. After longer incubation times, only the cells cultivated on polystyrene wells, without recombinant proteins, proliferated significantly. In the wells coated with RC films, either with or without proteins, there is no significant increase in cell number. The few attached cells to these wells were always

round, meaning there were not strongly attached. Thus, it seems that the recombinant fusion protein, RGDChBM does not improve fibroblast adhesion to the RC films.

Discussion

The sequence encoding for the human chitin-binding module was used to obtain a fusion protein, RGDChBM. The proteins ChBM and RGDChBM were successfully expressed in *E. coli* Tuner(DE3) (Figure 2.2A), fused at the C-terminal to a hexa-histidine tag that allowed the purification using a nickel column (Figure 2.2B).

The affinity assays performed (Figure 2.3), showed that the human chitin-binding modules present in the recombinant proteins were active, binding specifically to chitin. We also found that the recombinant proteins were only eluted from chitin using harsh conditions, such as 1% SDS (data not shown) [32], indicating a strong interaction between the fusion proteins and chitin, as already stated by Tjoelker and coworkers [29]. This ability to bind strongly and specifically to chitin can also be used to successfully purify the recombinant proteins produced. Some authors have already shown that the chitin-binding module can be used as a affinity tag to purify fusion proteins expressed in different microorganisms [33-35]. Even though 1% SDS was used to elute the proteins from chitin, the specificity and ability of the recovered protein to bind to chitin was maintained (data not shown) [32].

Cell-surface interaction is very important on cell adhesion and growth, both microtopography and the surface chemistry influencing the cell-surface interactions. In a serum-containing medium, it is likely that the surface become covered with adsorbed proteins, with adhesion molecules, enhancing cell attachment.

By coating wells with the recombinant fusion protein we were expecting to provide a supply of adhesion molecules, in this case RGD, to the growing fibroblast culture in DMEM without serum, allowing its normal adhesion or

even improving it. Other authors were able to improve the adhesion of cells to different biomedical materials, by coating them with fusion proteins containing carbohydrate-binding modules and RGD sequences. In 1995, Wizerba *et al* [36] described a fusion protein between a RGD and a cellulose-binding domain (CBD) from the *Cellulomonas fimi* endoglucanase A (CenA) that promoted the attachment of green monkey Vero cell to polystyrene and cellulose acetate. Wang and coworkers [22], used a self-designed bifunctional RGD-containing fusion protein (BFP) made of two GRGDS sequences separately fused to the C-terminus and N-terminus of the *Trichoderma koningii* cellobiohydrolase I gene cellulose-binding domain. This BFP, grafted on the Petri dish, improved human keratinocytes and dermal fibroblasts adhesion.

In our laboratory, two different fusion proteins containing carbohydrate-binding modules and RGD sequences were tested. Andrade *et al* [30] tested a recombinant fusion protein (RGDCBM) between RGD and cellulose-binding module from the cellulosome of the bacteria *Clostridium termocellum* and Moreira *et al* [31] developed a fusion protein, containing a C-terminal starch binding module (SBM), from an α-amylase from *Bacillus* sp. TS-23 and an N-terminal RGD sequence (RGDSBM). Comparing to the control wells, the images obtained in the work show (Figure 2.4) that CBM and SBM have no significant effect on fibroblast adhesion; ChBM, on the other hand, seems to inhibit cell adhesion. We can also notice that RGDCBM and RGDSBM really improve cell adhesion and proliferation, while RGDChBM has the contrary effect. In fact, as can be seen in Figures 2.3, 2.4 and 2.6, it seems that the recombinant proteins, ChBM and RGDChBM inhibits cellular adhesion to the wells, regardless the presence of RGD sequence.

Chitosan is a biocompatible polymer. It was already shown that chitosan-based materials do not elicit allergic reactions after implantation, injection or topical application in the human body. Chitosan is commonly obtained by the N-deacetylation of chitin. The degree of acetylation (DA) of chitosan represents the proportion of N-acetyl-D-glucosamine units relatively to the total number of units. This is a structural parameter that influences several physicochemical and biological properties. DA exerts influence in cell

adhesion and proliferation, but does not change the cytocompatibility of chitosan [37]. Some authors have already studied the influence of chitosan DA on human fibroblast [38], keratinocytes [37] and chick dorsal root ganglion (DRG) neurons [39]. These authors conclude that, for some cell lines, cell viability and adhesion decrease as DA increases. Chatelet *et al* [37] also shows that, whatever their DA, fibroblasts do not proliferate in chitosan, because they adhere very strongly to the material, interacting in a way that would inhibit their growth.

It is predictable that fibroblasts would adhere poorly to RC films, as our results also shows. In Figure 2.6 it is visible that the number of cells adhered to RC films is very low and that this number does not increase over time. By using proteins that specifically and strongly bind to chitin we were aiming to improve the fibroblast adhesion and proliferation in RC films. ChBM could be used to modify chitosan with different DA, addressing fused bioactive peptides, such as RGD (tested in this work), to the surface of the biomaterial. Stable binding of RGD peptides to a surface is essential to promote strong cell adhesion that is fundamental for fibroblast growth. It is already known that simple adsorption can lead to poor cell attachment. However, RGDChBM do not seem to improve significantly cell adhesion to the RC films. In RC films with and without proteins, the cells (photographs not shown) show comparable morphology to the cells adhered to polystyrene wells coated with the recombinant proteins (Figs. 2.3 and 2.4): they are very few, round and do not proliferate. It is not clear why ChBM, a chitin-binding module present in the human chitinase whose cDNA is the sixth transcript found in macrophages [29], exhibits this surprising ability to inhibit fibroblast adhesion. Given its pI of about 6, its small size (72 amino acids) and amino acid composition, it would not be expected that ChBM had this kind of effect on the animal cells used. The reason for this effect is not clear at this stage.

Conclusions

Two recombinant proteins, containing a human chitin-binding module, were successfully expressed soluble and active in *E. coli*. These proteins were purified and used to test its effect on fibroblast adhesion. The recombinant ChBM affect negatively the fibroblasts adhesion. In the presence of ChBM and RGDChBM cells do not attach to surface of the biomaterials or seem to stop growing. It was already demonstrated that RGD sequences fused with carbohydrate-binding modules improve fibroblast adhesion to biomaterials, so it looks like, the chitin-binding module, fused or not with RGD peptide, interferes with the anchorage of the cells, fundamental to cell survival, cell division and proliferation.

References

(1) Tsigos, I.; Martinou, A.; Kafetzopoulos, D.; Bouriotis, V., *Trends Biotechnol* **2000,** 18, (7), 305-312.

(2) Hirano, S., *Biotechnol Annu Rev* **1996,** 2, 237-58.

(3) Dodane, V.; Vilivalam, V. D., *Pharm Sci Technol To* **1998,** 1, (6), 246-253.

(4) Shahidi, F.; Arachchi, J. K. V.; Jeon, Y. J., *Trends Food Sci Tech* **1999,** 10, (2), 37-51.

(5) Illum, L.; Farraj, N. F.; Davis, S. S., *Pharmaceut Res* **1994,** 11, (8), 1186-1189.

(6) Felt, O.; Buri, P.; Gurny, R., *Drug Dev Ind Pharm* **1998,** 24, (11), 979-993.

(7) Madihally, S. V.; Matthew, H. W. T., *Biomaterials* **1999,** 20, (12), 1133-1142.

(8) Shigemasa, Y.; Minami, S., *Biotechnol Genet Eng Rev* **1996,** 13, 383-420.

(9) Koide, S. S., *Nutr Res* **1998,** 18, (6), 1091-1101.

(10) Peluso, G.; Petillo, O.; Ranieri, M.; Santin, M.; Ambrosio, L.; Calabro, D.; Avallone, B.; Balsamo, G., *Biomaterials* **1994,** 15, (15), 1215-1220.

(11) Stevens, M. M.; George, J. H., *Science* **2005,** 310, (5751), 1135-1138.

(12) Lutolf, M. P.; Hubbell, J. A., *Nat Biotechnol* **2005,** 23, (1), 47-55.

(13) Sakiyama-Elbert, S. E.; Hubbell, J. A., *Ann Rev Mater Res* **2001,** 31, 183-201.

(14) Hubbell, J. A., *Curr Opin Biotech* **1999,** 10, (2), 123-129.

(15) Elbert, D. L.; Hubbell, J. A., *Annu Rev Mater Sci* **1996,** 26, 365-394.

(16) Hubbell, J. A., *Bio-Technol* **1995,** 13, (6), 565-576.

(17) Ikada, Y., *Biomaterials* **1994,** 15, (10), 725-736.

(18) Plow, E. F.; Haas, T. K.; Zhang, L.; Loftus, J.; Smith, J. W., *J Biol Chem* **2000,** 275, (29), 21785-21788.

(19) van der Flier, A.; Sonnenberg, A., *Cell Tissue Res* **2001,** 305, (3), 285-298.

(20) Hersel, U.; Dahmen, C.; Kessler, H., *Biomaterials* **2003,** 24, (24), 4385-4415.

(21) Hsu, S. H.; Chu, W. P.; Lin, Y. S.; Chiang, Y. L.; Chen, D. C. H.; Tsai, C. L., *J Biotechnol* **2004,** 111, (2), 143-154.

(22) Wang, T. W.; Wu, H. C.; Huang, Y. C.; Sun, J. S.; Lin, F. H., *J Biomed Mater Res B* **2006,** 79B, (2), 379-387.

(23) Yang, F.; Williams, C. G.; Wang, D. A.; Lee, H.; Manson, P. N.; Elisseeff, J., *Biomaterials* **2005,** 26, (30), 5991-5998.

(24) Levesque, S. G.; Shoichet, M. S., *Biomaterials* **2006,** 27, (30), 5277-5285.

(25) Ugarova, T. P.; Zamarron, C.; Veklich, Y.; Bowditch, R. D.; Ginsberg, M. H.; Weisel, J. W.; Plow, E. F., *Biochemistry-Us* **1995,** 34, (13), 4457-4466.

(26) Chiba, M.; Malik, S. W.; Specks, U., *J Immunol Methods* **1996,** 191, (1), 55-63.

(27) Renkema, G. H.; Boot, R. G.; Muijsers, A. O.; Donkerkoopman, W. E.; Aerts, J. M. F. G., *J Biol Chem* **1995,** 270, (5), 2198-2202.

(28) Boot, R. G.; Renkema, G. H.; Verhoek, M.; Strijland, A.; Bliek, J.; de Meulemeester, T. M. A. M. O.; Mannens, M. M. A. M.; Aerts, J. M. F. G., *J Biol Chem* **1998,** 273, (40), 25680-25685.

(29) Tjoelker, L. W.; Gosting, L.; Frey, S.; Hunter, C. L.; Le Trong, H.; Steiner, B.; Brammer, H.; Gray, P. M., *J Biol Chem* **2000,** 275, (1), 514-520.

(30) Andrade, F. K.; Moreira, S. M.; Domingues, L.; Gama, F. M., *J Biomed Mater Res A* **2010,** 92, (1), 9-17.

(31) Moreira, S. M.; Andrade, F. K.; Domingues, L.; Gama, M., *BMC Biotechnol* **2008,** 8, 78.

(32) Carvalho, V.; Gama, M.; Domingues, L., *J Biotechnol* **2007,** 131, (2), S255-S255.

(33) Chong, S. R.; Mersha, F. B.; Comb, D. G.; Scott, M. E.; Landry, D.; Vence, L. M.; Perler, F. B.; Benner, J.; Kucera, R. B.; Hirvonen, C. A.; Pelletier, J. J.; Paulus, H.; Xu, M. Q., *Gene* **1997,** 192, (2), 271-281.

(34) Babu, K. S.; Antony, A.; Muthukumaran, T.; Meenakshisundaram, S., *Protein Expres Purif* **2008,** 57, (2), 201-205.

(35) Khatuntseva, S. A.; Eldarov, M. A.; Redo, V. A.; Skryabin, K. G., *J Biotechnol* **2008,** 133, (1), 123-126.

(36) Wierzba, A.; Reichl, U.; Turner, R. F. B.; Warren, R. A. J.; Kilburn, D. G., *Biotechnol Bioeng* **1995,** 46, (3), 185-193.

(37) Chatelet, C.; Damour, O.; Domard, A., *Biomaterials* **2001,** 22, (3), 261-268.

(38) Hamilton, V.; Yuan, Y.; Rigney, D. A.; Puckett, A. D.; Ong, J. L.; Yang, Y.; Elder, S. H.; Bumgardner, J. D., *J Mater Sci-Mater M* **2006,** 17, (12), 1373-1381.

(39) Freier, T.; Koh, H. S.; Kazazian, K.; Shoichet, M. S., *Biomaterials* **2005,** 26, (29), 5872-5878.

Chapter 3 | Preliminary studies on dextrin nanogels as an IL-10 carrier system

Adapted from: *International Journal of Pharmaceuticals* (2010) **400**:234-242

Interleukin-10 (IL-10) is an anti-inflammatory cytokine, which active form is a non-covalent homodimer with two intramolecular disulphide bonds essential for its biological activity. A mutated form of murine IL-10 was successfully expressed in E. coli, recovered and purified from inclusion bodies. Its ability to reduce tumor necrosis factor α synthesis and down-regulate class II major histocompatibility complex molecules expression on endotoxin-stimulated bone marrow-derived macrophages was confirmed, and shown to be similar to that of a commercially available IL-10. Given the potential of IL-10 for application in various medical conditions, it is essential to develop systems that can effectively deliver the protein. In this work it is shown that a dextrin nanogel effectively incorporated IL-10, stabilized, and enabled the slow release of biologically active IL-10 over time. Altogether, these results demonstrate the suitability of dextrin nanogel to be used as a system for the controlled release of IL-10.

Introduction

Interleukin-10 (IL-10) is produced by various cell types including T and B cells, monocytes, and macrophages [1, 2]. This cytokine is highly pleiotropic in its biological activity that includes: inhibition of the synthesis of several cytokines, including IL-1, IL-2, IL-3, IL-6, IL-8, IL-12, tumor necrosis factor α (TNF-α), and interferon γ (IFN-γ) [3]; immunosuppressive effects on monocytes/macrophages [4-6]; as well as immunostimulatory activity on a broad range of cells types, including T cells [7], B cells [8], and mast cells. Furthermore, IL-10 down-regulates constitutive and IFN-γ- or IL-4-induced class II major histocompatibility complex (MHC-II) molecules expression on monocytes, dendritic cells, and Langerhans cells [9, 10] as well as adhesion and co-stimulatory molecules on antigen-presenting cells (APCs) [11, 12] and, suppresses the release of reactive oxygen intermediates [4, 6]. IL-10 conditioned APC may also promote the differentiation of counter-inflammatory regulatory T cells [13, 14]. IL-10 has thus a strong anti-inflammatory activity and may act as a general suppressor factor of immune responses. Due to its immunoregulatory properties, this cytokine has been proposed to be used in several clinical applications [15].

Interleukin-10 pleiotropic activities are conveyed to cells by a high-affinity interaction with its cell surface receptor (IL-10R). The IL-10R is a member of the class 2 cytokine receptor family and is composed of at least two subunits, IL-10R1 and IL-10R2, which are members of the interferon receptor family [1, 2]. The interaction of IL-10 with IL-10R seems to be highly complex [15] and the receptor neutralization blocks IL-10 activity [1].

IL-10 DNA sequence from different species is highly conserved and contains an open reading frame encoding for a secreted polypeptide of about 178 amino acids, with an N-terminal hydrophobic leader sequence of 18 amino acids, with well conserved domains [1]. Biologically active IL-10 has been

shown to exist in solution predominantly as a non-covalent symmetric homodimer [16, 17]. Human IL-10 is composed of two polypeptide chains of 160 amino acids each. The very similar murine IL-10 consists of 157 amino acids and presents a 73% overall sequence identity with the human IL-10. Biophysical characterization of the human and murine IL-10 [18, 19] showed the presence of two disulfide bonds that link the first to the third and the second to the fourth cysteine residues, bonds that are essential to the biological activity of the protein [1, 2, 15, 16, 20]. The murine IL-10 also revealed a fifth cysteine that exists as a free sulfhydryl [18]. Rat IL-10 has a 83% identity with murine IL-10, including the existence of a fifth unpaired cysteine, and it has been shown [21] that, due to the high reactivity of the fifth unpaired cysteine, rat IL-10 produced from the native sequence presents a severely reduced biological activity. The same work [21] showed that a mutated form of rat IL-10, where the fifth unpaired cysteine at position 149 was substituted with tyrosine, possesses the full biological activity of the native physiological rat IL-10 homodimer.

As already stated, cytokines, like IL-10, have attracted great attention due to their potential application in various medical fields, such as: vaccines [22], allergies [23], infectious diseases [24], acute inflammatory diseases [15], etc. Normally, proteins are expensive to produce on a large scale, are easily denatured loosing their bioactivity, and have a quite short half-life *in vivo*. So, it is essential to develop new delivery systems that allow efficient therapeutic effects at a minimum dosage. A promising method is the encapsulation using polymeric nanohydrogels or nanogels (also called polymeric or macromolecular micelles), which, by trapping the proteins in a hydrated polymer-network, minimizing denaturation, and enabling slow-release, while maintaining an effective concentration for the necessary period of time [25-28].

Dextrin is a very promising biomaterial, available in medical grade and accepted by the United States Food and Drug Administration (FDA) [29, 30] for human application. In previous work, we have developed and characterized a nanogel obtained by self-assembling of hydrophobized dextrin [31, 32]. The nanogel obtained have high colloidal stability and spherical shape. Size

distribution, obtained by dynamic light scattering, showed two distinct populations, with 25 and 150 nm, the former being the predominant one. *In vitro* studies, by Gonçalves *et al.*, showed that dextrin nanogel is non-toxic and does not elicit a reactive response when in contact with macrophages [33]. Therefore, the dextrin nanogel presents itself as a promising carrier for IL-10.

This work describes: (1) the expression in *E. coli* and purification of a mutated murine IL-10 form (rIL-10). In this mutated form, the unpaired cysteine (Cys 149) was replaced with tyrosine, as in the human IL-10 homologue; (2) the evaluation of rIL-10 biological activity, using bone marrow derived macrophages (BMDM), and its comparison with that of a commercially available IL-10 (cIL-10); (3) the incorporation/release of IL-10 into/from the dextrin nanogel, and the stability and bioactivity of rIL-10 in the nanogel/rIL-10 complex.

Experimental

Materials

All reagents used were of laboratory grade and purchased from Sigma-Aldrich (USA), unless stated otherwise. Commercial IL-10 (cIL-10) was purchased from eBioscience (San Diego, CA, USA). Purified anti-human CD210 (IL-10 R) (denominated as AntiIL-10R) was obtained from BioLegend (San Diego, CA, USA).

Recombinant IL-10 expression and purification

Construction of the expression plasmid.

The DNA encoding for murine IL-10 was synthesised by GenScript Corporation (NJ, USA) with optimized codons for bacterial expression and delivered cloned, into the *Nde*I and *Xho*I restriction sites, on the expression vector pET28a(+) (Novagen, USA), yielding pET28aIL-10.

Site directed mutagenesis.

To remove the hexahistidine tag (HisTag) coded by the pET28aIL-10 construction, the HisTag and the linker coding sequences from the N-terminus were deleted using a site directed mutagenesis kit. The same kit was used to obtain the Cys149Tyr mutant [21]. For that purpose, the primers listed in Table 3.1 were used.

Table 3.1 – Primers used for the deletion of HisTag (dHisTag) and to obtain the Cys149Tyr mutant (C149Y).

Name	Sequence
dHisTag-forward	5′-CTTTAAGAAGGAGATATACCATGTCTCGTGGCCAGTACTCTCGTGAAG-3′
dHisTag-reverse	5′-CTTCACGAGAGTACTGGCCACGAGACATGGTATATCTCCTTCTTAAAG-3′
C149Y-forward	5′-GAATTTGACATCTTCATCAACTATATTGAAGCTTACATGATGATCAAAATGAAAAGC-3′
C149Y-reverse	5′-GCTTTTCATTTTGATCATCATGTAAGCTTCAATATAGTTGATGAAGATGTCAAATTC-3′

The mutagenesis was performed using the QuikChange Site-Directed Mutagenesis Kit (Stratagene, CA, USA) according to the manufacturer's instructions. The deletion of the HisTag and the linker coding sequences was accompanied by the loss of *Nco*I and *Nde*I restriction endonuclease sites. The primers designed to obtain the C149Y mutant also induced a novel *Hind*III restriction endonuclease site. These changes allowed the identification of the positively deleted/mutated clones by restriction endonuclease analysis. Automated DNA sequencing analysis later confirmed the positive clones identified.

Recombinant IL-10 expression, refolding, and purification.

The culture of *E. coli* BL21 star (Invitrogen, CA, USA), transformed with the expression construct, was grown in Luria-Bertani (LB) medium supplemented with 50 μg/ml kanamycin at 37^{o}C, 185 rpm. The expression of IL-10 C149Y (termed rIL-10 ahead in this paper) was induced by the addition of isopropyl-β-D-thiogalactopyranoside into the culture medium at mid-log phase ($O.D._{600nm}$ = 0.6) to 0.5 mM final concentration. After 3 h incubation, cells were

harvested, resuspended in 50 mM Tris, 50 mM NaCl (pH 7.4) and lysed by adding 100 μg/ml lysozime. After freeze and thawing, 100 μg/ml deoxyribonuclease I and 100 mM $MgCl_2$ were added and the extract incubated at 4ºC for 1 h. The inclusion bodies were then washed for 3 h with 50 mM Tris, 50 mM NaCl (pH 7.4), pelleted at 10,000 x g and then washed again for another 3 h with 50 mM Tris, 50 mM NaCl (pH 7.4), 0.1% triton X-100 (v/v) followed by centrifugation at 10,000 x g. The pelleted inclusion bodies were then dissolved in 6 M guanidine.HCl, pH 8.5 and dithiothreitol was added to a final concentration of 5 mM and, after a ultracentrifugation step (100,000 x g, 20 min, 4ºC) to remove any insoluble material, the protein was refolded by rapid dilution (20-fold) into 50 mM Tris pH 8.0, 2 mM glutathione (reduced form), 0.2 mM glutathione (oxidized form), 50 mM NaCl, 5 mM EDTA. The refolded solution was kept in cold room until purification (usually between 3-4 days to a week).

The refolded rIL-10 solution was first concentrated by tangential flow ultrafiltration (Sartocon Slice – Sartorius, Germany) to approximately 150 ml, followed by a N_2 pressurized stirred cell concentrator (Amicon 8200 – Millipore, MA, USA) to 12-15 ml. After ultracentrifugation to clarify the solution (100,000 x g, 20 min, 4ºC), the protein was applied to a Superdex 200 26/60 column (Amersham, England) pre-equilibrated at room temperature with 25 mM phosphate buffer, pH 7.25 at 2.0 ml/min. The collected fractions with elution volume corresponding to rIL-10 dimer were pooled and applied to a Mono S HR 5/5 (Amersham, England) column equilibrated with 25 mM phosphate buffer, pH 7.25 at 0.75 ml/min. The elution was done by a linear NaCl gradient from 0 to 0.5 M.

The purity of the protein was assessed by SDS-PAGE using 12.5% gels in a BioRad Mini Protean III (CA, USA) electrophoresis apparatus according to the method of Laemmli, and stained with Coomassie brilliant Blue R-250.

Cytokine analysis

IL-10 and TNF-α were quantified by a enzyme-linked immunosorbent assay (ELISA) commercial kit, Mouse IL-10 ELISA Ready-SET-Go!, and Mouse TNF-a ELISA Ready-SET-Go! (eBioscience, San Diego, CA, USA), respectively, following the manufacturer's instructions.

Culture of murine bone marrow-derived macrophages (BMDM)

Macrophages were obtained from mouse bone marrow as follows: mice were sacrificed and femurs and tibias removed under aseptic conditions. Bones were flushed with Hanks' balanced salt solution. The resulting cell suspension was centrifuged at 500 x g and resuspended in RPMI 1640 medium supplemented with 10 mM HEPES, 10% heat-inactivated fetal bovine serum (FBS), 60 μg/ml penicillin/streptavidin, 0.005 mM β-mercaptoethanol (complete RPMI [cRPMI]), and 10% L929 cell conditioned medium. To remove fibroblasts or differentiated macrophages, cells were cultured, on cell culture dishes (Sarstedt, Canada), overnight at 37°C in a 5% CO_2 atmosphere. Then, nonadherent cells were collected with warm cRPMI, centrifuged at 500 x g, distributed in 96-well plates (Sarstedt, Canada) at a density of 1 x 10^5 cells/well, and incubated at 37°C in a 5% CO_2 atmosphere. Four days after seeding, 10% of L929 cell conditioned medium was added, and the medium was renewed on the seventh day. After ten days in culture, cells were completely differentiated into macrophages. This method allows for the differentiation of a homogenous primary culture of macrophages that retain the morphological, physiological and surface markers characteristics of these phagocytic cells [34-36].

Bioassay of IL-10

IL-10 bioactivity was assayed by its ability to inhibit the production of TNF-α and the surface expression of major histocompatibility complex class II (MHC-II) molecules in lipopolysacharide (LPS) and IFN-γ activated macrophages (endotoxin-stimulated macrophages).

IL-10, recombinant (rIL-10) and commercial (cIL-10), in concentrations ranging from 0.1 ng/ml to 250.0 ng/ml, were added to the BMDM, and the cells incubated at 37°C in a 5% CO_2 atmosphere for 1 h. Then, 0.1 ng/ml LPS and 1.0 ng/ml IFN-γ were added to the cells to promote macrophage activation, and incubated for 24 h. As a positive control of macrophage activation, cells stimulated with LPS and IFN-γ, without IL-10, were used; as a negative control, cells cultured in cRPMI alone were used. After incubation, culture supernatants were removed and stored at -80°C until TNF-α quantification. The attached cells were collected, with 5 mM EDTA in PBS, for MHC-II expression analysis by flow cytometry (FACS analysis).

Anti-IL-10R assay.

The inhibition of rIL-10 biological activity by anti-IL-10R monoclonal antibody was tested in BMDM cultures performed as in the previous assay.

rIL-10 (100.0 ng/ml) and anti IL-10R monoclonal antibody (AntiIL-10R) (0, 12.5, 25.0, 50.0 μg/ml) were added to the cells, and incubated for 1 h at 37°C in a 5% CO_2 atmosphere. Then, 0.1 ng/ml LPS and 1.0 ng/ml IFN-γ were added to the cells, to induce macrophage activation, that were incubated for further 24 h. After incubation, culture supernatants were removed and stored at -80°C until TNF-α quantification. The attached cells were collected, with 5 mM EDTA in PBS, for FACS analysis of MHC-II expression as described below.

FACS analysis

To determine the surface expression of MHC-II molecules, cells were labeled for 20 minutes on ice with 1:300 MCHII-PE antibody (BD Pharmingen™, USA) in FACS buffer (PBS, 1% BSA). Then, cells were washed with FACS buffer and transferred to FACS-tubes containing 1:100 5 μg/ml propidium iodide in FACS buffer.

Labeled cell samples were analyzed in a FACScan (Becton Dickinson, San Jose, CA, USA) with the CellQuest software (Becton Dickinson, San Jose, CA, USA).

Nanogel/rIL-10 complex formation and stability

Preparation of the nanogel/rIL-10.

Dextrin-MVA-SC_{16} (MVA: vinyl methacrylate; SC_{16}: alkyl chain) was synthesized as previously described [32, 37], with the exception that the transesterification was made with vinyl methacrylate instead of vinyl acrylate.

The size distribution was determined with a Malvern Zetasizer MODEL NANO ZS (Malvern Instruments Limited, UK). A dispersion of the nanogel was analyzed at 25°C in a polystyrene disposable cell, using a He-Ne laser-wavelength of 633 nm and a detector angle of 173°.

To form the self-assembled nanogel, lyophilized dextrin-VMA-SC_{16} was dissolved in cRPMI, at a concentration of 1.0 mg/ml. The dissolution was accomplished after approximately 16 h at room temperature with stirring. The nanogel formation was confirmed by dynamic light scattering. All suspensions were sterilized by filtration through a 0.45 μm membrane.

The complex nanogel/rIL-10 was formed by dissolving rIL-10 in cRPMI, without FBS, and then by mixing lyophilized dextrin-VMA-SC_{16} (1.0 mg/ml).

The dissolution was accomplished after approximately 16 h at room temperature with stirring.

Evaluation of rIL-10 incorporation into the nanogel/rIL-10 complex.

rIL-10 incorporation into the dextrin nanogel was verified quantifying the amount of rIL-10 free in solution by ELISA. Briefly, the complex nanogel/rIL-10 was formed, as described previously, using concentrations of rIL-10 ranging from 10 ng/ml to 10000 ng/ml. Then, the complex was washed three times, using the Ultra-Filtration device Amicon®Ultra-15 100 kDa (Millipore, MA, USA), to elute unbound protein. Finally, rIL-10 free in solution was quantified, by ELISA, to evaluate the amount of rIL-10 incorporated.

Circular dichroism (CD) measurements.

The secondary structure of rIL-10, free or complexed with the nanogel, was investigated using CD. Spectra were obtained on a Olis DSM 20 circular dichroism spectropolarimeter continuously purged with nitrogen, equipped with a Quantum Northwest CD 150 temperature-controlled cuvette and controlled by the Globalworks software.

CD spectra of free rIL-10 (0.5 mg/ml or 0.25 mg/ml) and rIL-10 complexed with the nanogel (1 mg/ml), in PBS, were collected using a 0.2 mm path length cuvette, between 190 and 260 nm at 1 nm intervals. Three scans with an integration time of 4 s were averaged for each measurement. Spectra were acquired at 4 or 37°C. The results are expressed in terms of mean residue ellipticity $[\theta]_{MRW}$ in deg cm^2 $dmol^{-1}$, according to the equation $[\theta]_{MRW} = \theta_{obs} \times 100\ MW / (lcN)$, where θ_{obs} is the observed ellipticity in mdeg, MW is the protein molecular weight in g/mol, l is the cuvette path length in cm, c is the protein concentration in g/l and N is the number of residues of the protein.

rIL-10 stability, free or complexed with the nanogel (0.25 mg/ml rIL-10, 1 mg/ml nanogel), at 37°C and at 4°C, was accessed by obtaining CD spectra of the samples, at determined intervals of time.

Bioactivity of the complex nanogel/rIL-10

Evaluation of rIL-10 release from the nanogel/rIL-10 complex.

The release of rIL-10 from the complex nanogel/rIL-10 was assessed in a BMDM culture.

The complex nanogel/rIL-10 was formed with 2000 ng/ml rIL-10, as described above, and 20% FBS was added to the suspension. Then, the suspension (200 μL/well) was added to BMDM cells (1 x 10^5 cells/well) and incubated at 37°C in a 5% CO_2 atmosphere. At determined times, supernatants were collected and stored at -80°C until IL-10 quantification.

Bioactivity of rIL-10 released from the nanogel/rIL-10 complex.

Suspensions of nanogel and nanogel/rIL-10 complex were prepared as described previously. Then, 20% FBS was added and the suspensions (200 μL/well) added to BMDM cells (1 x 10^5 cells/well). After 2 h of incubation at 37°C in a 5% CO_2 atmosphere, 0.1 ng/ml LPS and 1.0 ng/ml IFN-γ were added to the cells to promote macrophage activation, and incubated for further 24 h. After incubation, culture supernatants were removed and stored at -80°C until TNF-α quantification. The attached cells were collected, with 5 mM EDTA in PBS, for MHC-II expression analysis by flow cytometry. As controls, wells without LPS and IFN-γ stimulation were used.

Results and discussion

IL-10 expression and purification

Interleukin-10 is a very important immunoregulatory protein hence drawing great interest for its potential regarding biomedical applications [15, 22-24].

The active form of IL-10 is known to be a non-covalent homodimer and, as already stated, human and murine IL-10 have two disulfide bonds that are essential to the biological activity of the protein [18, 19]. However, murine IL-10,

and alike the rat IL-10, has also a fifth unpaired cysteine (Cys149). In the rat, this additional cysteine has been shown to reduce significantly the IL-10 biological activity [21]. In order to eliminate the unwanted and predictable reactivity of Cys149, this amino acid was replaced by directed mutagenesis with tyrosine. Amino acid sequence and structure of human, murine, rat and porcine IL-10 dimer, suggests that both amino acids surrounding cys149 are conserved [16] and therefore, the replacement of cysteine 149 for tyrosine, the corresponding amino acid in human and porcine IL-10, was least likely to disrupt the dimer active conformation [21].

After deletion of the hexahistidine tag and the C149Y mutagenesis, the recombinant vector was transformed into *E. coli* BL21 star cells. The mutated murine IL-10 protein (rIL-10) was expressed in bacteria, yielding about 50% of the total cell protein, bearing an apparent molecular weight close to the expected (18 kDa), as shown in the SDS-PAGE analysis (Figure 3.1A, lane 1). However, the expression of soluble and functional eukaryotic proteins in heterologous systems is not always straightforward [38] and usually overexpressed recombinant proteins accumulate either in the cytoplasm and/or periplasmic space in form of inclusion bodies, which are amorphous granules of misfolded protein with no biological activity [39]. The formation of inclusion bodies led to the recovery of rIL-10 by a process of solubilization in 6 M guanidine, renaturation and re-oxidation of the dissulphides. Then, the retrieval of the soluble protein from the renaturation solution was made by gel filtration, using the stationary phase Superdex 200 (Figure 3.1B), to collect the dimeric form of the recombinant protein. The fractions containing the rIL-10 dimer, collected between 205 and 225 ml (Figure 3.1A, lane 2), were pooled and combined for further purification by ion-exchange chromatography, in a Mono S column (Figure 3.1C). SDS-PAGE (Figure 3.1A, lanes 3, 4, 5, and 6) analysis confirmed the apparent molecular weight of the proteins as well as their purity. The oligomerization state of the collected fractions (either from the Superdex 200 column as from Mono S column) was verified by analytical gel filtration and shown to be dimeric (data not shown).

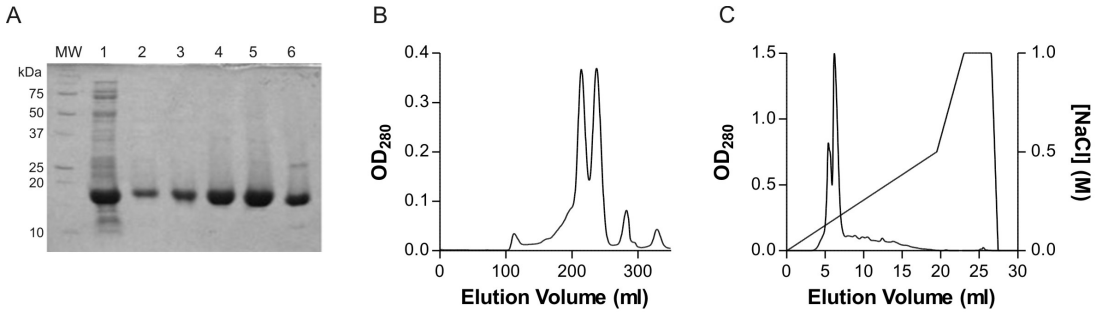

Figure 3.1 (A) SDS-PAGE: MW – molecular weight marker; 1 – Insoluble fraction applied to Superdex 200; 2 – Fractions eluted from Superdex 200 and applied to Mono S; 3, 4 – first peak eluted from Mono S; 5, 6 – second peak eluted from Mono S; (B) Chromatogram obtained using Superdex 200; (C) Purification of the rIL-10 dimer in a Mono S column.

So, rIL-10 was recovered as the active non-covalent homodimer and the yield of protein (about 1.0-1.5 mg/l culture, quantified by ELISA) was high enough to the subsequent assays, and stable between batches. Both fractions eluted from Mono S column were shown to be in dimeric state, and were then tested for biological activity.

Biological activities of rIL-10

In order to evaluate whether the rIL-10 recovered from the inclusion bodies was biologically active, BMDM cultures were used. Active macrophages exhibit a higher production of several cytokines, as well as oxygen reactive intermediates. IL-10 is known to deactivate macrophages, reducing the production of cytokines and oxygen reactive intermediates, and also to down-regulate MHC-II expression [1-4, 6, 9, 10].

As it can be seen in Figure 3.2A, in the range of 0.1 ng/ml to 1.0 ng/ml, rIL-10 showed a dose-dependent ability to reduce the TNF-α production. At 1.0 ng/ml, TNF-α is reduced by about 80%; increasing the rIL-10 concentration does not seem to further reduce TNF-α production significantly. It is also noticeable that rIL-10 ability to reduce TNF-α production is similar to that of tested cIL-10, in the analyzed range of concentrations.

As antigen presenting cells, macrophages have a constitutive expression of MHC-II molecules that is however increased upon activation [40]. The results shown in Figure 3.2B are normalized taking as reference (100%) the MHC-II

expression by cells treated only with LPS and INF-γ (positive control of macrophage activation). Treating cells with rIL-10 reduces MHC-II expression of the stimulated macrophages to the level detected in the negative control (Figure 3.2B). In the range of 1.0 ng/ml to 50.0 ng/ml the effect of cIL-10 and rIL-10, on the expression of MHC-II molecules, is identical.

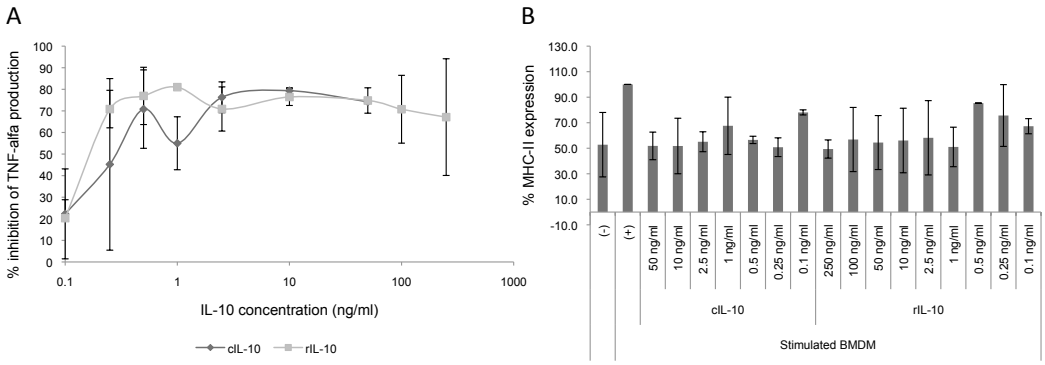

Figure 3.2 – Biological activity of rIL-10 and cIL-10. (A) Percentage of inhibition of TNF-α production, by 0.1 ng/ml LPS and 1.0 ng/ml INF-γ stimulated BMDM. (B) Percentage of MHC-II expression induced by cIL-10 and rIL-10 treatment of stimulated BMDM. Data points are the means±SD (standard deviation) of duplicate independent assays with triplicate cell incubations each. (+) – positive control of macrophage activation; (-) – negative control of macrophage activation.

The two fractions eluted from Mono S column were tested and presented similar results.

To further test the specificity of rIL-10 bioactivity, a blocking IL-10R antibody was used. IL-10 exhibits a wide variety of activities when it binds specifically to its cellular receptor, signaling through the IL-10R results not only in the inhibition of the synthesis of several cytokine genes, but also prevents several cytokines from inducing their biological activities on their target cells [1, 2]. The information about the interaction of rIL-10 with IL-10R is important to determine whether rIL-10 acts as "genuine" IL-10 or if it mimics its function indirectly by, for instance, facilitating endogenous IL-10 expression or release.

As shown in Figure 3.3A, in the presence of AntiIL-10R, TNF-α production by stimulated macrophages is high meaning that rIL-10 activity was thus exerting its activity through binding to the IL-10R. The effect of rIL-10 on MHC-II expression was similarly blocked (Figure 3.3B). It should be noticed that, in the absence of the blocking antibody, rIL-10 presented biological

activity, decreasing TNF-α production and MHC-II expression. It was also observed that, in the presence of the blocking antibody, TNF-α production and MCH-II expression were higher than in the positive control (+) meaning that even the activity of endogenous IL-10, expressed by the macrophages in response to LPS and INF-γ, was blocked.

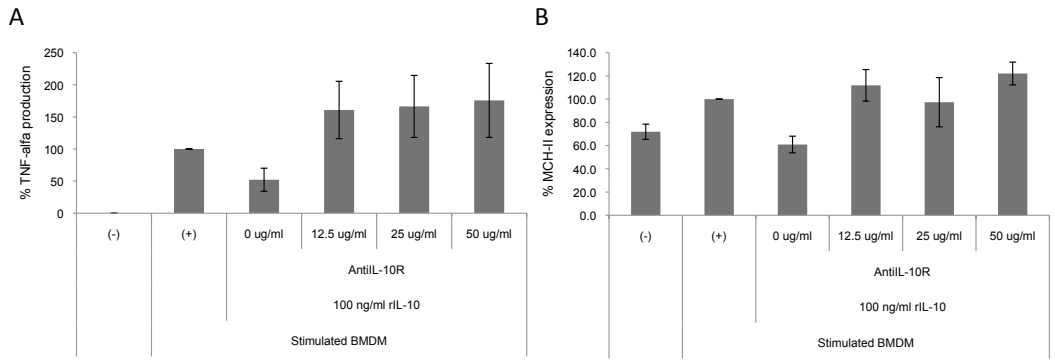

Figure 3.3 – Anti IL-10R activity. (A) Percentage of TNF-α production, by 0.1 ng/ml LPS and 1.0 ng/ml INF-γ stimulated BMDM. (B) Percentage of MHC-II expression induced by AntiIL-10R and rIL-10 treatment of stimulated BMDM. Data points are the means±SD of triplicate independent assays with triplicate cell incubations each. (+) – positive control of macrophage activation; (-) – negative control of macrophage activation.

Taken together, these results demonstrate that the rIL-10 is biologically active and exerts its activity specifically through IL-10 receptor binding, acting thus like endogenous IL-10.

Nanogel/rIL-10 complex formation and stability

Polymer formulations, including polymer-protein conjugates, are finding increasing clinical use. Synthetic and natural polymers have been explored as drug carriers, but most polymers used clinically are still non-biodegradable synthetic ones [29]. The proven clinical tolerability of dextrin and its efficient absorption due to degradation by amylases, suggest that this polymer might be ideal for development as a drug carrier [29]. Furthermore, dextrin is readily excreted due to its low molecular weight, hence accumulation in the tissues is unlikely.

Self-assembled dextrin nanogel, dispersed in water at a concentration of 1.0 mg/ml, was observed using dynamic light scattering (DLS) after filtration through a 0.45 μm membrane, as comprehensively described in previous work [31-33], and illustrated by Scheme 3.1.

Scheme 3.1 – Synthesis of Dex-VMA-SC16

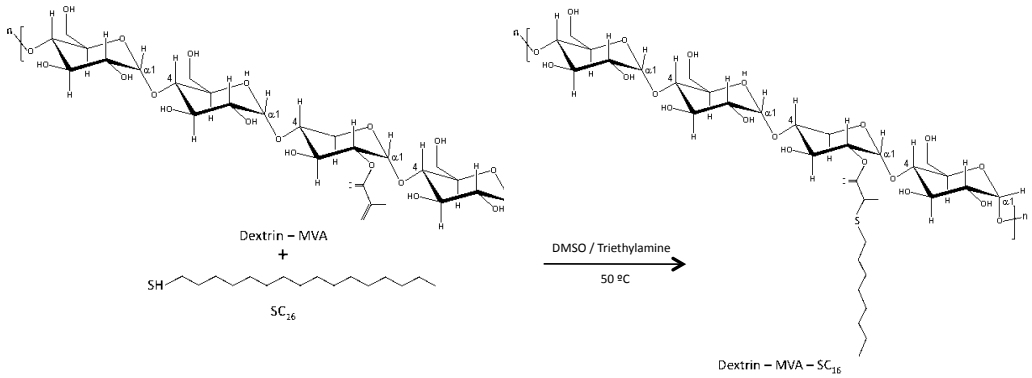

The DLS analysis, in the intensity distribution, revealed two populations with roughly 25 and 150 nm. The conversion to number distribution highlighted only the smaller population of particles, the predominant one. Thus, the nanogel used in this study present a diameter of about 25 nm, in water, upon self-aggregation. The z-value obtained was 23.6 nm, representative of the average size of polydisperse colloids. The polysdispersity index (PdI) provides information on the homogeneity of the dispersion and the obtained PdI for the nanogel was low (< 0.5), meaning the sample may be considered homogeneous, consisting of one main population with 23.6 nm. Additionally, the variation of the hydrodynamic diameter (z-value) and zeta-potential of the nanogel with pH was evaluated [31]. In the pH range studied, the zeta potential was almost constant and close to zero. Although the low zeta potential, the nanogel is stable. The stability can be attributed to the solvation forces, as discussed by Gonçalves and Gama (2008).

Cytokines are proteins bearing a short half-live, *in vivo*. The encapsulation of rIL-10 in the dextrin nanogel was attempted as a mean to augment its bioavailability and stability. By trapping rIL-10 in a hydrated polymer-

network, the nanogel is expected to minimize denaturation and enable a slow release profile, hence maintaining an effective concentration.

In order to confirm the incorporation of rIL-10 by the nanogel, the cytokine detectable using the ELISA was quantified after formation of the complexes nanogel/rIL-10. The encapsulation was achieved simply mixing the cytokine and nanogel, as described in the methods section. Irrespective of the concentration of rIL-10 incubated with the nanogel (10, 100, 1000 and 10000 ng/ml), rather low amounts (1.5-2.0 ng/ml) were detected in each case. Thus, even when 10000 ng/ml of rIL-10 is used, only 0.02 % of the rIL-10 remains detectable in solution. Indeed, even lower amounts of rIL-10 (less than 1 ng/ml) were detected in permeates collected after ultrafiltration of the complex nanogel/rIL-10 using a membrane with a cutoff of 100kDa, thus allowing the filtration only of the free cytokine. Altogether, these results show that rIL-10 is efficiently and spontaneously incorporated in the nanogel complex. The difference in the concentrations detected in the ultrafiltration permeate (<1ng/ml) and in the mixture nanogel/rIL10 (1,5-2,0 ng/ml) is assigned to protein on the surface of the nanogel, allowing its detection by ELISA.

The CD spectra of soluble rIL-10 (0.5 mg/ml) and nanogel/rIL-10 (1 mg/ml nanogel, 0.5 mg/ml rIL-10) are shown in Figure 3.4A.

The secondary structure of free soluble rIL-10 is mainly helical, as expected [16, 20, 41], and the complexation with the nanogel did not induce any conformational change. Similar results were obtained using other concentrations of rIL-10. Furthermore, the nanogel (1 mg/ml) did not interfere in the CD observations, under the conditions employed.

The stability of the free and complexed rIL-10 was accessed at the physiological temperature, 37ºC, by recording the CD spectra over time. Samples of rIL-10 and nanogel/rIL-10 complex were incubated at 37ºC, in PBS, and CD spectra obtained at determined intervals of time (Figure 3.4B and C, thick grey lines represent the CD spectra of the samples at beginning of the experiment). After 6 days incubation, CD spectrum of free rIL-10 completely looses its characteristic pattern (thick black line in Figure 3.4B)

while rIL-10 complexed with the nanogel still presents a typical CD spectrum of a helical protein even after 16 days incubation at 37ºC (thick black line in Figure 3.4C). The mean residual ellipticity (θ) variation, at 222 nm, shows that rIL-10 stability is significantly increased when rIL-10 is complexed with the dextrin nanogel.

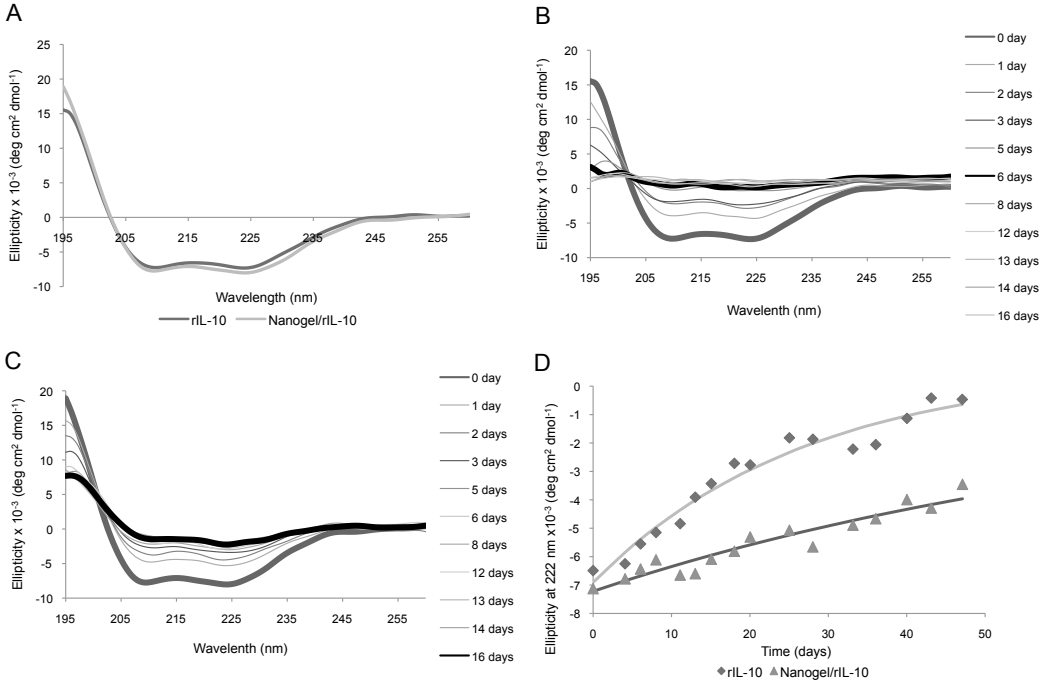

Figure 3.4 – CD spectra of (A) free rIL-10 (0.25 mg/ml) and complex nanogel/rIL-10 (1 mg/ml nanogel and 0.25 mg/ml rIL-10) at 37ºC in PBS; (B) free rIL-10 (0.25 mg/ml) and, (C) complex nanogel/rIL-10 (1 mg/ml nanogel and 0.25 mg/ml rIL-10) incubated at 37ºC, in PBS for several days; and, (D) variation of the mean residual ellipticity at 222 nm of rIL-10 and nanogel/rIL-10 incubated at 4ºC for several days.

These results suggest that the nanogel stabilize rIL-10, avoiding its denaturation and precipitation and thus preserving bioavailability for longer periods of time, at physiological temperature. In addition, the stability improvement of the formulation during storage, at lower temperatures, is also significant (Figure 3.4D). The dextrin nanogel may thus effectively perform as stability enhancer, not only as a protein carrier.

Biological activities of rIL-10 released from the nanogel/rIL-10 complex.

The complex nanogel/rIL-10 suspension was added to BMDM cultures to evaluate the release of the cytokine, measured by ELISA, to the culture medium in the presence of serum proteins (Figure 3.5). The spontaneous dissociation of rIL-10 from the complex was barely observed in culture medium without serum. On the other hand, rIL-10 was released from the nanogel/rIL-10 complex when FBS was added to the system. Worth noticing that, the BMDM culture (without the nanogel/rIL-10) did not produce IL-10 in significant amounts. After 2 h of incubation in the presence of 20% FBS, the released rIL-10 reaches a maximum, stable concentration of 35 ng/ml, which is still constant after 24 h. A similar release profile is observed in culture medium without BMDM (Figure 3.5).

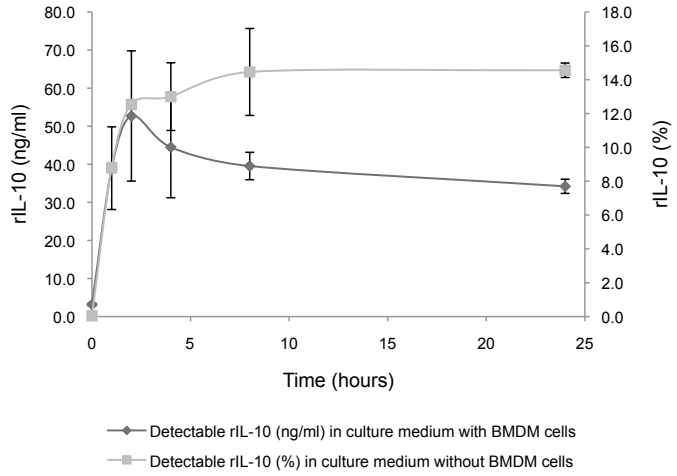

Figure 3.5 – IL-10 release profile on a BMDM culture and on culture medium alone. Data points are the means ± SD of duplicate independent assays with triplicate incubations each.

The rIL-10 release is probably due to the exchange of rIL-10 with serum proteins. Indeed, when the nanogel/rIL-10 complex is placed in medium containing serum proteins, a partition equilibrium (incorporated versus free rIL-10) is established in approximately 2 h, with or without BMDM cells. However, it must be remarked that the rIL-10 released correspond only to approximately 15% of the protein incorporated initially in the nanogel (Figure

3.5). The protein released in this experimental set-up probably corresponds to the commonly observed - in drug release systems - initial burst release of the less tightly adsorbed proteins, less stabilized by the hydrophobic cores present inside the nanogel, as previously discussed [31, 32]. Theoretically, the constant concentration of IL-10 in the culture medium may be due to 1) a partition equilibrium of the cytokine between the nanogel and the culture medium, or, 2) to a strong interaction of the cytokine, more likely a denatured fraction, with the hydrophobic domains inside the nanogel. Along time, in sink conditions, the release rate is expected to slow-down, as protein stabilized deeper within the nanogel and interacting more tightly with the hydrophobic cores is being exchanged. Furthermore, in the dynamic situation *in vivo*, with continuous depletion of rIL-10 (at different rates, depending on the administration route), the protein is expected to be fully released. Probably, a different release profile will be obtained with different proteins. This release profile is likely to depend on the hydrophobicity of the protein and affinity for the hydrophobic domains in the nanogel and on its stability. A more comprehensive characterization of the interaction protein-nanogel - using different proteins - of the release kinetics in sink conditions will be performed in future work.

The bioactivity of the rIL-10 released from the nanogel was also analyzed. A suspension of nanogel/rIL-10 was added to a BMDM culture and incubated for 2 h, such that enough rIL-10 could be released from the complex. Then, LPS and INF-γ was added to activate the macrophages. After 24 h incubation, the amount of TNF-α produced and the expression of MHC-II were evaluated. The rIL-10 released from the nanogel/rIL-10 complex was able to inhibit TNF-α production and MHC-II expression at the same level as the soluble rIL-10, as Figure 3.6 shows.

So, the results demonstrate that the rIL-10 released from the nanogel/rIL-10 complex is able to inhibit macrophages at the same level as the soluble rIL-10. We can also conclude that the nanogel encapsulation, besides not inducing any alteration on the rIL-10 secondary conformation (as seen in Figure 3.4A), does not alter the biological properties of the protein.

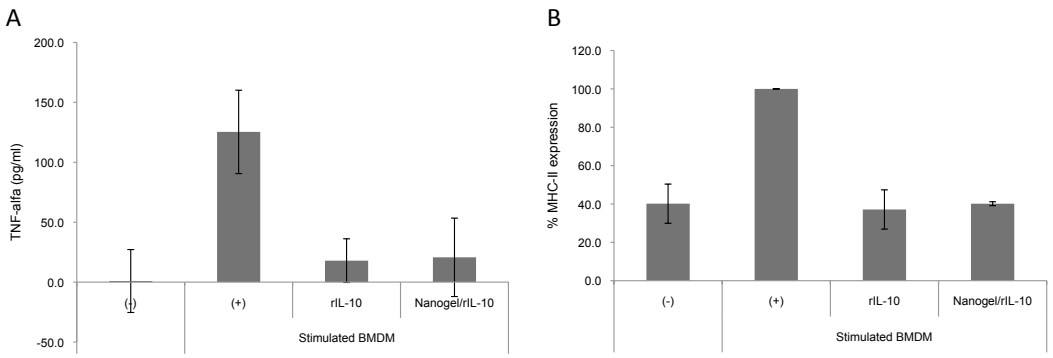

Figure 3.6 – Biological activity of rIL-10 released from nanogel/rIL-10 complex. (A) TNF-α concentration (pg/ml), produced by 0.1 ng/ml LPS and 1.0 ng/ml INF-γ stimulated BMDM, treated with rIL-10 and nanogel/rIL-10. (B) MHC-II induced, in stimulated BMDM, by 50 ng/ml rIL-10 and nanogelrIL-10. Data points are the means ± SD of duplicate independent assays with triplicate cell incubations each. (+) – positive control of macrophage activation; (-) – negative control of macrophage activation.

Conclusions

A mutated form of murine IL-10 was successfully expressed in *E. coli*. This recombinant protein was recovered and purified from inclusion bodies and demonstrated biological activity similar to a commercially available IL-10. Dextrin self-assembled nanogel was able to efficiently encapsulate and protect rIL-10 from denaturation at 37ºC, and also enables rIL-10 to be released in biologically significant amounts over time. The biological activity of the released rIL-10 was confirmed by the evaluation of the production of TNF-α and expression of MHC-II on endotoxin-stimulated BMDM. The simplicity of the preparation of the nanogel/rIL-10 complex, associated to the enhancement of protein stability and controlled release, makes this a very promising system.

IL-10 has potential application in various medical fields, such as in acute inflammatory diseases, namely rheumatoid arthritis, and these results point to dextrin nanogel as a promising carrier of IL-10, which enables the protein sustained release.

References

(1) Moore, K. W.; de Waal Malefyt, R.; Coffman, R. L.; O'Garra, A., *Annu Rev Immunol* **2001,** 19, 683-765.

(2) Pestka, S.; Krause, C. D.; Sarkar, D.; Walter, M. R.; Shi, Y.; Fisher, P. B., *Annu Rev Immunol* **2004,** 22, 929-79.

(3) de Waal Malefyt, R.; Abrams, J.; Bennett, B.; Figdor, C. G.; de Vries, J. E., *J Exp Med* **1991,** 174, (5), 1209-20.

(4) Fiorentino, D. F.; Zlotnik, A.; Mosmann, T. R.; Howard, M.; O'Garra, A., *J Immunol* **1991,** 147, (11), 3815-22.

(5) Gazzinelli, R. T.; Oswald, I. P.; James, S. L.; Sher, A., *J Immunol* **1992,** 148, (6), 1792-6.

(6) Bogdan, C.; Vodovotz, Y.; Nathan, C., *J Exp Med* **1991,** 174, (6), 1549-55.

(7) MacNeil, I. A.; Suda, T.; Moore, K. W.; Mosmann, T. R.; Zlotnik, A., *J Immunol* **1990,** 145, (12), 4167-73.

(8) Defrance, T.; Vanbervliet, B.; Briere, F.; Durand, I.; Rousset, F.; Banchereau, J., *J Exp Med* **1992,** 175, (3), 671-82.

(9) Groux, H.; Bigler, M.; de Vries, J. E.; Roncarolo, M. G., *J Immunol* **1998,** 160, (7), 3188-93.

(10) de Waal Malefyt, R.; Haanen, J.; Spits, H.; Roncarolo, M. G.; te Velde, A.; Figdor, C.; Johnson, K.; Kastelein, R.; Yssel, H.; de Vries, J. E., *J Exp Med* **1991,** 174, (4), 915-24.

(11) Willems, F.; Marchant, A.; Delville, J. P.; Gerard, C.; Delvaux, A.; Velu, T.; de Boer, M.; Goldman, M., *Eur J Immunol* **1994,** 24, (4), 1007-9.

(12) Creery, W. D.; Diaz-Mitoma, F.; Filion, L.; Kumar, A., *Eur J Immunol* **1996,** 26, (6), 1273-7.

(13) Steinbrink, K.; Graulich, E.; Kubsch, S.; Knop, J.; Enk, A. H., *Blood* **2002,** 99, (7), 2468-76.

(14) Steinbrink, K.; Wolfl, M.; Jonuleit, H.; Knop, J.; Enk, A. H., *J Immunol* **1997,** 159, (10), 4772-80.

(15) Asadullah, K.; Sterry, W.; Volk, H. D., *Pharmacol Rev* **2003,** 55, (2), 241-69.

(16) Zdanov, A.; Schalk-Hihi, C.; Gustchina, A.; Tsang, M.; Weatherbee, J.; Wlodawer, A., *Structure* **1995,** 3, (6), 591-601.

(17) Walter, M. R.; Nagabhushan, T. L., *Biochemistry* **1995,** 34, (38), 12118-25.

(18) Windsor, W. T.; Syto, R.; Tsarbopoulos, A.; Zhang, R.; Durkin, J.; Baldwin, S.; Paliwal, S.; Mui, P. W.; Pramanik, B.; Trotta, P. P.; et al., *Biochemistry* **1993,** 32, (34), 8807-15.

(19) Bondoc, L. L., Jr.; Varnerin, J. P.; Tang, J. C., *Anal Biochem* **1997,** 246, (2), 234-8.

(20) Zdanov, A.; Schalk-Hihi, C.; Wlodawer, A., *Protein Sci* **1996,** 5, (10), 1955-62.

(21) Ball, C.; Vigues, S.; Gee, C. K.; Poole, S.; Bristow, A. F., *Eur Cytokine Netw* **2001,** 12, (1), 187-93.

(22) Berzofsky, J. A.; Ahlers, J. D.; Belyakov, I. M., *Nat Rev Immunol* **2001,** 1, (3), 209-19.

(23) Pullerits, T., *Curr Pharm Des* **2002,** 8, (20), 1845-53.

(24) Hubel, K.; Dale, D. C.; Liles, W. C., *J Infect Dis* **2002,** 185, (10), 1490-501.

(25) Murthy, N.; Thng, Y. X.; Schuck, S.; Xu, M. C.; Frechet, J. M., *J Am Chem Soc* **2002,** 124, (42), 12398-9.

(26) Murthy, N.; Xu, M.; Schuck, S.; Kunisawa, J.; Shastri, N.; Frechet, J. M., *Proc Natl Acad Sci U S A* **2003,** 100, (9), 4995-5000.

(27) Leonard, M.; De Boisseson, M. R.; Hubert, P.; Dalencon, F.; Dellacherie, E., *J Control Release* **2004,** 98, (3), 395-405.

(28) Kim, S.; Kim, J. H.; Jeon, O.; Kwon, I. C.; Park, K., *Eur J Pharm Biopharm* **2009,** 71, (3), 420-30.

(29) Hreczuk-Hirst, D.; Chicco, D.; German, L.; Duncan, R., *Int J Pharm* **2001,** 230, (1-2), 57-66.

(30) Treetharnmathurot, B.; Dieudonne, L.; Ferguson, E. L.; Schmaljohann, D.; Duncan, R.; Wiwattanapatapee, R., *Int J Pharm* **2009,** 373, (1-2), 68-76.

(31) Gonçalves, C.; Gama, F. M., *European Polymer Journal* **2008,** 44.

(32) Goncalves, C.; Martins, J. A.; Gama, F. M., *Biomacromolecules* **2007,** 8, (2), 392-8.

(33) Goncalves, C.; Torrado, E.; Martins, T.; Pereira, P.; Pedrosa, J.; Gama, M., *Colloids Surf B Biointerfaces* **2009,** 75, (2), 483-9.

(34) Tushinski, R. J.; Oliver, I. T.; Guilbert, L. J.; Tynan, P. W.; Warner, J. R.; Stanley, E. R., *Cell* **1982,** 28, (1), 71-81.

(35) Zhang, X.; Goncalves, R.; Mosser, D. M., *Curr Protoc Immunol* **2008,** Chapter 14, Unit 14 1.

(36) Mosmann, T., *J Immunol Methods* **1983,** 65, (1-2), 55-63.

(37) Carvalho, J.; Goncalves, C.; Gil, A. M.; Gama, F. M., *European Polymer Journal* **2007,** 43, (7), 3050-3059.

(38) Dyson, M. R.; Shadbolt, S. P.; Vincent, K. J.; Perera, R. L.; McCafferty, J., *BMC Biotechnol* **2004,** 4, 32.

(39) Sorensen, H. P.; Mortensen, K. K., *Microb Cell Fact* **2005,** 4, (1), 1.

(40) Ma, J.; Chen, T.; Mandelin, J.; Ceponis, A.; Miller, N. E.; Hukkanen, M.; Ma, G. F.; Konttinen, Y. T., *Cell Mol Life Sci* **2003,** 60, (11), 2334-46.

(41) Josephson, K.; DiGiacomo, R.; Indelicato, S. R.; Ayo, A. H.; Nagabhushan, T. L.; Parker, M. H.; Walter, M. R., *Journal of Biological Chemistry* **2000,** 275, (18), 13552-13557.

Chapter 4 | Self-assembled dextrin nanogel as a IL-10 carrier: biocompatibility and IL-10 *in vivo* release and activity

Interleukin-10 (IL-10) is an anti-inflammatory cytokine, which active form is a non-covalent homodimer. Given the potential of IL-10 for application in various medical conditions, it is essential to develop systems for its effective delivery.

In previous work, it has been shown that a dextrin nanogel effectively incorporated and stabilized rIL10, enabling its release over time. In this work, the delivery system based on dextrin nanogels was further analyzed. The biocompatibility of the nanogel was comprehensively analyzed, through cytotoxicity (lactate dehydrogenase release, MTS, Live and Dead) and genotoxicity (comet) assays. The release profile of rIL-10 and its biological activity were evaluated in vivo, in C57 Bl/6 mice. Although able to maintain a stable concentration of IL-10 for at least 4 hours in the serum of mice, the amount of protein released is rather low. Despite this, the amount of rIL-10 released from the complex is biologically active inhibiting TNF-α production, in vivo, after LPS challenge.

Introduction

Interleukin-10 (IL-10) is produced by various cell types including T and B cells, monocytes, and macrophages [1, 2]. This cytokine is highly pleiotropic in its biological activity that includes: inhibition of the synthesis of several cytokines, including IL-1, IL-2, IL-3, IL-6, IL-8, IL-12, tumor necrosis factor α (TNF-α), and interferon γ [3]; immunosuppressive effects on monocytes/macrophages [4-6]; as well as immunostimulatory activity on a broad range of cell types, including T cells [7], B cells [8], and mast cells. Furthermore, IL-10 down-regulates constitutive and IFN-γ- or IL-4-induced class II major histocompatibility complex molecules expression on monocytes, dendritic cells, and Langerhans cells [9, 10] as well as adhesion and co-stimulatory molecules on antigen-presenting cells [11, 12] and, suppresses the release of reactive oxygen intermediates [4, 6]. IL-10 has thus a strong anti-inflammatory activity and may act as a general suppressor factor of immune responses and might be an efficient agent to prevent LPS toxicity *in vivo*, in mice [13-15].

Due to its immunoregulatory properties, this cytokine has been proposed to be used in vaccination [16] or in the treatment of allergies [17], infectious diseases [18], acute inflammatory diseases [19], etc. Normally, proteins of this kind are expensive to produce on a large scale and denature easily, loosing their bioactivity, thus having a quite short half-life *in vivo*. So, it is essential to develop new delivery systems that allow efficient therapeutic effects at a minimum dosage. A promising method is protein encapsulation by polymeric nanogels (or hydrogel nanoparticles), which, by trapping them in a hydrated polymer-network, minimize denaturation, and enabling slow-release, while maintaining an effective concentration for the necessary period of time [20-23].

In previous work [24], a dextrin self-assembled nanogel have been used to effectively incorporate a recombinant biologically active mutated murine IL-

10 form (rIL-10) and shown to enable its release over time. In this work, we present a further characterization of the complex nanogel/rIL-10, including the nanogel's cellular citotoxicity and the *in vivo* rIL-10 release from the nanogel complex, after subcutaneous injection in C57 BL/6 mice. The effect of rIL-10 and nanogel/rIL-10 administration before LPS challenge (endotoxin-induced shock) in C57 BL/6 mice, focusing on the systemic TNF-α release, was also analyzed.

Experimental

All reagents used were of laboratory grade and purchased from Sigma-Aldrich, unless stated otherwise. IL-10 and TNF-α were quantified by a enzyme-linked immunosorbent assay (ELISA) commercial kit, Mouse IL-10 ELISA Ready-SET-Go!, and Mouse TNF-a ELISA Ready-SET-Go! (eBioscience, San Diego, CA, USA), respectively, following the manufacturer's instructions.

Preparation of nanogel and complex nanogel/rIL-10

Dextrin nanogel and the complex nanogel/rIL-10 were prepared as described in Vera Carvalho *et al* [24]. Briefly, the self-assembled nanogels were obtained by dissolving the lyophilized dextrin-VMA-SC_{16} in cell culture medium or phosphate-buffered saline (PBS) pH 7.4 (2.7 mM KCl, 137 mM NaCl, 10 mM $HPO_4.2H_2O$, 2 mM KH_2PO_4), at a concentration of 1.0 mg/ml. The dissolution was accomplished after approximately 16 hours at room temperature, with stirring. The nanogel formation was confirmed by dynamic light scattering, as described previously [24-27]. The concentration was adjusted to 0.4, 0.1 and 0.05 mg/ml by dilution of the 1 mg/ml suspension.

The complex nanogel/rIL-10 was formed by dissolving rIL-10 in cell culture medium or PBS, followed by dissolution of lyophilized dextrin-VMA-SC_{16}, for approximately 16 hours at room temperature with stirring. The rIL-10 incorporation was confirmed by quantifying the amount of rIL-10 free in

solution using the ELISA commercial kit, following the manufacturer's instructions.

All suspensions were sterilized by filtration through a 0.45 μm membrane.

Cell cultivation

Mouse embryo fibroblasts 3T3.

Mouse embryo fibroblasts 3T3 (ATCC CCL-164) were grown in Dulbecco's modified Eagle's media supplemented with 10% newborn calf serum (Invitrogen, UK) and 1 μg/ml penicillin/streptavidin (DMEM complete medium [cDMEM]) at 37ºC in a 95% humidified air containing 5% CO_2. At 80% confluency, 3T3 fibroblasts were harvested with 0.05% (w/v) trypsin-EDTA and subcultivated in the same medium.

Murine bone marrow-derived macrophages (BMDM).

Macrophages were obtained from mouse bone marrow as follows: mice were sacrificed and femurs and tibias removed under aseptic conditions. Bones were flushed with Hanks' balanced salt solution. The resulting cell suspension was centrifuged at 500 x g and resuspended in RPMI 1640 medium supplemented with 10 mM HEPES, 10% heat-inactivated fetal bovine serum (FBS), 60 μg/ml penicillin/streptavidin, 0.005 mM β-mercaptoethanol (RPMI complete medium [cRPMI]), and 10% L929 cell conditioned medium (LCCM). To remove fibroblasts or already differentiated macrophages, cells were cultured, on cell culture dishes (Sarstedt, Canada), overnight at 37°C in a 5% CO_2 atmosphere. Then, nonadherent cells were collected with warm cRPMI, centrifuged at 500 x g, distributed in 96-well plates (Sarstedt, Canada) at a density of 1 x 10^5 cells/well, and incubated at 37°C in a 5% CO_2 atmosphere. Four days after seeding, 10% of LCCM was added, and the medium was renewed on the seventh day. After ten days in culture, cells were completely differentiated into macrophages. This method allows for the differentiation of a homogenous primary culture of macrophages that retain the morphological, physiological and surface markers characteristics of these phagocytic cells [28-30].

Evaluation of nanogel cellular citotoxicity

Cellular cytotoxicity was assessed using the MTS, live and dead and comet assays, and by measuring the release of lactate dehydrogenase (LDH). Although all these methods are usually used to evaluate cell viability, they address different features, namely the cell integrity or metabolic activity. In our experience, using the different methods allows a more comprehensive and consistent detection of cytotoxicity.

Mouse embryo fibroblasts 3T3 were seeded (4 x 10^5 cells/well in a 96-well polystyrene plate or 1 x 10^6 cells/well in a 6-well polystyrene plate) and incubated at 37ºC, 5% CO_2 for two hours. Then, the culture medium was removed and replaced with cDMEM containing a different concentration of NPs suspension (0.05 mg/ml to 1 mg/ml) and cells further incubated for 24 or 48 hours. In a similar way, on the tenth day of BMDM differentiation, the culture medium was replaced with NPs suspensions (0.05 mg/ml to 1 mg/ml), in cRPMI, and cells further incubated for 24 or 48 hours. Control cells were incubated with fresh medium and wells containing only growth medium were used as blanks.

Exceptionally, the culture medium used for the LDH release assay had only 1% serum and the incubation times were 3 and 20 hours.

All assays were made with triplicate cell incubations.

MTS assay.

Cellular viability, was assessed by measuring cell concentration via mitochondrial reduction of the tetrazolium salt MTS (3-(4,5-dimethyl-2-yl)-5-(3-carboxy-methoxyphenyl)-2-(4-sulfophenyl)-2H-tetrazolium) in the presence of 5% phenazine methosulfate over a one hour incubation period. The coloured reaction product formazan is soluble in the culture medium and can be measured spectrophotometrically at a wavelength of 490 nm with a reference wavelength of 570 nm.

After the incubation time, the culture medium of each well was replaced with 100 μL of fresh culture medium and 20 μL of CellTiter 96® AQueous One

Solution Reagent (Promega) was added and the plate further incubated for 1 hour at 37°C, 5% CO_2, as indicated by the manufacturer. The amount of soluble formazan produced by cellular reduction of MTS was measured at 490 nm.

Live and Dead assay.

The LIVE/DEAD® Viability/Cytotoxicity Kit for mammalian cells (Invitrogen, UK) was used to determine cell viability. This kit provides two-colour fluorescence cell viability assay, based on the simultaneous determination of live and dead cells with two probes that measure intracellular esterase activity and plasma membrane integrity.

Briefly, after the incubation time, 200 μL of a solution of 2 μM calcein AM and 4 μM ethidium homodimer-1, in sterile PBS, were added to the wells, incubated for 30 to 45 minutes at 37ºC, 5% CO_2 (as indicated by the manufacturer) and visualized in a fluorescence microscope.

Lactate dehydrogenase (LDH) release.

The Cytotoxicity Detection Kit^{PLUS} (LDH) (Roche) is a colorimetric assay for quantitating cytotoxicity/cytolysis by measuring LDH activity released from damaged cells.

The amount of LDH released was measured using the Cytotoxicity Detection Kit^{PLUS} (LDH) following manufacturer's instructions. In few words, after cell incubation with nanogel, 100 μL of Reaction Mixture was added to each well and the plate incubated at room temperature for 9 minutes, in the dark. Then, 50 μL of Stop Solution was added to each well and the absorbance of the samples was measured at 492 nm. Three controls were included: background control (determines the LDH activity in the assay medium) made with 1% serum culture medium; low control (determines the LDH activity released from the untreated normal cells) made with cells incubated with 1% serum culture medium; and, high control (determines the maximum releasable LDH activity in the cells) made with cells incubated with 1% serum culture medium where 5 μL of Lysis Solution was added before LDH quantification.

To determine the percentage cytotoxicity, the average absorbance values of the triplicate samples and controls were calculated; the average absorbance

value obtained in the background control was subtracted to the value obtained using the samples. Citotoxicity percentage values were obtained substituting the resulting values in the following equation:

Cytotoxicity (%) = (sample value – low control) / (high control – low control) x 100

Comet assay.

The comet assay (single-cell gel electrophoresis) is a simple method for detecting DNA damage at the level of individual cells [31]. Cells embedded in agarose on a microscope slide are lysed with detergent and high salt to form nucleiods containing supercoiled loops of DNA linked to the nuclear matrix. Electrophoresis at high pH results in structures resembling comets, observed by flourescence microscopy; the intensity of the comet tail relative to the head reflects the number of DNA breaks.

The comet assay was performed as described by Costa *et al* [32], with some exceptions. Briefly, collected cells were centrifuged (7500 x g for 3 min), suspended in 100 μL of 0.6% low-melting-point agarose in PBS and dropped onto a slide precoated with a layer of 1% normal melting point agarose and covered with coverslips. Slides were placed on ice and allowed to solidify. Coverslips were then removed and slides were immersed in freshly prepared lysing solution (2.5 M NaCl, 100 mM Na_2EDTA, 10 mM TrisBase, 0.25 M NaOH, pH 10) for 1 h at 4ºC, in the dark. After lyses, slides were placed on a horizontal electrophoresis tank and the tank filled with freshly made alkaline electrophoresis solution (1 mM Na_2EDTA, 300 mM NaOH, pH 13) to cover the slides, and left for 20 min in the dark to allow DNA unwinding and alkali-labile site expression. Then, electrophoresis was carried out for 20 min at 30 V and 300 mA (1.13 V/cm) and after, the slides were washed for 10 min with neutralizing solution (0.4 M TrisBase, pH 7.5). After neutralization, the slides were left to dry overnight in the dark. Afterwards, the slides were rehydrated for 30 minutes with ice-cold bidistilled water and stained with ethidium bromide solution (20 g/ml) for 20 min. After staining, the slides were washed again twice with ice-cold bidistilled water for 20 min. Each experimental condition was carried out twice with mouse embryo fibroblasts 3T3 and once with BMDM, and one slide was prepared for each sample. A 'blind' scorer

examined 100 randomly selected cells in each slide using a magnification of 500x. The DNA damages were evaluated by image analysis performed with Comet Assay IV software (Perceptive Instruments). Data collected from each cell included tail length, tail intensity, and tail moment.

In vivo assays

In vivo rIL-10 release from the nanogel/rIL-10.

C57 BL/6 mice were purchased from Charles River Laboratories España S. A. (Spain).

Mice were injected with 200 μL of nanogel/rIL-10 suspension in PBS (12.5 μg/ml rIL-10 and 5 mg/ml nanogel), rIL-10 solution in PBS (12.5 μg/ml), nanogel suspension in PBS (5 mg/ml) or PBS via subcutaneous (sc) route. Blood samples were taken at given intervals of time and serum concentrations of rIL-10 were assayed by ELISA.

In vivo effects of rIL-10 and nanogel/rIL-10 in endotoxin-induced shock mice.

C57 BL/6 mice were injected intraperitoneally (i.p.) with 100 μg of LPS 30 minutes after an i.p. administration of rIL-10 (2.5 μg), nanogel/rIL-10 (1 mg nanogel, 2.5 μg rIL-10), and nanogel (1 mg). Serum TNF-α levels were determined by ELISA 1.5 and 6 hours after LPS challenge. As controls, serum TNF-α levels were determined, in mice injected with PBS with and without LPS challenge.

Data analysis

Data are presented as means ± SD of the indicated number (n) of determinations. Statistical analysis was performed using the variance analysis method (*One way ANOVA*). Significant differences between samples were determined through *Dunnet Test*.

Results and Discussion

Nanogel cellular citotoxicity assays

Polymer formulations, including polymer-protein conjugates, are finding increasing clinical use. Synthetic and natural polymers have been explored as drug carriers, but almost all polymers used clinically are still non-biodegradable synthetic polymers [33]. The proven clinical tolerability of dextrin and preliminary observations that dextrin is readily degraded by amylases, suggest that this polymer might be ideal for the development of drug carriers [33]. Furthermore, dextrin is readily excreted due to its low molecular weight, hence accumulation in the tissues is unlikely. In this work, dextrin is used to produce self-assembled nanogels following methodologies described in previous work.

Self-assembled dextrin nanogels, dispersed in water at a concentration of 1.0 mg/ml, were observed using dynamic light scattering (DLS) after filtration through a 0.45 μm membrane. The DLS analysis, in the intensity distribution, revealed two populations with roughly 25 and 150 nm [25, 27]. The conversion to number distribution highlighted only the smaller population of particles, the predominant one. The z-value obtained was 23.6 nm, representative of the average size of polydisperse colloids. The obtained polysdispersity index for the nanogel was low (< 0.5), meaning the sample may be considered homogeneous, consisting of one population with 23.6 nm. Previously [25], the variation of the hydrodynamic diameter (z-value) and zeta-potential of the nanogel with pH was studied and found to be almost constant and close to zero. Although the low zeta potential, the nanogel is stable. This stability can be attributed to the solvation forces, as discussed by Gonçalves and Gama (2008) [25].

In order to evaluate the biocompatibility of the dextrin nanogel, *in vitro* experiments were carried out using mouse embryo fibroblasts 3T3 and bone marrow derived macrophages (BMDM). Cytotoxicity, defined as the "*in vitro* evaluation of toxicological risks using cell culture", is a way to assess the *in*

vitro biocompatibility of materials to be used in biomedical applications. Assays deal with the assessment of various aspects of cellular function such as cell viability and proliferation, loss of membrane integrity, reduced cell adhesion, biosynthetic activity and altered cell morphology [34]. Moreover, the information gained from these types of investigations may be used in the design of further *in vivo* experiments. Given the concerns related to the possible toxicity associated to nanoparticulated materials, we find appropriate to perform a comprehensive characterization of biocompatibility of the nanogel. In this case we address the cytotoxicity and genotoxicity analysis.

Nanogel was resuspended in culture medium at different concentrations ranging between 0.05 and 1 mg/ml. Cells were incubated for 24 or 48 hours with the nanogel suspensions and then tested for cell viability and proliferation using MTS, LDH, Comet and, Live and Dead assays. It should be noted that the higher concentration used was intentionally rather high, as to detect any possible effects caused to the cells by the nanogel, but it must be acknowledged that such a concentration is not likely to be reached in any biomedical application of the material.

Figure 4.1A illustrates the MTS absorbance values obtained for fibroblasts cultured with the nanogel. Fibroblasts in control wells (wells with cDMEM without nanogel) behave normally: the cells adhere after seeding and proliferate, reaching confluency after 48 hours. In wells with the higher concentration of the nanogel (1 mg/ml), cell proliferation is inhibited, especially after 48 hours incubation. In wells treated with 0.1 and 0.05 mg/ml, cells proliferate normally and also reach confluency after 48 hours.

MTS was also used to evaluate BMDM cells viability (Figure 4.1B). In control wells (with cRPMI), the number of cells is relatively constant over time meaning that cells are kept alive. As seen with fibroblasts, after 48 hours, the absorbance values are very low in wells treated with the higher concentration of the nanogel, meaning that cells die to a significant extent after 48 hours of incubation time. Cells treated with the lower concentrations (0.1 and 0.05 mg/ml) show a behavior similar to control wells.

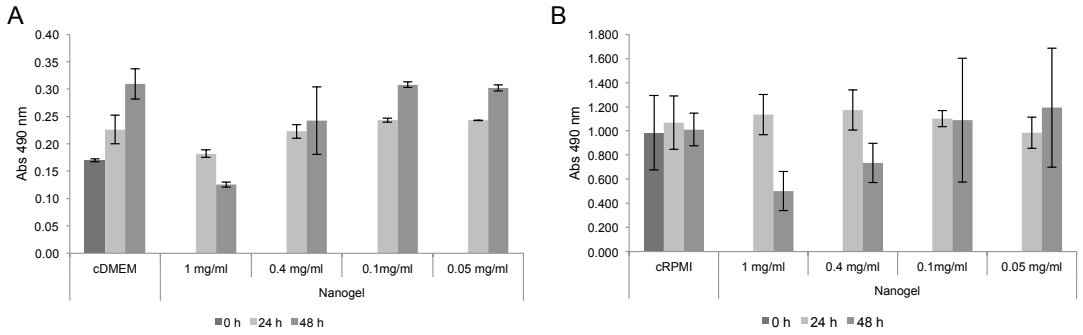

Figure 4.1 – MTS absorbance results. (A) nanogel incubation with mouse embryo fibroblasts 3T3 and (B) nanogel incubation with BMDM. Shown are mean ± SD values (n=3).

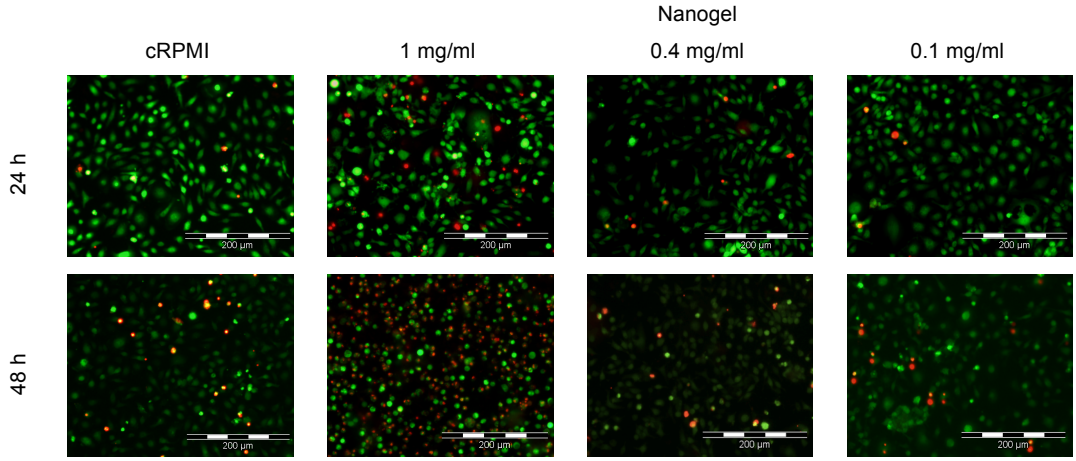

Figure 4.2 – Fluorescence photographs of BMDM cells incubated with the nanogel (0.1 to 1 mg/ml) stained with LIVE/DEAD® Viability/Cytotoxicity Kit for mammalian cells. Live cells are stained in green and dead cells stained in red.

To further evaluate the nanogel cytotoxicity, the Live and Dead® assay was performed using the nanogel in concentrations ranging from 0.1 mg/ml to 1 mg/ml. In Figure 4.2, fluorescence images of BMDM cells, after 24 or 48 hours incubation with the nanogel are shown. These images translate what was revealed by the MTS results: in wells with cRPMI (control wells) the number of living cells (stained in green) is far superior to the number of dead cells (stained in red) and this proportion is maintained over time. When cells are treated with 1 mg/ml of the nanogel, the number of cells stained in red augments, especially after 48 hours incubation. Lower concentrations of the nanogel did not alter significantly the number of living cells comparatively to control wells and the number of green live cells is fairly the same over time.

Similar results were obtained using mouse embryo fibroblasts 3T3 (images not shown).

Table 4.1 reports the percentage of the nanogel citotoxicity in mouse embryo fibroblasts 3T3 and BMDM, measured by the LDH activity released from damaged cells.

Table 4.1 – Percentage of the nanogel citotoxicity in mouse embryo fibroblasts 3T3 and BMDM, evaluated by Cytotoxicity Detection Kit^{PLUS} (LDH). Percentage values where obtained as described in the experimental section. Shown are mean ± SD values (n=3).

Nanogel	Citotoxicity (%) ± SD (%)			
	3 h		20 h	
	3T3 fibroblasts	BMDM	3T3 fibroblasts	BMDM
1 mg/ml	9.9 ± 4	0.5 ± 0	39.8 ± 15	6.5 ±3
0.4 mg/ml	2.8 ± 2	ND[a]	15 ± 5	ND
0.1 mg/ml	ND	ND	ND	ND
0.05 mg/ml	ND	ND	ND	ND

[a] ND, not detected

In agreement with the previous results, 1 mg/ml of the nanogel showed higher toxicity towards fibroblasts. After 20 hours incubation, 0.1 and 0.05 mg/ml of the nanogel did not show any citotoxicity. Citotoxicity was also measured in BMDM cultures by measuring LDH activity released from damaged cells (Table 4.1) and confirmed the previous results.

The genotoxicity of a material may be measured by analyzing the damage caused on DNA. The comet assay or single-cell gel electrophoresis assay is a rapid, sensitive and relatively simple procedure to detect DNA damage [31]. It combines the simplicity of biochemical techniques for detecting DNA single strand breaks (strand breaks and incomplete excision repair sites), alkali-labile sites and cross-linking, using the single cell approach. The advantages of the comet assay, relative to other genotoxicity tests, include its high sensitivity for detecting low levels of both single and double stranded breaks in damaged DNA, the requirement for small numbers of cells per sample, flexibility, low cost, and ease of application [35-37]. Moreover, the comet assay is arguably one of the most widely used tests for genotoxicity available [38, 39], being already described as a reproducible assay to evaluate nanoparticles

genotoxicity [35], and suggested as a diagnostic tool for clinical management of cancer [36]. The genotoxicity of a nanomaterial may result from a direct interaction with DNA, or from an indirect response caused by several factors, including surface stress through direct particle influences on DNA, the release of toxic ions from soluble nanoparticles, or generation of oxidative stress [40].

The comet assay is based on the ability of negatively charged loops/fragments of DNA to be drawn through an agarose gel, in response to an electric field. The extent of DNA migration depends directly on the DNA damage present in the cells [36]. It should be pointed out, that DNA lesions consisting of strand breaks after treatment with alkali either alone or in combination with certain enzymes (as endonucleases) increases DNA migration, whereas DNA-DNA and DNA-protein cross-links result in retarded DNA migration compared to those in concurrent controls [41]. In the procedure described, a suspension of cells, previously treated with different concentrations of the nanogel, was mixed with low melting agarose and spread in slides precoated with normal melting point agarose. After lysis of cells with detergent at high salt concentration, DNA unwinding and electrophoresis was carried out at a specific pH, to be precise pH 13. Unwinding of the DNA and electrophoresis at neutral pH (7-8) predominantly makes possible the detection of double strand breaks and cross-links; at pH 12.2-12.4 the detection of single and double strand breaks, incomplete excision repair sites and cross-links is facilitated; while unwinding and electrophoresis at a pH greater than 12.6, as it was done in this study, expresses alkali labile sites in addition to all types of lesions listed above [42]. When an electric field is applied, the DNA migrates out of the cell, in the direction of the anode, looking like a comet. The size and shape of the comet is related with the extent of the DNA damage [43].

Although it was collected information on different comet assay parameters, data presented here concerns only tail length (TL) as this was the parameter that offered the more reproducible results in duplicates.

Results show that DNA damage assessed by means of TL increases with concentration and time of exposure to nanogel in both studied cell types (3T3

fibroblasts and BMDM). Figure 4.3 presents observed means of TL in each experimental condition.

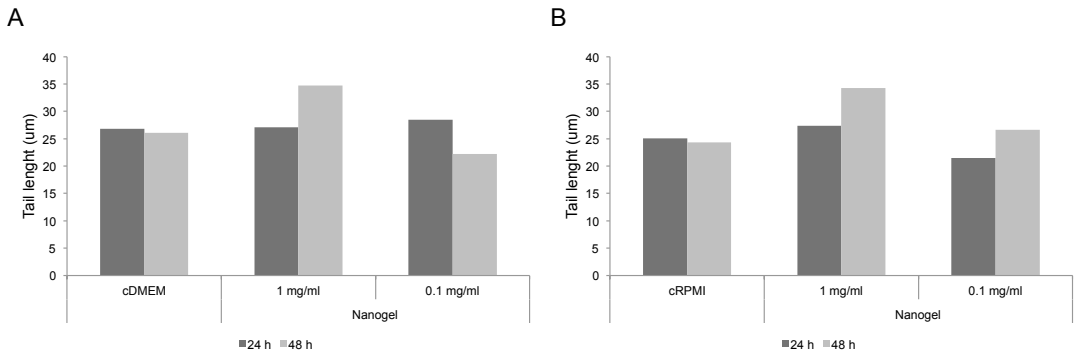

Figure 4.3 – Mean TL values obtained for (A) mousse embryo 3T3 fibroblasts and (B) BMDM.

As one can observe, it can be concluded that 1 mg/ml of the nanogel, after 48 hours incubation, is the experimental condition that leads to higher DNA damage levels relatively to the negative control samples (cDMEM and cRPMI, for fibroblasts and BMDM cultures, respectively). In addition, it seems that the smaller concentration of the nanogel (0.1 mg/ml) did not induce noteworthy DNA damage, since the medium culture (negative control) and samples with the nanogel present similar values of tail length.

The overall obtained results, predominantly indicate a high level of cytocompatibility for the lower concentrations of the nanogel (0.1 and 0.05 mg/ml), under the conditions tested and for the two cell lines used. The results obtained with the higher concentrations, especially 1 mg/ml, indicated that, in the assays conditions, nanogel can present moderate cytotoxicity, inhibiting mouse embryo 3T3 fibroblasts proliferation and diminishing BMDM viability, although no significant DNA damages were detected.

In vivo release and biological activity of rIL-10

Aiming at achieving an effective protein delivery *in vivo*, carriers such as liposomes, polymer micelles, and micro or nanogels have been developed [23, 44-49]. Among them, nanometer-sized polymer hydrogels (nanogels) have

attracted growing interest. By trapping proteins in a hydrated polymer-network, nanogels minimize denaturation, simultaneously allowing a slow, continuous and controlled release of the protein, ideally maintaining an effective concentration for the necessary period of time [20-23]. Nanocarriers enable localized and specific targeting to their intended tissues or cells, thereby allowing the use of lower drug doses [46]. The ideal protein delivery system should be able to enhance the protein solubility; allow its controlled and sustained release; improve biodistribution and targeting of the diseased tissue, *in vivo* [50]. In addition, the nanocarrier must not compromise the bioactivity of the protein. On the other hand, binding/trapping must be stable enough as to allow release only at the site of action, in a sustained, controlled way.

The rIL-10 incorporation by the nanogel suspension was described in a previous work [24], where it has been shown that a part of the encapsulated cytokine may be displaced by adding FBS to the colloidal suspension. In all the *in vitro* experiments, the initial rate release of rIL-10, in the presence of serum proteins, was rapid and then stabilized or even diminished after approximately 8 hours incubation. The rapid initial release rate probably corresponds to the initial fast release of less adsorbed and less stabilized proteins, commonly observed in drug delivery systems, as discussed previously in Carvalho *et al* [24], Gonçalves *et al* [27] and, Gonçalves and Gama [25]. However, most of the protein was retained in the nanogel. We suppose that a strong interaction of the cytokine occur, more likely involving a denatured fraction of rIL-10 with the hydrophobic domains inside the nanogel, leading to the poor release of the cytokine. IL-10 exists in solution predominantly as a non-covalent symmetric homodimer that easily denatures, so it is likely that a considerable (denaturated) fraction rIL-10 becomes irreversibly bound to the nanogel. It also has been shown [24] that the nanogel significantly stabilizes rIL-10, as evaluated by circular dichroism. However, denaturation of the cytokine still proceeds, even when complexed in the nanogel. rIL-10 is a very unstable protein with a predicted half-life of 4.4 ± 0.7 days, at 37ºC in PBS, based on the evaluation of the mean residual ellipticity (θ) variation, at 222 nm [24]. Probably,

the release rate is dependent on the properties of the protein incorporated in the dextrin nanogel. Properties such as hydrophobicity, long-term stability and binding affinity can condition the incorporation and the release profile from (nano)hydrogels [51, 52]. It is likely that a different release profile could be achieved using other kind of bioactive molecules. This possibility will be exploited in forthcoming work using other bioactive proteins.

Indeed, a protein release system based on cholesterol-bearing pullulan (CHP)-based nanogels (a nanogel similar to the one used in this work) for interleukin-12 (IL-12) was described recently [53, 54]. IL-12 is an immunostimulatory cytokine that can suppress not only tumor growth and metastasis, but also infection and allergy. However, as for IL-10, it is difficult to maintain its plasma concentration at an effective level due to its short half-life *in vivo*. The CHP-based nanogels effectively incorporated IL-12 and maintained relatively high serum IL-12 levels in plasma after subcutaneous injection in mice for 12-24 hours. Additionally, tumor growth was successfully inhibited by weekly administrations of CHP/IL-12 complex. Later on, the same group [54] prepared raspberry-like assembled nanogels (A-CHPNG) by cross-linking an acrylate group-modified cholesterol-bearing pullulan nanogel with thiol group-modified poly(ethylene glycol) (PEGSH). They showed that, even in the presence of a high concentration of BSA (50 mg/ml), A-CHPNG did not release IL-12 for at least 72 hours. As with the nanogel/rIL-10 complex, the IL-12 release is driven mainly by an exchange mechanism between IL-12 and BSA proteins and this exchange seem to be minimized by PEG chain which offer a structural stability and a proteins-repellent property. This modification also allowed the maintenance of high plasma IL-12 levels for 72 hours.

A similar approach was attempted in this work using the nanogel-rIL-10 complex. *In vivo* kinetics of rIL-10 release was examined by administrating nanogel/rIL-10 into mice. Figure 4.4 illustrates the levels of IL-10 measured in the sera after administration of rIL-10 and nanogel/rIL-10.

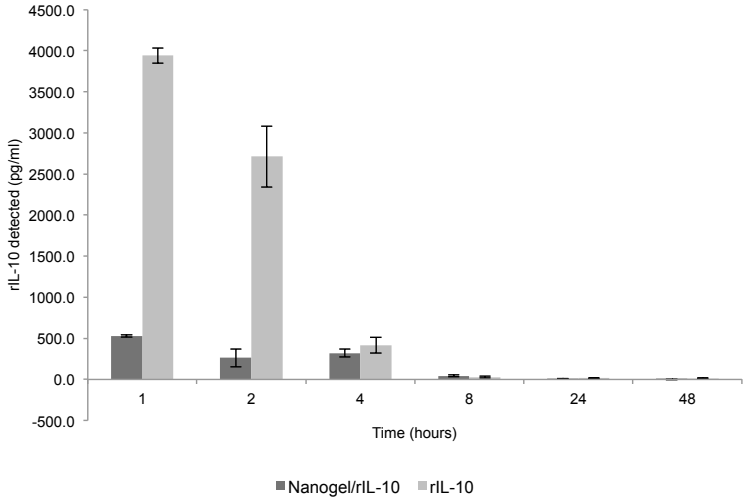

Figure 4.4 – Serum concentrations of IL-10, evaluated by ELISA, after subcutaneous administration of soluble rIL-10 (2.5 μg/mouse) or nanogel/rIL-10 (1 mg/mouse nanogel, 2.5 μg/mouse rIL-10). Shown are means ± SD of IL-10 concentrations (n=3).

After a subcutaneous injection with a rIL-10 solution, the IL-10 concentration in the sera peaked at 1 hour, followed by a rapid decrease. In contrast, serum IL-10 levels remained relatively constant in the nanogel/rIL-10 treated mice. These data suggests that the subcutaneous administration of nanogel/rIL-10 leads to a persistent IL-10 serum concentration for about 4 hours. Again, it is noticeable that the release of the protein occurs to a limited extent. Indeed, as compared with the injected free protein, a much lower amount of protein reaches the blood (about 0.05%, after 1 hour). Again, we stress that this effect is likely due to the instability of the cytokine, other proteins – more stable – may perform better. Interestingly, it is possible to see that while a quick concentration reduction occurs over time in the case of the free protein, the nanogel formulation allows a more constant concentration to be obtained, a highly desirable feature. However, the time frame of the observed release is still limited.

Endotoxin (LPS) from gram-negative bacteria is a major causative agent in the pathogenesis of septic shock, and injection of LPS is a widely used experimental model of systemic inflammation. The toxic effects of LPS are mostly related to macrophage activation leading to the release of multiple inflammatory mediators, as TNF-α and/or IL-1. Previously, we demonstrated that rIL-10 as well as the complex nanogel/rIL-10, efficiently blocked the *in*

vitro production of TNF-α by LPS-activated bone marrow derived macrophages [24]. So, rIL-10 might be an efficient agent to diminish LPS toxicity *in vivo*.

To assess the *in vivo* effects of rIL-10 and nanogel/rIL-10 administration on LPS-induced TNF-α release, rIL-10, nanogel/rIL-10 complex and nanogel were given intraperitoneally (i.p.) to C57 BL/6 mice 30 minutes before the i.p. administration of 100 μg LPS. Blood samples were taken 1.5 h and 6 h after LPS challenge and serum TNF-α quantified by ELISA (Figure 4.5). As controls, mice were also pretreated with PBS (with and without LPS challenge).

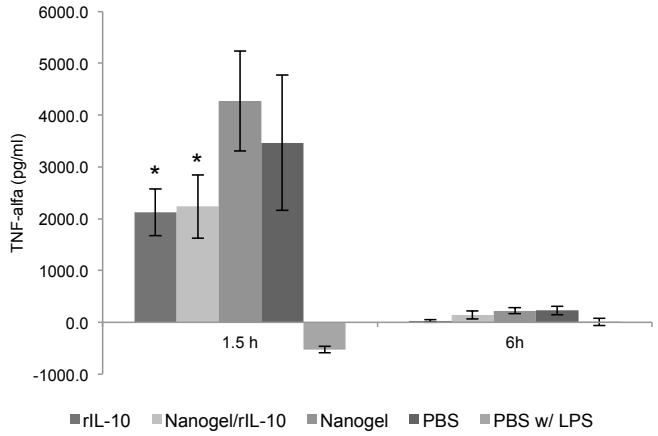

Figure 4.5 – Serum concentrations of TNF-α induced by LPS challenge after 30 minutes i.p. administration of soluble rIL-10 (2.5 μg/mouse), nanogel/rIL-10 (1 mg/mouse nanogel, 2.5 μg/mouse rIL-10) and nanogel (1 mg/mouse). As controls, mice were pretreated with PBS and challenged (PBS) or not (PBS w/ LPS) with LPS. TNF-α was quantified by ELISA and shown are means ± SD of TNF-α concentrations (n=4). * $p < 0.05$ compared to TNF-α values obtained with PBS after LPS challenge.

Sera from blood collected 1.5 h after LPS challenge indicates a substantial reduction in circulating TNF-α in animals receiving rIL-10 and nanogel/rIL-10 prior to LPS administration, comparing to animals receiving the nanogel or PBS. The inhibition of circulating TNF-α is directly related to the protection of mice from lethal endotoxemia [55, 56], an effect that could be observed both with soluble and the nanogel/rIL-10 complex, contributing to the protection against lethal endotoxemia by inducing the suppression of TNF-α.

Despite the low amounts of IL-10 released from the complex nanogel/rIL-10, it is noticeable that the available protein is capable to efficiently diminish TNF-α production to levels achieved with the soluble protein. Therefore, it can be assumed that the rIL-10 is been released from the complex nanogel/rIL-10 in biological significant amounts. Further characterization of the rIL-10 – nanogel interaction is required to better evaluate the potential of this formulation. However, the instability of the cytokine, although stabilized to some extent in the nanogel, apparently does not allow the development of controlled release systems performing in a long time frame.

Conclusions

The therapeutic potential of many pharmaceutical proteins could profit considerably from the availability of controlled released systems for the constant release of the intact biologically active protein. IL-10 has potential application in various medical fields, such as in acute inflammatory diseases, so it is important to develop IL-10 release systems, in order to prevent IL-10 denaturation and to enable a slow controlled release.

We have previously demonstrated that the dextrin nanogel enhances rIL-10 stability and allows the release of biologically active rIL-10 *in vitro* [24]. This work further shows that the dextrin nanogel is biocompatible and that is able to release rIL-10 in biologically relevant amounts over 72 hours, after subcutaneous administration in mice. It also shown that rIL-10, complexed with the nanogel or not, is able to reduce TNF-α production after LPS challenge *in vivo*. Consequently, rIL-10 can be considered as a potential agent of protection against lethal endotoxemia.

The major limitation to this system seems to lie on the strong interaction of IL-10 with the nanogel, due to fast denaturation in spite of the stabilizing effect of the nanogel.

References

(1) Moore, K. W.; de Waal Malefyt, R.; Coffman, R. L.; O'Garra, A., *Annu Rev Immunol* **2001,** 19, 683-765.

(2) Pestka, S.; Krause, C. D.; Sarkar, D.; Walter, M. R.; Shi, Y.; Fisher, P. B., *Annu Rev Immunol* **2004,** 22, 929-79.

(3) de Waal Malefyt, R.; Abrams, J.; Bennett, B.; Figdor, C. G.; de Vries, J. E., *J Exp Med* **1991,** 174, (5), 1209-20.

(4) Fiorentino, D. F.; Zlotnik, A.; Mosmann, T. R.; Howard, M.; O'Garra, A., *J Immunol* **1991,** 147, (11), 3815-22.

(5) Gazzinelli, R. T.; Oswald, I. P.; James, S. L.; Sher, A., *J Immunol* **1992,** 148, (6), 1792-6.

(6) Bogdan, C.; Vodovotz, Y.; Nathan, C., *J Exp Med* **1991,** 174, (6), 1549-55.

(7) MacNeil, I. A.; Suda, T.; Moore, K. W.; Mosmann, T. R.; Zlotnik, A., *J Immunol* **1990,** 145, (12), 4167-73.

(8) Defrance, T.; Vanbervliet, B.; Briere, F.; Durand, I.; Rousset, F.; Banchereau, J., *J Exp Med* **1992,** 175, (3), 671-82.

(9) Groux, H.; Bigler, M.; de Vries, J. E.; Roncarolo, M. G., *J Immunol* **1998,** 160, (7), 3188-93.

(10) de Waal Malefyt, R.; Haanen, J.; Spits, H.; Roncarolo, M. G.; te Velde, A.; Figdor, C.; Johnson, K.; Kastelein, R.; Yssel, H.; de Vries, J. E., *J Exp Med* **1991,** 174, (4), 915-24.

(11) Willems, F.; Marchant, A.; Delville, J. P.; Gerard, C.; Delvaux, A.; Velu, T.; de Boer, M.; Goldman, M., *Eur J Immunol* **1994,** 24, (4), 1007-9.

(12) Creery, W. D.; Diaz-Mitoma, F.; Filion, L.; Kumar, A., *Eur J Immunol* **1996,** 26, (6), 1273-7.

(13) Leon, L. R.; Kozak, W.; Rudolph, K.; Kluger, M. J., *Am J Physiol* **1999,** 276, (1 Pt 2), R81-9.

(14) Howard, M.; Muchamuel, T.; Andrade, S.; Menon, S., *J Exp Med* **1993,** 177, (4), 1205-8.

(15) Gerard, C.; Bruyns, C.; Marchant, A.; Abramowicz, D.; Vandenabeele, P.; Delvaux, A.; Fiers, W.; Goldman, M.; Velu, T., *J Exp Med* **1993,** 177, (2), 547-50.

(16) Berzofsky, J. A.; Ahlers, J. D.; Belyakov, I. M., *Nat Rev Immunol* **2001,** 1, (3), 209-19.

(17) Pullerits, T., *Curr Pharm Des* **2002,** 8, (20), 1845-53.

(18) Hubel, K.; Dale, D. C.; Liles, W. C., *J Infect Dis* **2002,** 185, (10), 1490-501.

(19) Asadullah, K.; Sterry, W.; Volk, H. D., *Pharmacol Rev* **2003,** 55, (2), 241-69.

(20) Murthy, N.; Thng, Y. X.; Schuck, S.; Xu, M. C.; Frechet, J. M., *J Am Chem Soc* **2002,** 124, (42), 12398-9.

(21) Murthy, N.; Xu, M.; Schuck, S.; Kunisawa, J.; Shastri, N.; Frechet, J. M., *Proc Natl Acad Sci U S A* **2003,** 100, (9), 4995-5000.

(22) Leonard, M.; De Boisseson, M. R.; Hubert, P.; Dalencon, F.; Dellacherie, E., *J Control Release* **2004,** 98, (3), 395-405.

(23) Kim, S.; Kim, J. H.; Jeon, O.; Kwon, I. C.; Park, K., *Eur J Pharm Biopharm* **2009,** 71, (3), 420-30.

(24) Carvalho, V.; Castanheira, P.; Faria, T. Q.; Goncalves, C.; Madureira, P.; Faro, C.; Domingues, L.; Brito, R. M. M.; Vilanova, M.; Gama, F. M., *Int J Pharm* **2010,** 400, 234-242.

(25) Goncalves, C.; Gama, F. M., *Eur Polym J* **2008,** 44, (11), 3529-3534.

(26) Goncalves, C.; Torrado, E.; Martins, T.; Pereira, P.; Pedrosa, J.; Gama, M., *Colloid Surface B* **2010,** 75, (2), 483-489.

(27) Goncalves, C.; Martins, J. A.; Gama, F. M., *Biomacromolecules* **2007,** 8, (2), 392-398.

(28) Tushinski, R. J.; Oliver, I. T.; Guilbert, L. J.; Tynan, P. W.; Warner, J. R.; Stanley, E. R., *Cell* **1982,** 28, (1), 71-81.

(29) Zhang, X.; Goncalves, R.; Mosser, D. M., *Curr Protoc Immunol* **2008,** Chapter 14, Unit 14 1.

(30) Mosmann, T., *J Immunol Methods* **1983,** 65, (1-2), 55-63.

(31) Singh, N. P.; Mccoy, M. T.; Tice, R. R.; Schneider, E. L., *Exp Cell Res* **1988,** 175, (1), 184-191.

(32) Costa, S.; Coelho, P.; Costa, C.; Silva, S.; Mayan, O.; Santos, L. S.; Gaspar, J.; Teixeira, J. P., *Toxicology* **2008,** 252, (1-3), 40-8.

(33) Hreczuk-Hirst, D.; Chicco, D.; German, L.; Duncan, R., *Int J Pharm* **2001,** 230, (1-2), 57-66.

(34) Chiellini, E. E.; Chiellini, F.; Solaro, R., *J Nanosci Nanotechnol* **2006,** 6, (9-10), 3040-7.

(35) Collins, A. R.; Dobson, V. L.; Dusinska, M.; Kennedy, G.; Stetina, R., *Mutat Res-Fund Mol M* **1997,** 375, (2), 183-193.

(36) Collins, A. R.; Oscoz, A. A.; Brunborg, G.; Gaivao, I.; Giovannelli, L.; Kruszewski, M.; Smith, C. C.; Stetina, R., *Mutagenesis* **2008,** 23, (3), 143-151.

(37) Brendler-Schwaab, S.; Hartmann, A.; Pfuhler, S.; Speit, G., *Mutagenesis* **2005,** 20, (4), 245-254.

(38) Anderson, D.; Plewa, M. J., *Mutagenesis* **1998,** 13, (1), 67-73.

(39) Anderson, D.; Yu, T. W.; McGregor, D. B., *Mutagenesis* **1998,** 13, (6), 539-555.

(40) Barnes, C. A.; Elsaesser, A.; Arkusz, J.; Smok, A.; Palus, J.; Lesniak, A.; Salvati, A.; Hanrahan, J. P.; de Jong, W. H.; Dziubaltowska, E.; Stepnik, M.; Rydzynski, K.; McKerr, G.; Lynch, I.; Dawson, K. A.; Howard, C. V., *Nano Lett* **2008,** 8, (9), 3069-3074.

(41) Tice, R. R.; Agurell, E.; Anderson, D.; Burlinson, B.; Hartmann, A.; Kobayashi, H.; Miyamae, Y.; Rojas, E.; Ryu, J. C.; Sasaki, Y. F., *Environ Mol Mutagen* **2000,** 35, (3), 206-221.

(42) Miyamae, Y.; Iwasaki, K.; Kinae, N.; Tsuda, S.; Murakami, M.; Tanaka, M.; Sasaki, Y. F., *Mutat Res-Gen Tox En* **1997,** 393, (1-2), 107-113.

(43) Fairbairn, D. W.; Olive, P. L.; Oneill, K. L., *Mutat Res-Rev Genet* **1995,** 339, (1), 37-59.

(44) Haag, R.; Kratz, F., *Angew Chem Int Ed Engl* **2006,** 45, (8), 1198-215.

(45) Nair, L. S.; Laurencin, C. T., *Adv Biochem Eng Biot* **2006,** 102, 47-90.

(46) Devalapally, H.; Chakilam, A.; Amiji, M. M., *J Pharm Sci* **2007,** 96, (10), 2547-65.

(47) Lukyanov, A. N.; Torchilin, V. P., *Adv Drug Deliv Rev* **2004,** 56, (9), 1273-89.

(48) Branco, M. C.; Schneider, J. P., *Acta Biomater* **2009,** 5, (3), 817-31.

(49) Nayak, S.; Lyon, L. A., *Angew Chem Int Ed Engl* **2005,** 44, (47), 7686-708.

(50) Tan, M. L.; Choong, P. F.; Dass, C. R., *Peptides* **2010,** 31, (1), 184-93.

(51) Lee, K. Y.; Yuk, S. H., *Prog Polym Sci* **2007,** 32, (7), 669-697.

(52) Lee, K. Y.; Mooney, D. J., *Chem Rev* **2001,** 101, (7), 1869-1879.

(53) Shimizu, T.; Kishida, T.; Hasegawa, U.; Ueda, Y.; Imanishi, J.; Yamagishi, H.; Akiyoshi, K.; Otsuji, E.; Mazda, O., *Biochem Bioph Res Co* **2008,** 367, (2), 330-335.

(54) Hasegawa, U.; Sawada, S.; Shimizu, T.; Kishida, T.; Otsuji, E.; Mazda, O.; Akiyoshi, K., *Journal of Controlled Release* **2009,** 140, (3), 312-317.

(55) Wan, J. M.; Sit, W. H.; Lee, C. L.; Fu, K. H.; Chan, D. K., *Int Immunopharmacol* **2006,** 6, (5), 750-8.

(56) Tang, Y.; Li, B.; Wang, N.; Xie, Y.; Wang, L.; Yuan, Q.; Zhang, F.; Qin, J.; Peng, Z.; Ning, W.; Hu, G.; Li, J.; Tao, L., *Int Immunopharmacol* **2010,** 10, (5), 580-3.

Chapter 5 | Development of an injectable and biodegradable dextrin hydrogel and hydrogel/nanogel

Dextrin, a naturally occurring polymer, was used to develop a biodegradable hydrogel without using chemical initiators. Dextrin was first oxidized (oDex) with sodium periodate and then crosslinked with adipic acid dihidrazide, a non-toxic and non-mutagenic covalent crosslinking molecule. Further, a new bidimensional composite hydrogel, made of oxidized dextrin and with incorporated dextrin nanogels (oDex-nanogel), was also developed. The mechanical properties and biocompatibility of the obtained oDex hydrogel were analysed. The porous structure of both hydrogels was evaluated by Cryo-scanning electron microscopy and their degradation kinetics analysed. The dextrin nanogel release from the oDex-nanogel hydrogel, along with the degradation in vitro, was evaluated by fluorimetry, using a FITC-labelleled nanogel. Preliminary assays on the potential of this material as a delivery system were performed using curcumin (CM), interleukin-10 (IL-10) and β-galactosidase (β-Gal).

The oDex hydrogels showed good mechanical properties and biocompatibility, allowing the proliferation of mouse embryo fibroblasts 3T3 cultured on top of the gel. The gelification time may be controlled selecting the concentrations of the polymer and reticulating agent. Typically, gelification times in the range of the 2-10 minutes were observed, thus allowing its injectability. Both the oDex and oDex-nanogel hydrogels are biodegradable and present a three-dimensional network with a continuous porous structure. The obtained oDex-nanogel hydrogel enables the release of the dextrin nanogel over an extended period of time, paralleling the mass loss curve due to the degradation of the material. The dextrin nanogel allowed the efficient incorporation of CM, IL-10 and β-Gal in the oDex hydrogel.

Introduction

Hydrogels are three-dimensional, cross-linked networks of water-soluble polymers that can be prepared from virtually any water-soluble polymer, encompassing a variety of chemical compositions and bulk physical characteristics [1]. In addition, hydrogels can be formulated in a wide range of physical forms, as slabs, microparticles, nanoparticles (nanogels), coatings, and films. They are usually used in clinical practice and experimental medicine in diverse applications, including tissue engineering and regenerative medicine, diagnostics, cellular immobilization, as barrier materials to regulate biological adhesions, and as drug delivery systems [1-5]. Hydrogels can be obtained from natural sources or prepared through synthetic pathways. Natural polymers are usually biodegradable and offer excellent biocompatibility; on the other hand, synthetic polymers are available in a wide variety of compositions with readily adjustable properties [6].

However, hydrogels present some limitations regarding drug delivery: the high water content and large pore sizes frequently result in relatively rapid release. In the last decade, composite systems where micro or nanogels are incorporated in a bulk hydrogel matrix, appeared as a platform for drug delivery [7-10]. The micro or nanogel particles can act as a drug reservoir from which release can be triggered by a suitable stimulus, or simply released in a diffusion-controlled manner. Simultaneous diffusion of different molecules at different rates can be obtained from the same platform, by adding two (or more) populations of micro or nanogels, each loaded with one kind of drug, in the same hydrogel matrix [8, 10]. The major advantage relies on the improvement of the kinetic release profile of the drug, as the nanogel phase provides an additional diffusion barrier moderating or eliminating the initial burst release typically observed in hydrogel or nanogel drug delivery systems.

Starch-based polymers, as dextrin, are examples of natural polymers with great potential for the development of hydrogels, as reported in the literature [11, 12]. Dextrin derives from starch by partial thermal degradation under acidic conditions or enzymatic hydrolysis. It is a α-1,4 poly(glucose) polymer with minimal branching. The proven clinical tolerability [13] of dextrin and its efficient absorption due to degradation by amylases [14], suggest that this polymer might be ideal for development as a drug carrier [15]. Furthermore, dextrin is readily excreted due to its low molecular weight (~2kDa), hence accumulation in the tissues is unlikely. Additionally, if longer plasma circulation times are required, dextrin's main polymeric chain can be reproducibly modified to slow the rate of degradation, which provides the opportunity to design conjugates with greater capacity for tissue targeting [15].
Recently Carvalho *et al* [11, 12] produced dextrin hydrogels, namely dextrin-VA and dextrin-HEMA, and verified its non-citotoxicity, as well as its appealing diffusivity and degradability profiles for targeted delivery therapeutics. Moreover, Gonçalves *et al.* developed and characterized a nanogel obtained by self-assembling of hydrophobized dextrin [16, 17]. The nanogel obtained has high colloidal stability and spherical shape. In preceding work [18], it was shown that dextrin nanogels effectively incorporated and stabilized a recombinant mutated interleukin-10 (rIL-10), allowing for the release of biologically active rIL-10 over time.
In this work, an expeditious methodology initially developed by Bouhadir and colleagues [19] was used to prepare degradable injectable hydrogels from oxidized dextrin (oDex) and adipic acid dihydrazide, without the use of any chemical initiator. The networks were evaluated regarding their rheological properties, as well their degradation at physiologic pH. A composite system made from dextrin nanogel and oDex hydrogel is also described. Their degradation and nanogel release profile were also evaluated. Simultaneously, curcumin (CM), an anti-inflammatory and anti-cancer molecule [20-23]; interleukin-10 (IL-10), an immuno-regulatory cytokine with strong anti-inflammatory activity [24-29]; and β-galactosidase (β-Gal) were incorporated in

the dextrin nanogel and their release profiles from the composite system evaluated.

Experimental

Materials

All reagents used were of laboratory grade and purchased from Sigma-Aldrich, unless stated otherwise. Dextrin - Koldex 60 starch was a generous gift from Tate & Lyle. All other chemicals and solvents used in this work were of the highest purity commercially available.

Preparation of oDex hydrogels

Dextrin oxidation.

Briefly, aqueous solutions of dextrin (2% w/v) were oxidized with a 2 mL sodium m-periodate solution (Panreac), whose concentration varied according to the desired theoretical degree of oxidation (DO_t). The flasks were wrapped in aluminium foil and the reaction was developed while stirring for 20h at room temperature, after which an equimolar amount of diethylene glycol was added dropwise, to reduce any unreacted periodate. The resulting solution was dialyzed for 3 days against water, using a dialysis membrane with a MWCO 1000 Da, and then lyophilized for 10 days

Determination of aldehyde groups by ^{1}H NMR analysis.

The degree of oxidation (DO) of oDex is defined as the number of oxidized residues per 100 glucose residues, quantified using the *tert*-butylcarbazate (tBC) method as described elsewhere [19, 30]. Briefly, oDex was dissolved in phosphate buffer pH 6.0, 0.1M (1 mL, 1% w/v); subsequently a 5-fold excess of tBC was dissolved in the same buffer (1 mL) and added separately. The mixture was allowed to react for 24h at room temperature. Excess low-molecular weigh tBC was then removed using a PD-10 desalting column system and the filtrate was lyophilized for 48h. Afterwards the resulting

product was dissolved in deuterated water (D_2O) (7.5 mg/ml) and analyzed by ^1H NMR. The ^1H NMR spectrum was used to determine DO, calculated as a peak area ratio in the NMR spectra according to equation 5.1.

$$DO\ (\%) = (X/Y) \times 100 \quad \text{(Eq. 5.1)}$$

Where, X is the average integral corresponding to the peak at δ 7.3 ppm and Y is the average integral of the anomeric protons at δ 4.8 ppm and δ 5.4 ppm

Preparation of oDex-ADH hydrogels.

oDex was dissolved in phosphate buffer pH 6.0, 0.1M (30% w/v) at room temperature and an adipic acid dihydrazide (ADH) solution (prepared separately) was added at different concentrations (5%, 15% and 30% in molar base, taking into account the number of glucose residues in the original dextrin). The crosslinking reaction was allowed to proceed during 2h. The material was considered as gelified when it stopped slipping along a 90° inclined surface.

Preparation of oDex-nanogel hydrogels.

Dextrin nanogel was prepared as described in Vera Carvalho *et al* [18]. Briefly, the self-assembled hydrogel nanoparticles were obtained by dissolving the lyophilized dextrin-VMA-SC_{16} in PBS. The dissolution was accomplished after approximately 16 hours at room temperature, with stirring. The nanogel formation was confirmed by dynamic light scattering, as described previously [18, 31-33]. oDex, DO 35%, (30% w/v) was dissolved in PBS (oDex) or in a suspension of nanogel (oDex-nanogel) for approximately 16 hours at room temperature. Then, the oDex suspensions were mixed with 5% (in molar base taking into account the number of glucose residues in the original dextrin) adipic acid dihydrazide with the pipette tip. The crosslinking was allowed to proceed at room temperature for about 2 hours.

Mechanical analysis

The mechanical properties of crosslinked dextrin hydrogels were assessed using a Mechanical Tester - Shimadzu-AG-IS 1 kN Testing Instrument. Each hydrogel disc (superficial area = 133 mm^2) was placed between two parallel

metallic circumferential plates, so that the compressive force would be uniform along the sample, and compressed at room temperature with a constant deformation rate of 0.5 mm min^{-1}. For each condition, samples in triplicate were analysed; the values given in the results section represent the mean and the standard deviation.

Standard biocompatibility assays

The cell cytotoxicity was evaluated for un-crosslinked macromonomer solutions, crosslinked hydrogels and hydrogel degradation extracts using Live and Dead® and MTT assays, as described below.

Mouse embryo fibroblasts 3T3 culture.

Mouse embryo fibroblasts 3T3 (ATCC CCL-164) were grown in Dulbecco's modified Eagle's media (Sigma) supplemented with 10% newborn calf serum (Invitrogen, UK) and 1 μg/ml penicillin/streptavidin (DMEM complete medium) at 37ºC in a 95% humidified air containing 5% CO_2. At 80% confluency, 3T3 fibroblasts were harvested with 0.05% (w/v) trypsin-EDTA and subcultivated in the same medium.

Live and Dead assay.

The LIVE/DEAD® Viability/Cytotoxicity Kit for mammalian cells (Invitrogen, UK) was used to determine cell viability. This kit provides two-colour fluorescence cell viability assay, based on the simultaneous determination of live and dead cells with two probes that measure intracellular esterase activity and plasma membrane integrity.

Briefly, mousse embryo fibroblasts 3T3 were seeded (5 x 10^4 cells/well) in a 6 well polystyrene plate (Orange Scientific) and incubated at 37ºC, 5% CO_2 for 24 hours. Then, the culture medium was removed and hydrogel discs (Ø4mm, 2 mm thickness) were placed on the wells, in direct contact with cells. At regular time intervals, 200 μL of a solution of 2 μM calcein AM and 4 μM ethidium homodimer-1, in sterile PBS, were added to the wells, incubated for 30 to 45 minutes at 37ºC, 5% CO_2 (as indicated by the manufacturer) and

visualized in a fluorescence microscope. Latex discs and agar gel (U.S. Pharmacopeia) were used as positive and negative controls, respectively.

MTT assay.

The viability of the 3T3 fibroblast cells was determined using 3-[4,5-dimethylthiazol-2-yl]-2,5-diphenyl tetrazolium bromide (MTT) assay (Sigma-Aldrich, USA). The MTT assay accurately measure the activity of living cells via mitochondrial dehydrogenase activity. Mitochondrial dehydrogenases of viable cells cleave the tetrazolium ring, yielding purple MTT formazon crystals that can be dissolved in DMSO, resulting in a purple solution that is spectrophotometrically measured. The increase in cell number results in an increase in absorbance.

The fibroblasts adhesion to oDex hydrogels was also evaluated, by MTT assay. For this assay, oDex hydrogels were formed at the bottom of the wells of a 96 well polystyrene culture plate. After 2h of polymerization, the oDex hydrogels were washed with PBS and three times with cDMEM. Then, 3T3 fibroblasts cells were added ($3x10^3$ cells/well) to each well. The culture medium was refreshed every 2 days. For the control assays, cells were grown directly in the bottom of the wells. After 48h, hydrogels were carefully washed three times with PBS, to remove floating cells, and the cell layer was detached before conducting the MTT assay, as previously described by Carvalho et al [12].

The biocompatibility of the hydrogels degradation extracts was also evaluated. In a few words, 3T3 fibroblasts cells were seeded ($5x10^2$ cells/well) in a 96 well polystyrene plate and exposed to hydrogel degradation extracts (200 μL; 1:1, 1:2 and 1:4 dilutions) obtained separately from three oDex hydrogels (DO 40%). After 48h of incubation at 37°C, the cytotoxicity of the extracts was evaluated using the MTT assay.

Furthermore, oxidized dextrin and ADH alone were also tested for their cytotoxic potential. Briefly, 3T3 cells ($5x10^2$ cells/well) seeded in a 96 well polystyrene plate were exposed to increasing concentrations of these components for 48h at 37°C, after which the cytotoxicity was evaluated using the MTT assay. Oxidized dextrin was firstly sterilized by ethylene oxide (EtO)

sterilization process. All biocompatibility measurements were made in triplicate or more and the results given are the mean.

Cryo-scanning electron microscopy (Cryo-SEM) analysis

The topography and porosity of the hydrogels were studied by Cryo-SEM. The oDex and oDex-nanogel hydrogels (30% w/v oDex, 10 mg/ml nanogel) were rapidly immersed in liquid nitrogen slush at -210ºC for 2 min and vacuum transferred to an Alto 2500 (Gatan Inc., CA) cryo preparation chamber attached to a JEOL JSM 6301F scanning electron microscope. Frozen samples were fractured at -185ºC, etched during 90 seconds (to partially sublimate water from the fractured hydrogel surface), and finally gold-coated for 2 min. Samples were viewed at -130ºC and the resulting SEM images were analyzed using ImageJ software (National Institutes of Health, USA).

Hydrogel's degradation profile

After being prepared and weighted (W_i), the hydrogels were immersed in PBS or cDMEM (diffusion medium), and incubated at 37ºC. At regular intervals, they were removed from the solutions, blotted with filter paper, weighed (W_t) and returned to the same container. The buffer solution was replaced at each measurement and the old one stored for further analysis. The percentage of mass loss was determined using equation 5.2:

$$\text{Mass loss } (\%) = 100 - [(W_t / W_i) \times 100] \quad \text{(Eq. 5.2)}$$

Release assays

In order to assess the oDex and oDex-nanogel hydrogels potential for drug delivery, the nanogel release from the oDex-nanogel hydrogels was accessed, followed by the evaluation of the release of several molecules incorporated directly in the oDex hydrogel or in the dextrin nanogel.

Nanogel/FITC.

FITC is a fluorescent probe commonly used in biological studies, owing to its biocompatibility. To obtain nanogels labeled with FITC, a nanogel solution was formed by dissolving 10 mg of dextrin-VMA-SC_{16} in 1.3 ml 0.1M sodium phosphate buffer pH 7 and stirred for 30 min. Simultaneously, a fluorescein solution was prepared by dissolving 5 mg of SAMSA [(5-(2-(and-3)-S-(acetylmercapto)succinoyl) amino) Invitrogen] fluorescein in 0.5 ml of 0.1 M NaOH and stirred for 15 min. Then, 7 µl of 6M HCl and 0.1 ml of 0.5M NaPO4 buffer pH 7 were added and stirred for 10 min. Finally, the nanogel solution and the fluorescein solution were mixed and stirred for 30 min. Unbound FITC was separated using a Sephadex G25 PD10 column (Amersham Biosciences) equilibrated with PBS, and the labelled nanogel (nanogel/FITC) was eluted with PBS.

The oDex-nanogel/FITC hydrogel was obtained as described previously (preparation of oDex-nanogel hydrogel). Degradation assays were performed also as described above. The nanogel/FITC release from the oDex-nanogel hydrogels was evaluated by fluorimetry. The fluorescence intensity of the supernatant collected from the degrading hydrogels, at regular intervals, was measured using a spectrofluorimeter (Fluorolog Horiba Jobin Yvon). Fluorescence spectra were collected using an excitation wavelength of 460 nm and recording emission between 470 and 600 nm at 1 nm intervals. The slit width was set at 6.0 nm for the excitation and emission. The fluorescence intensity was measured at the maximum of the peak obtained (520 nm).

The percentage of nanogel/FITC released from the oDex-nanogel hydrogel was obtained by equation 5.3:

$$\text{Nanogel/FITC release (\%)} = [\text{nanogel/FITC}]_{det} / [\text{nanogel/FITC}]_{tot} \times 100 \quad \text{(Eq. 5.3)}$$

where, $[\text{nanogel/FITC}]_{det}$ is the fluorescence intensity detected in the PBS supernatant collected during degradation and $[\text{nanogel/FITC}]_{tot}$ is the fluorescence intensity obtained dispersing the nanogel/FITC in the same volume as used in the degradation assays.

Nanogel/CM.

A curcumin (CM) solution was prepared by dissolving CM in ethanol (1 mg/ml). The complex nanogel/CM was formed by adding CM (0.03 mg/ml

or 0.1 mg/ml), to the nanogel suspension (3 mg/ml or 10 mg/ml nanogel, respectively). The incorporation was accomplished after approximately 16 h, at room temperature with stirring. The oDex-nanogel/CM hydrogel was obtained as described previously (preparation of oDex-nanogel hydrogel), immersed in PBS and incubated at 37ºC.

The CM incorporation and release from the oDex-nanogel hydrogels was evaluated by visually comparing the color of the hydrogels after being submersed in PBS. A spectrophotometric quantitative evaluation of the release rate was not possible due to the presence of colored material being released from the hydrogel while degrading.

Nanogel/rIL-10.

The nanogel/rIL-10 complex was obtained by dissolving the lyophilized dextrin-VMA-SC_{16} in a rIL-10 solution (5 mg/ml nanogel, 25 μg/ml rIL-10), as previously described [18].The oDex-nanogel/rIL-10 hydrogel was then prepared as described. The oDex hydrogel with incorporated free rIL-10 was obtained by dissolving oDex in a rIL-10 solution (25 ug/ml) and then by adding adipic acid dihydrazide has already described.

The rIL-10 release from the oDex hydrogels, after being immersed in PBS with 10% FBS and incubated at 37ºC, was evaluated by quantifying by ELISA, the free rIL-10 in the diffusion medium. The percentage of rIL-10 released was obtained by the following equation (equation 5.4):

$$\text{rIL-10 release (\%)} = [\text{rIL-10}]_{det} / [\text{rIL-10}]_{tot} \times 100 \qquad \text{(Eq. 5.4)}$$

where, $[\text{rIL-10}]_{det}$ is the amount of rIL-10 detected in the diffusion medium at determined time and $[\text{rIL-10}]_{tot}$ is the total amount of rIL-10 entrapped in the dextrin nanogel or in the hydrogel.

Circular dichroism (CD) measurements of rIL-10. The secondary structure of rIL-10 was investigated using CD. Spectra were obtained on an Olis DSM 20 circular dichroism spectropolarimeter continuously purged with nitrogen, equipped with a Quantum Northwest CD 150 temperature-controlled cuvette and controlled by the Globalworks software.

rIL-10 stability, at 37ºC, was accessed by obtaining CD spectra of the sample, at determined intervals of time. CD spectra of rIL-10 (0.25 mg/ml) in PBS,

were collected using a 0.2 mm path length cuvette, between 190 and 260 nm at 1 nm intervals. Three scans with an integration time of 4 s were averaged for each measurement. Spectra were acquired at 37°C. The results are expressed in terms of mean residue ellipticity $[\theta]_{MRW}$ in deg cm^2 $dmol^{-1}$, according to the equation $[\theta]_{MRW} = \theta_{obs} \times 100\ MW/(lcN)$, where θ_{obs} is the observed ellipticity in mdeg, MW is the protein molecular weight in g/mol, l is the cuvette path length in cm, c is the protein concentration in g/l and N is the number of residues of the protein.

Nanogel/β-Gal.

The complex nanogel/β-Gal was obtained by dissolving the lyophilized dextrin-VMA-SC_{16} in a β-Gal solution (3 mg/ml nanogel and 1 mg/ml β-Gal); the oDex-nanogel/β-Gal hydrogel was obtained as described previously (preparation of oDex-nanogel hydrogel). An oDex-β-Gal hydrogel was prepared by dissolving oDex in a β-Gal solution (1 mg/ml) and by adding adipic acid dihydrazide.

The β-Gal release from the oDex hydrogels, after being immersed in PBS, was evaluated by measuring β-Gal activity in the supernatant.

β-Gal was assayed by using a reaction mixture containing 5 mM o-nitrophenyl-β-D-galactopyranoside, 18 mM sodium phosphate, and the appropriately diluted supernatant collected from the controlled release assay. After incubation at 30ºC for 10 min, the reaction was stopped with 200 mM borate buffer (pH 9.8). The colour that developed as a result of o-nitrophenol liberation was measured at 410 nm. One unit of β-Gal corresponds to the release of 1.0 μmol of o-nitrophenol per minute at pH 4.5, at 30ºC.

The relative activity of the β-Gal released was obtained by the following equation (equation 5.5):

$$\text{Relative activity of β-Gal release (\%)} = [\beta\text{-Gal}]_{det} / [\beta\text{-Gal}]_{tot} \times 100 \quad \text{(Eq. 5.5)}$$

where, $[\beta\text{-Gal}]_{det}$ is the activity of the β-Gal detected in the supernatant at a determined time and $[\beta\text{-Gal}]_{tot}$ is the activity of the total β-Gal entrapped in the dextrin nanogel or in the hydrogel.

Data analysis

Data are presented as means ± SD of the indicated number (n) of determinations. Statistical analysis was performed using the variance analysis method (*One way ANOVA*). Significant differences between samples were determined through *Dunnet Test*.

Results and discussion

Hydrogel production

The periodate oxidation reaction of carbohydrates is widely known and routinely used as a tool for elucidating the structural features of polysaccharides [34, 35]. In homopolysaccharides, such as dextrin, this oxidation reaction is characterized by the specific cleavage of the C2-C3 linkage of glucopyranoside rings, yielding two aldehyde groups per glucose unit [36] (Scheme 5.1).

Scheme 5.1 – Periodate oxidation of dextrin, yielding two aldehyde groups at positions C2 and C3 of a D-glucose unit.

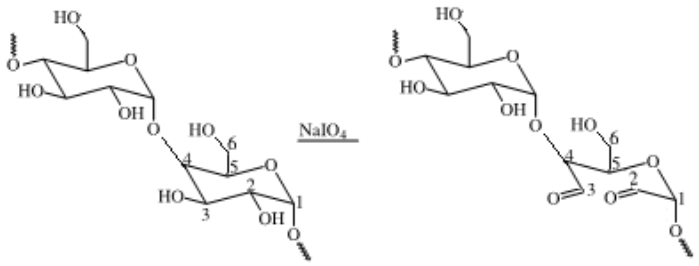

The quantification of aldehyde groups, i.e. oxidation degree (DO), was performed using tBC, as previously described by Jia *et al* and Bouhadir *et al* [19, 30]. Carbazates are well known to react with aldehydes to form stable carbazones in a similar manner to hydrazone formation, making it possible to determine the aldehyde content of dextrin by ^{1}H NMR spectroscopy analysis.

Figure 5.1 depicts a typical ^{1}H NMR spectra obtained for 25% oxidized dextrin (oDex 25%). The peaks between δ 4.0 and δ 3.4ppm are assigned to protons at positions 2, 3, 4, 5 and 6, while the peak at δ 5.4 ppm is attributed to the anomeric proton from the glucose unit. The spectrum also shows a small peak at δ 5.3 ppm corresponding to the anomeric proton in dextrin with α-1,6 linkages (<5% of the total dextrin [15]). The three peaks between δ 7.4 and δ 7.2 ppm are assigned to the proton attached to the carbon that was modified with tBC, and the singlet at δ 1.5 ppm assigned to tBC.

The degree of oxidation of oDex can be easily controlled by the relative quantity of sodium periodate used (the DO increased as the amount of added periodate increased – data not shown), enabling free aldehyde reactive groups to create covalent linkages with reticulating molecules (e.g. ADH), as well as with cellular adhesion binding peptides (e.g GRGDY [19]) or even with specific drugs for targeted controlled delivery systems.

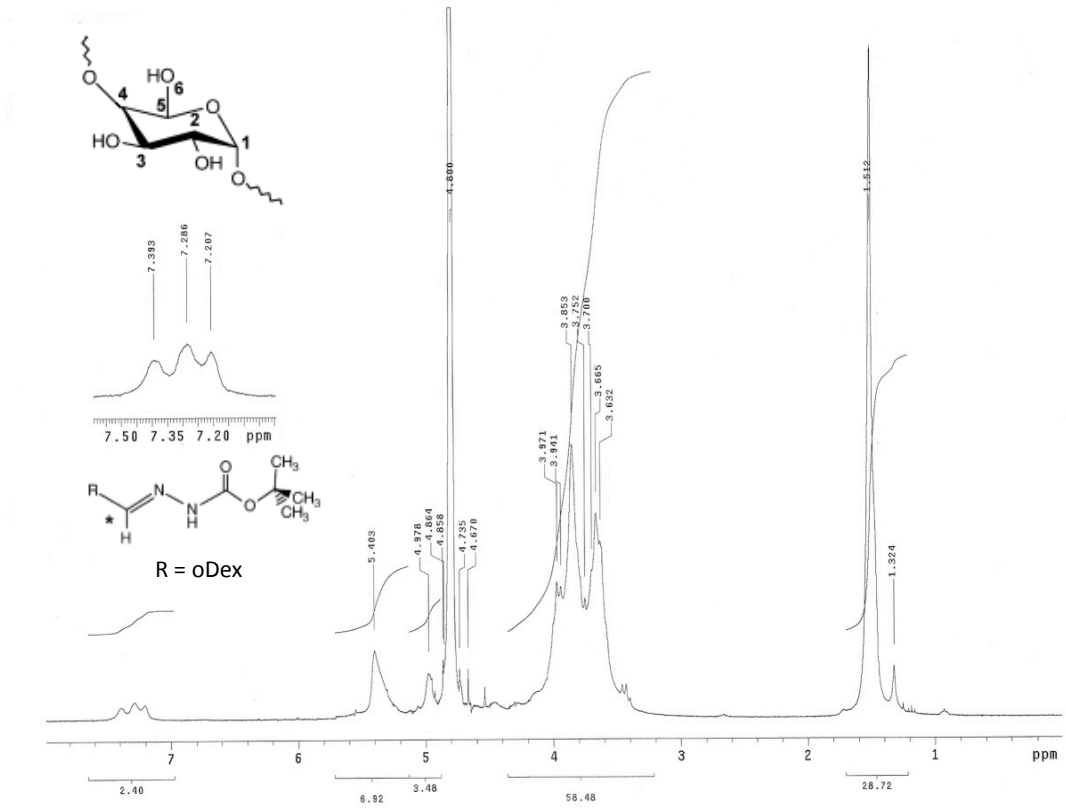

Figure 5.1 – Oxidized dextrin (DO 25%) ^{1}H NMR spectrum.

The hydrazide groups in ADH react with the aldehyde groups in oDex and form a network of hydrolysable hydrazone bonds (Scheme 5.2). Once these covalent bonds are cleaved, hydrazides and dextrin can easily diffuse across human tissues and be eliminated via renal clearance, owing to their low molecular weight, fairly below the renal threshold (~40,000 Da). Thus, besides the naturally occurring glycosidic bonds in dextrin, the hydrozone bonds provide an additional level of control over the mechanical properties of these hydrogels.

Scheme 5.2 – Polymerization reaction of oDex with ADH and degradation products obtained by hydrolysis.

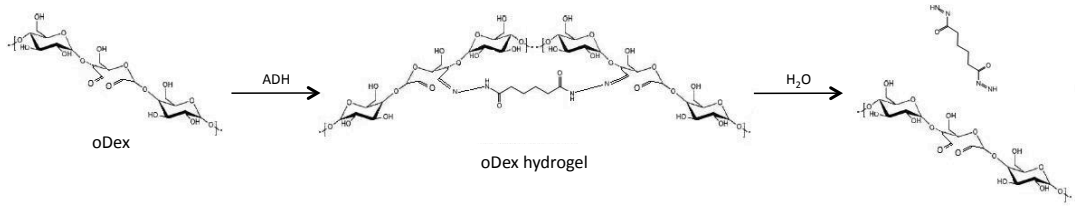

To evaluate the gelification profile of oDex hydrogels, the solubility pattern of oDex was accessed. Several oDex polymer solutions were prepared in phosphate buffer pH 6.0. It was noticed that above 30% (w/v) solutions were extremely viscous and practically impossible to homogenise. So, this concentration was considered as the threshold of oDex solubility in phosphate buffer pH 6.0, and was further on applied in the synthesis of all oDex hydrogels. Next, oDex was crosslinked with various concentrations of adipic dihydrazide. Twelve hydrogel samples were initially produced with DOs varying from 25% to 50% and ADH concentrations between 5% and 30% (in molar ratio, taking into account the number of glucose residues in the original dextrin).

Table 5.1 shows the approximate gelation periods obtained. As expected the crosslinking times decrease with increasing DOs, as well as with increasing amounts of reticulating agent. It was found that DOs above 40% yield very viscous solutions that react promptly with ADH, impairing good homogenization, and resulting in mat and brittle hydrogels. Through control

of DO and ADH concentrations, a good control over the gelification time is thus possible, making this hydrogel suitable as an injectable system.

Table 5.1 – Variation of crosslinking times with the degree of oxidation and adipic acid dihydrazide concentration. (+) over 1h gelation (++) gelation in less than 30 min (+++) gelation in less than 1min. The material was considered gelified when it stopped slipping along an 90° inclined surface. * Calculated as the molar ration of sodium periodate per initial glucose unit in dextrin. ** Calculated in molar base, taking into account the number of glucose residues in the original dextrin.

DO_T(%)*	ADH (%) **		
	5	15	30
25	+	+	+
32.5	++ (~30 min)	++ (~10min)	++ (~5 min)
40	++ (~2min)	+++	+++
50	+++	+++	+++

Mechanical properties

According to Anseth *et al* [37], the compressive modulus of hydrogels is directly proportional to the intermolecular crosslink density. Hence, the influence of the ADH concentration, DO and also the type of solvent used on the extent of intermolecular crosslinking was evaluated by quantifying the compressive modulus of oDex hydrogels. This approach was previously described by Bouhadir and co-workers [19]. Figure 5.2 presents a typical compression curve obtained for oDex hydrogels, from which the compressive modulus was determined, using equation 5.6:

Compressive modulus (KPa) = (Stress max / Superficial area) x 10^{-3} (Eq. 5.6)

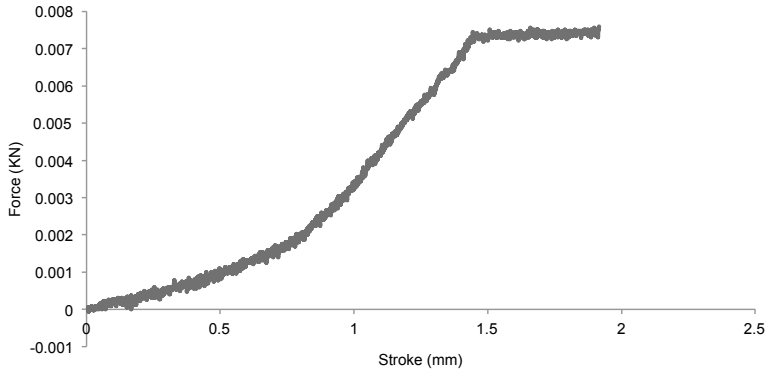

Figure 5.2 – Compression curve showing typical behavior for an oDex DO 35% with 4% ADH hydrogel.

The increasing concentration of ADH resulted in an increase in the compressive modulus of crosslinked oDex hydrogels (Figure 5.3A), suggesting the establishment of an increasing number of intermolecular bonds as more hydrazide groups become available to react. The same tendency was reported by Maia *et al* [38] with dextran hydrogels and by Bouhadir *et al* [19] with poly(aldehyde guluronate) hydrogels, the former revealing inferior compressive strength even with higher concentrations of reticulating agent. In fact, the maximum compressive modulus obtained with guluronate hydrogels was 560 KPa, with 150 mM ADH, while with ca. 130 mM (equivalent to 10% in molar ratio) a compressive modulus of 600 KPa for oDex 35% hydrogels was registered. Thus, dextrin hydrogels appear to have better mechanical properties.

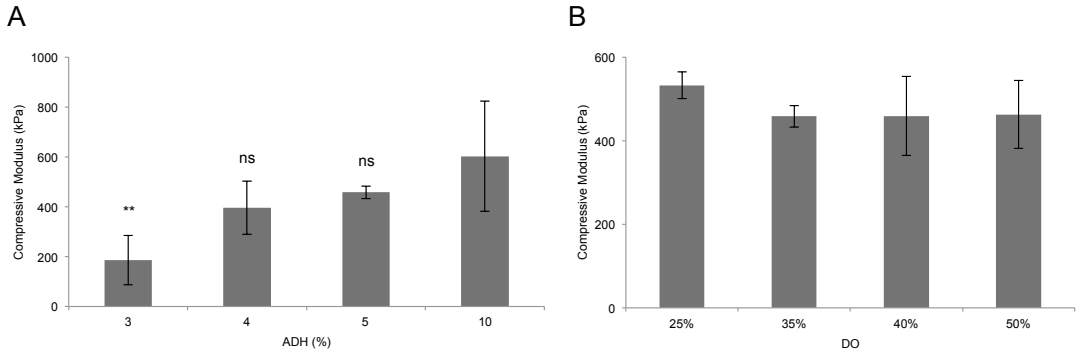

Figure 5.3 – Compressive modulus of (A) crosslinked oDex hydrogels as a function of the ADH concentration (in molar ratio, taking into account the number of glucose residues in the original dextrin, oDex DO 35% (30% w/v) in 0.1 M phosphate buffer, pH 6.0), and (B) crosslinked oDex hydrogels as a function of the degree of oxidation of dextrin (oDex DO 35% and 5% ADH in 0.1 M phosphate buffer, pH 6.0). Results presented as average ± SD, n=3. ns: non-significant, $p > 0.05$; ** $p < 0.01$, compared to the highest concentration of ADH used.

The influence of the degree of oxidation on the intermolecular crosslinks was evaluated, and no direct proportionality relationship between the compressive modulus and the DO was identified. Interestingly, oDex DO 25% hydrogels revealed the maximum compressive force (c.a. 533 KPa), although there was no significant difference ($p>0.05$) relatively to higher DO oDex hydrogels (Figure 5.3B). With 25% oxidation there is an average two to three

oxidized glucose residues per dextrin molecule (taking into account the average polymerization degree of dextrin which is ca. 10-12). Hence each molecule must participate in two distinct bonds with different molecules to be efficiently reticulated. These results suggest that the formation of more than two bonds does not necessarily imply an enhancement on hydrogel's mechanical properties. The excessive modification of the original polymeric chain, with the availability of a great number of reactive oxidized groups can be detrimental to the molecular organization of the new polymeric structure, by means of steric rearrangement impediment.

Injectable hydrogels should be able to prosecute its polymerization process *in situ*, meaning the interstitial fluids and/or blood should not interfere with it, for instance by influence of the media pH. Also, the intrinsic conditions necessary for the hydrogel's formation must not be harmful to the surrounding tissues. Hence, the pH influence on the density of intermolecular bonds was evaluated by measuring the compressive modulus of various oDex hydrogels prepared in four different solvents: dd water (c.a pH 5.77), 0.1M phosphate buffer (pH 6.0), PBS (pH 7.4) and cDMEM (c.a pH 7.5), respectively. Results are shown in Figure 5.4 and are in agreement to the tendency verified previously by Bouhadir *et al* [19]. In fact, it is well known that the reactivity of hydrazide groups with aldehydes is optimal at lower pH values. Under acidic conditions, aldehydes are protonated and are more susceptible to nucleophilic attack by the hydrazide groups. At neutral to basic conditions, however, slower kinetics are in effect and a longer time interval is required for the completion of the reaction, yielding a lower degree of functional crosslinking. A possible explanation for the low compressive modulus values (58 KPa) of hydrogels prepared in cDMEM, could be supported by the presence of aminoacids in solution, which might be interacting with aldehyde groups in oDex, following hydrolysis of hidrazone bonds.

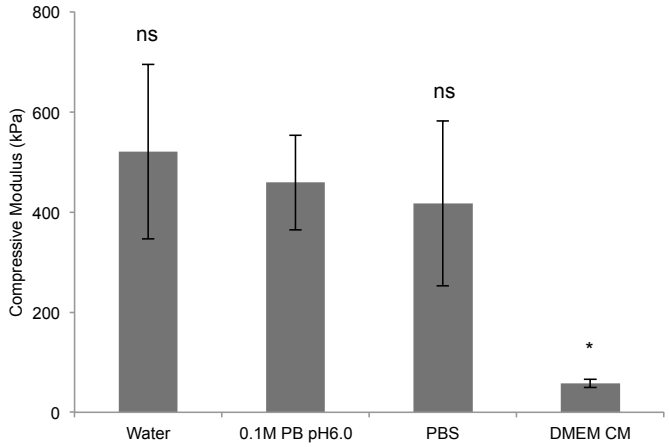

Figure 5.4 – Compressive modulus of crosslinked oDex hydrogels as a function of the solvent in which they are prepared. All hydrogels were prepared with oDex (30% w/v) and 5% ADH. Results presented as average ± SD, n=3. ns: non-significant, $p > 0.05$; * $p < 0.05$, compared to the solvent in which hydrogels are normally synthesized (0.1M phosphate buffer, pH 6.0).

Biocompatibility

As to characterize the biocompatibility of the oDex hydrogel, the cytotoxicity was evaluated for un-crosslinked macromonomer solutions and crosslinked hydrogels as well as its degradation products. Mouse embryo fibroblasts 3T3 cells were used. Cytotoxicity, defined as the "*in vitro* evaluation of toxicological risks using cell culture", is a way to assess the *in vitro* biocompatibility of materials to be used in biomedical applications. Assays deal with the assessment of various aspects of cellular function such as cell viability and proliferation, loss of membrane integrity, reduced cell adhesion, biosynthetic activity and altered cell morphology [39]. Moreover, the information gained from these types of investigations may be used in the design of further *in vivo* experiments.

Figure 5.5A and 5.5B depict the MTT absorbance values obtained after 48 hours incubation with different concentrations of ADH and oDex, respectively.

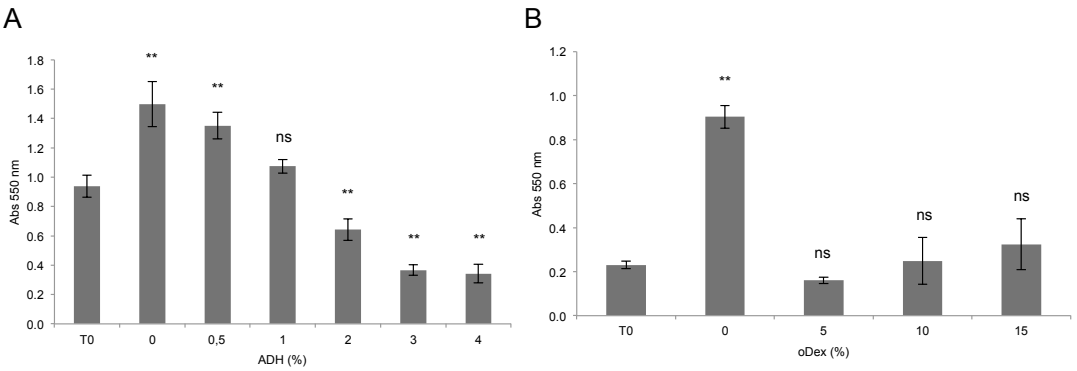

Figure 5.5 – MTT absorbance values obtained after 48h incubation of 3T3 cells in direct contact with (A) different concentrations of reticulating agent (ADH) alone, and (B) different concentrations of oxidized dextrin alone. Results presented as average ± SD, n=3. ** $p < 0.01$, compared to the T0 control (24h after cell seeding).

After 48 hours incubation, higher concentrations of ADH (2-4 % w/v) induce cell death. However, when the amount of ADH used to form the oDex hydrogels (5% molar base corresponding to 1% w/v) is incubated with 3T3 fibroblasts no significant difference is noted in MTT absorbance values. Additionally, oDex does not induce cell death, although proliferation is not observed in the presence of the material. Altogether, the results points to a high level of compatibility of the amount of ADH and oDex used for the oDex hydrogel production.

The products of the hydrogels degradation can be potentially cytotoxic; in order to evaluate its toxicity, the extracts obtained during degradation oDex hydrogel were incubated with mouse embryo fibroblasts 3T3 cells and MTT assay was used to measure 3T3 fibroblasts cellular viability. The results are shown in Figure 5.6.

Cellular death is observed when the oDex degradation products are in direct contact with cells, although this effect attenuates as the degradation products are diluted. In the wells where the degradation products are used (dilution 1:1), sedimentation of these degradation products was observed. This fact suggests that cellular death could be caused by the mechanical pressure or by the diminished oxygenation and nutrient diffusion caused by the products sedimentation. In fact, Massia and Stark [40] and Ferreira *et al* [41] described the same effect.

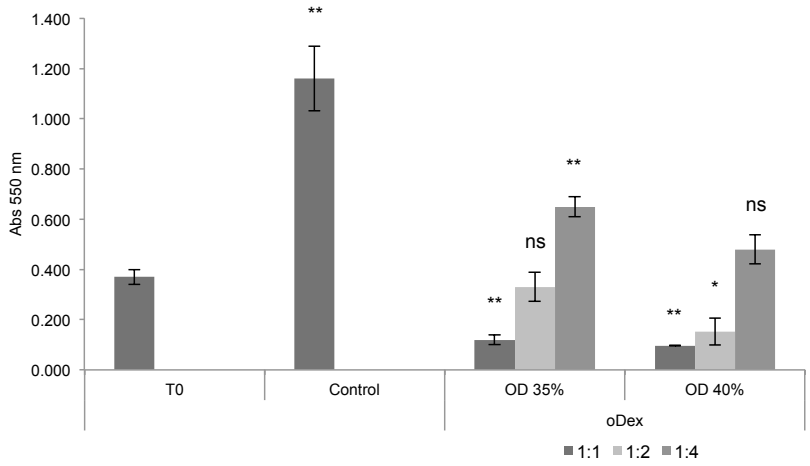

Figure 5.6 – MTT absorbance values obtained after 48h incubation of 3T3 cells with degradation products (1:1, 1:2 and 1:4 dilutions) of oDex hydrogels. T0 – initial cell abs; Control – abs after 48h incubated. Results presented as average ± SD, n=3. Ns: non-significant, $p>0.05$; *$p<0.05$; ** $p < 0.01$, compared to the T0 control.

Dextrin-HEMA hydrogels where previously developed by Carvalho and co-workers [12]. *In vivo* assays, performed by Moreira *et al* [42], showed that after implantation dextrin-HEMA hydrogels where quickly and completely degraded and reabsorbed even dough *in vitro* studies revealed citotoxicity associated with dextrin-HEMA degradation products. Thus, the rapid reabsorption and excretion is likely to minimize the biological impact observed in this assay.

To evaluate oDex cytotoxicity, the Live and Dead® assay was also performed. oDex (DO 35%) hydrogels were placed in direct contact with cells and latex discs and agar gels were used as positive and negative controls, respectively. In Figure 5.7 fluorescence images of mouse embryo fibroblasts 3T3 cells after 48 hours incubation are shown.

As expected, latex discs revealed high toxicity, for cells are majorly red (dead cells). On the contrary, with agar discs and oDex hydrogels the majority of cells are alive (green cells).

As Figure 5.8 illustrates, oDex hydrogels does not inhibit cell proliferation. Although the number of cells is inferior comparing to control wells, cells are adherent and retain the typical fibroblast morphology.

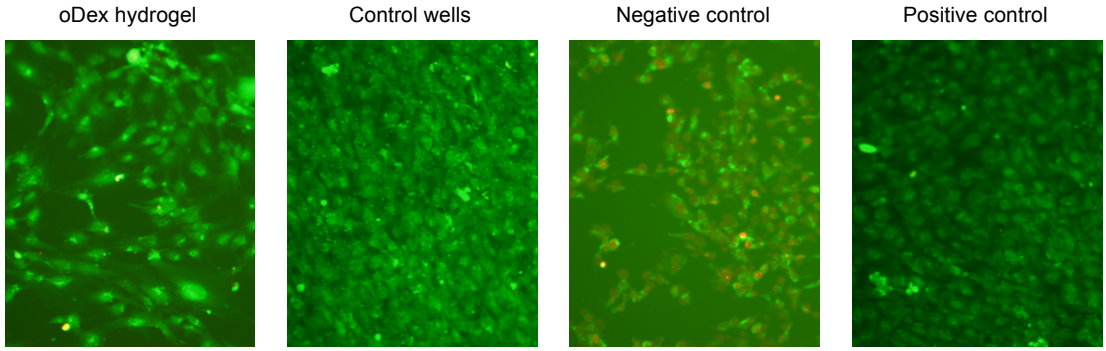

Figure 5.7 – Fluorescence photographs of mouse embryo fibroblasts 3T3 cells stained with Live and Dead® after 48 hours incubation. Live cells are stained in green and dead cells stained in red.

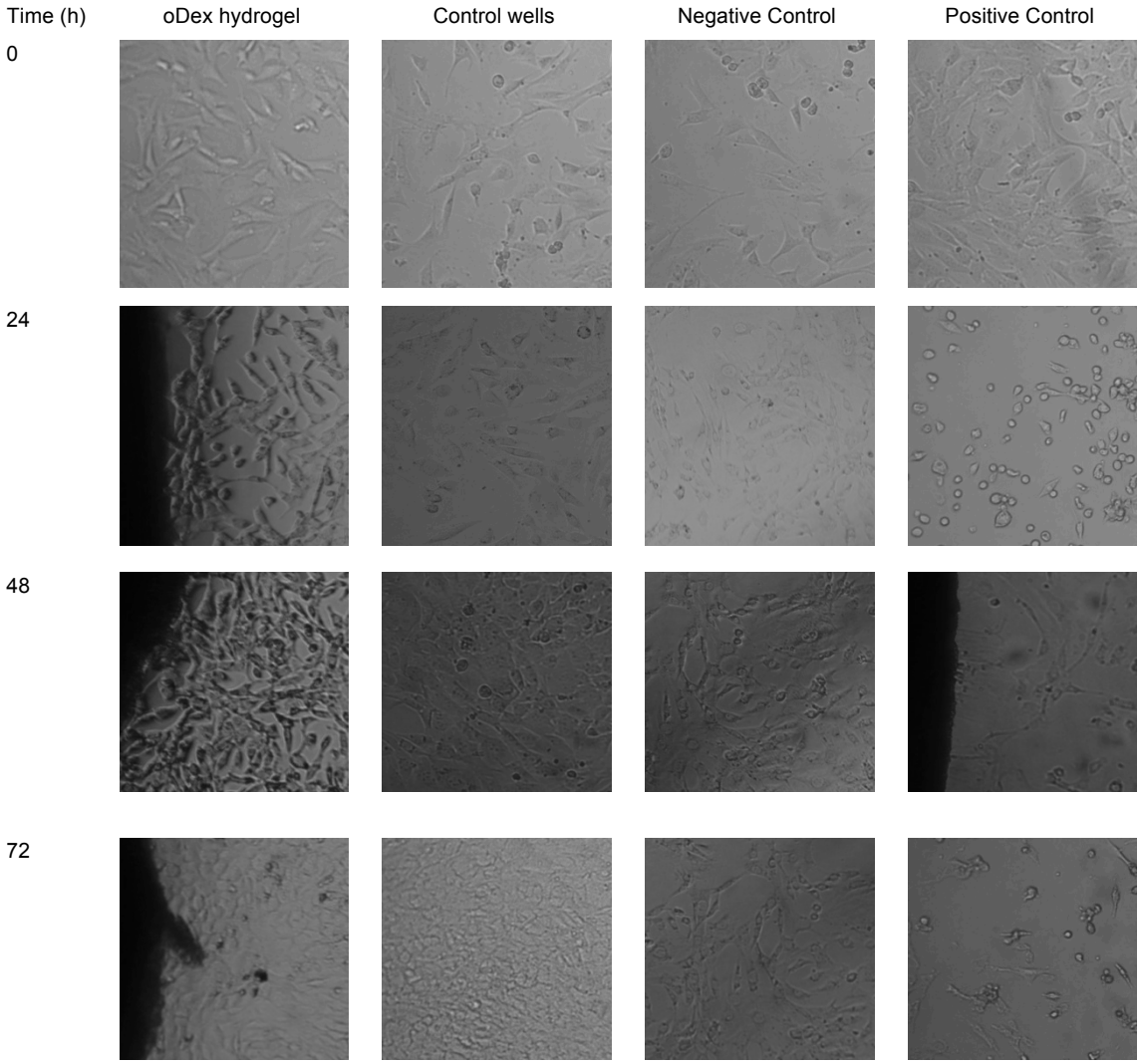

Figure 5.8 – Morphologic evaluation of 3T3 cells in direct contact with dextrin hydrogels (DO 35%), TCPS cell culture plates (control), agarose gel (negative control) and latex rubber (positive control). 10x magnification. Dark shadows on the left side show part of hydrogel or latex disc.

To evaluate the effects of the oDex hydrogels on the adhesion of mouse embryo fibroblasts 3T3, oDex (DO 35% and 40%) hydrogels were formed on the bottom of polystyrene wells and then cells were seeded. Polystyrene wells were used as control. The cellular adhesion was evaluated with MTT test as described by Carvalho et al [12].

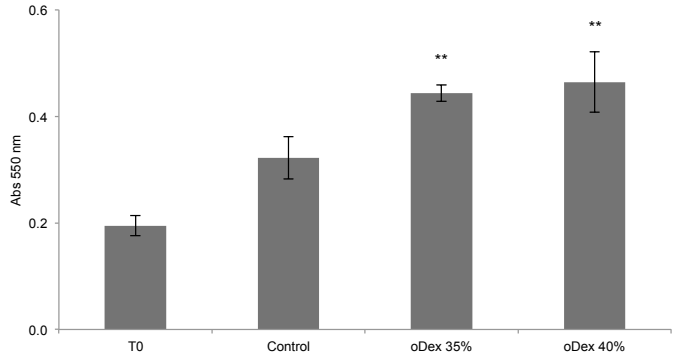

Figure 5.9 – MTT absorbance values obtained after 48h incubation of 3T3 cells on oDex (DO 35% and 40%) hydrogels. Results presented as average ± SD, n=3. ** $p < 0.01$, compared to the T0 control.

As seen in Figure 5.9, after 48 hours incubation the number of adhered cells is significantly higher in both oDex hydrogels comparing to the control (polystyrene wells). This is a somewhat unexpected and rather interesting result, since in other dextrin hydrogels developed in our lab, an improved proliferation as compared to polystyrene was not observed.

Recently, Maia et al [43] described oxidized dextran crosslinked with ADH hydrogels. These hydrogels were also shown to promote cell adhesion and proliferation. Such as dextrin, dextran is a neutrally charged molecule and is expected that this neutrality is maintained after the periodate oxidation reaction. Nevertheless, the crosslinking reaction with ADH yields hydrazone bonds that were reported to have a pK_a of 3-4. So, they hypothesized that due to the nature of the crosslinking bond, the dextran hydrogel zeta potential shifted negatively, allowing cell growth and proliferation.

It is well recognized that the surface chemistry of hydrogels can influence cell adhesion and proliferation. It has already been shown [44] that cell proliferation is sensitive to both hydrogel charge density and crosslinker concentration and

that cells adhere and proliferate easier in hydrogels with zeta potential below -20 mV. Other authors [45] also reported that the charge density of the hydrogel could regulate cell attachment.

Altogether the results predominantly indicate a high level of cytocompatibility for oDex hydrogels. Recently, Carvalho et al [12] also described two dextrin-based hydrogels that also presented negligible cell toxicity, allowing cell adhesion and proliferation.

Production and properties of the hydrogel/nanogel (oDex-nanogel)

The morphologies of the oDex hydrogels were examined by Cryo-SEM. As expected, the covalent cross-linking produced three-dimensional networks. As seen in Figure 5.10, the oDex hydrogels exhibits a continuous porous structure, with a diameter of about 1 μm. With a larger amplification, the nanogel particles present in oDex-nanogel hydrogel can be observed.

No obvious morphologic differences are noticeable comparing the oDex and oDex-nanogel hydrogel formulations. All hydrogels have random morphology and similar porous structure and the incorporated nanogels did not have significant influence in the morphology of the oDex hydrogel network.

In spite of their many favorable properties, hydrogels also have some limitations. The low tensile strength limits their use in load-bearing applications and, as a consequence, the premature dissolution or flow away of the hydrogel from the targeted local site can occur. Concerning drug delivery, the most important drawback of hydrogels relates to the quantity and homogeneity of drug loading, which may be limited, especially in the case of hydrophobic drugs; on the other hand, the high water content and large pores frequently result in relatively rapid drug release. In order to surmount these limitations, a nanogel previously developed and characterized in our lab was used to produce a new bidimensional hydrogel. Since this nanogel is obtained by self-assembling of amphiphilic molecules,

and have been shown to incorporate and stabilize both proteins and small hydrophobic pharmaceuticals, the presence of the nanophase may be useful for the formulation of hydrogels as a controlled drug release system.

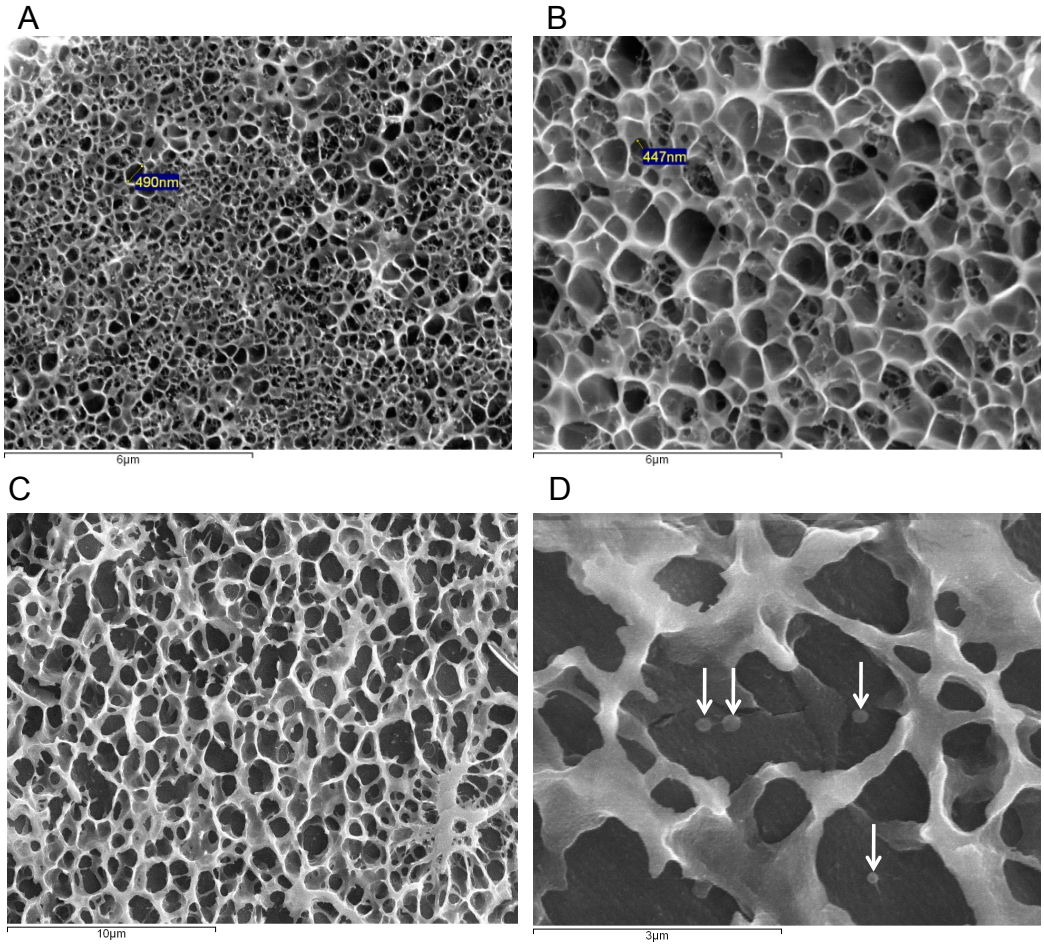

Figure 5.10 – Cryo-SEM images from cross-section of oDex hydrogel (A) before and (B) after immersion on PBS buffer for 24 hours and (C, D) oDex-nanogel hydrogel. Arrows show the dextrin nanogels (oDex DO 35%).

Figure 5.11 depicts the mass loss profile and nanogel release profile of oDex and oDex-nanogel hydrogels with different concentrations of nanogel (1 and 3 mg/ml) as a function of time, when incubated in PBS at 37ºC.

The oDex cross-link junctions are degraded along time, leading to a correspondingly gradual swelling. When the cross-links are hydrolyzed, the network swells, imbibing more water and leading to further hydrolysis. For the two kind of hydrogels (oDex and oDex-nanogel), there is a rapid initial increase in the mass loss, likely due to the hydrolysis of the hydrogel regions

with lower cross-linking density, followed by a slight decrease in the mass, probably owed to the degradation of high cross-linked regions, and then a final dissolution phase. Dextrin molecules may be reticulated through 1, 2 or 3 bonds; hence, their release rate is likely to be variable.

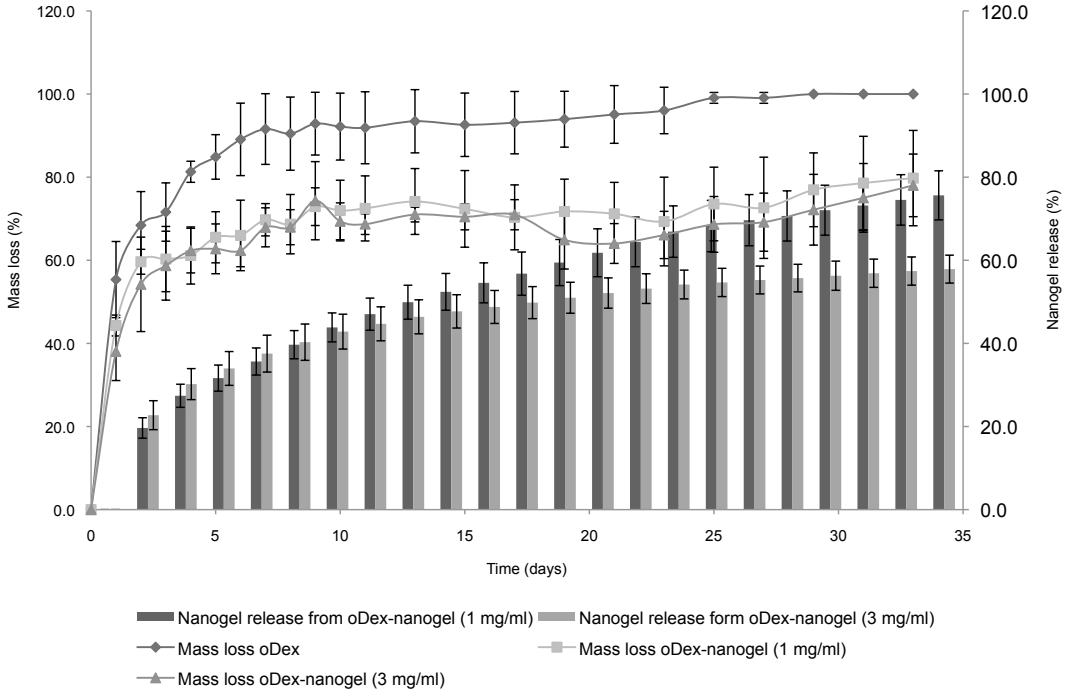

Figure 5.11 – Mass loss and nanogel cumulative release profiles of oDex, oDex-nanogel (1 mg/ml) and oDex-nanogel (3 mg/ml). Shown are mean ± SD, n=6.

It was also verified that in DMEM culture medium, the hydrogel degradation occurs faster than in PBS (as observed above for the oDex hydrogel; data not shown) possibly due to the presence of proteins from the culture medium that may favor the hydrolysis of the hydrazone bonds in the hydrogel network. The degradation rate of oDex hydrogels with DO 35% is slower than with oDex DO 40% (data not shown), due to the weaker mechanical properties.

According to mass loss studies, the degradation speed of oDex hydrogel is different from the one found in oDex-nanogel hydrogels. In approximately 25 days, the oDex hydrogel network is completely solubilized, while only about 70% mass loss was observed in oDex-nanogel hydrogels. On the other hand,

only a slight difference in mass loss is observed comparing the two formulations with different amounts of nanogel.

The slower degradation rate observed in the presence of the nanogel may be assigned to a further reticulation of the hydrogel network. Zhang *et al.* [46] described a composite system made of poly(N-isopropylacrylamide) (NIPAAm) hydrogel and hydroxyl-functionalized glycerol poly(ε-caprolactone) (PGCL)-based microspheres, where the incorporation of the hydrophobic PGCL-based microspheres into the hydrogel led to a greatly increased mechanical properties of the resulting networks. These improved mechanical properties were attributed to the existence of hydrophobic solid microspheres, which acted like reinforcing nodes. Nuño-Donlucas *et al.* [47] also reported similar findings of polyacrylamide hydrogels with increased mechanical properties by incorporating poly(methyl methacrylate) nanoparticles. Puig *et al.* [48] also presented a composite hydrogel of polyacrylamide nanoparticles in a polyacrylamide matrix with improved mechanical properties.

Depending on the chemical structure of the polymer backbone, hydrogel degradation can occur by either surface or bulk erosion. Surface erosion takes place when the rate of erosion exceeds the rate of water permeation into the bulk of the polymer. Bulk erosion occurs when water molecules permeate into the bulk of the matrix at a faster rate than erosion, thus exhibiting a complex degradation/erosion kinetics. Most of the biodegradable polymers used in drug delivery undergo bulk erosion, similar behavior being observed in hydrogels made form biodegradable polymers [49]. In oDex hydrogels, degradation mainly occurs by bulk erosion and it is characterized by non-linear degradation profile accompanied by an increasing pore size, as seen in Figures 5.10A and 5.10B. The variation in pore size during the degradation of the hydrogel network is important since it affects the swelling of the hydrogel, the diffusion of molecules, and the delivery of cells when the hydrogels are used for cell encapsulation [3, 50].

Release assays

The nanogel (labeled with FITC) release from the oDex-nanogel hydrogels was evaluated by fluorimetry (Figure 5.11). The nanogel was gradually released over time, paralleling the hydrogel degradation; the total fraction of nanogel released reached 75% and 54% for oDex-nanogel 1 mg/ml and oDex-nanogel 3 mg/ml, respectively, after 35 days. As the mass loss of the two oDex-nanogel hydrogels is similar, the amount of nanogel release from the oDex-nanogel 3 mg/ml is lower compared to the initial nanogel incorporated in the oDex hydrogel. Although a significant mass loss of the hydrogel is observed in the first few days, a steady and continuous release of nanogel is observed in an expanded time frame, up to 4 weeks. Preliminary assays on the study of the oDex-nanogelas a controlled release system for hydrophobic molecules and proteins were carried out.

Curcumin (CM) is a yellow pigment found in the rhizome of turmeric (*Curcuma longa L., Zingiberaceae*) and related species, and has a wide range of pharmacological and biological activity [20-23], including anti-cancer [20] and anti-inflammatory [21] activities. Despite its benefic properties, CM clinical application has been limited owing to its poor aqueous solubility and consequent minimal bioavailability. Drug delivery systems based on nanohydrogels (or nanogels) have already been used for augmenting hydrophobic agents, like CM [51], dispersibility in aqueous media, therefore circumventing the difficulties rendered by poor aqueous solubility.

CM was successfully encapsulated in the dextrin nanogels, allowing for CM solubilization in PBS. Then, the complex nanogel/CM was incorporated in oDex hydrogels (oDex-nanogel/CM hydrogel) forming bright yellow hydrogels (Figure 5.12, time 0 days).

Over time, the oDex-nanogel/CM hydrogels turns from bright to pale yellow translating a nanogel/CM release to the supernatant. Unfortunately, it is also noticeable that the oDex hydrogel became yellow over time, not allowing a proper quantification of the nanogel/CM release by spectrofotometry. Nevertheless, the efficient incorporation of nanogel/CM in the hydrogel, associated to the controlled release of the nanogel (Figure 5.11), suggests that

the oDex-nanogel may constitute a good platform for the controlled release of hydrophobic molecules.

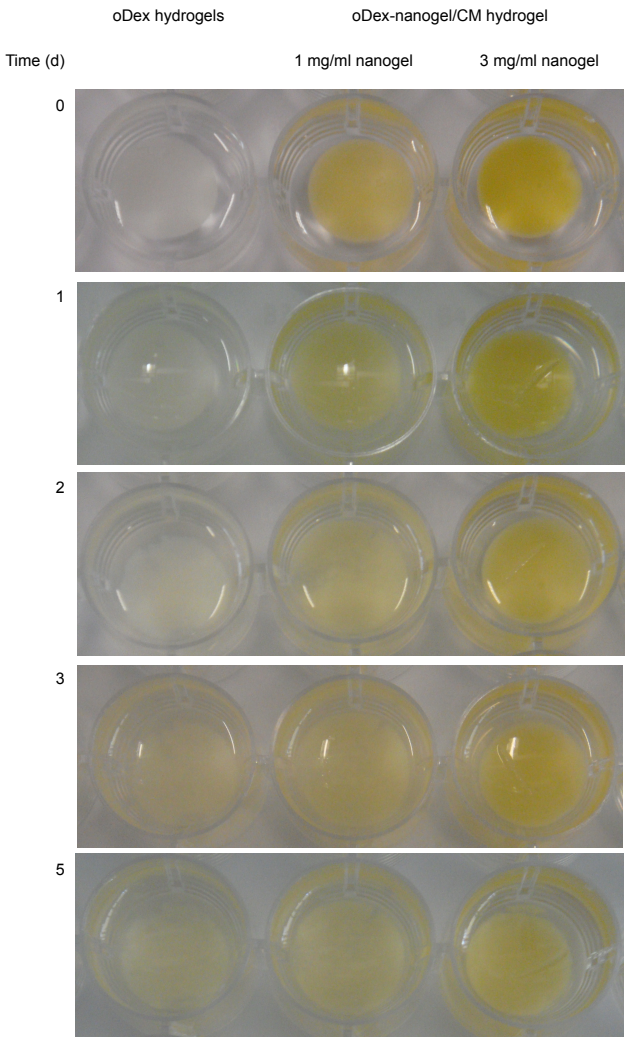

Figure 5.12 – Photographic evaluation of CM encapsulation on the oDex-nanogel/CM hydrogels. oDex hydrogel was used as controls.

The oDex hydrogels were also tested as protein delivery systems. Interleukin-10 (IL-10) is a cytokine with a strong anti-inflammatory activity acting as a general suppressor factor of immune responses [24-29]. Figure 5.13 shows the percentage of rIL-10 released from oDex and oDex-nanogel hydrogels in PBS with 10% FBS.

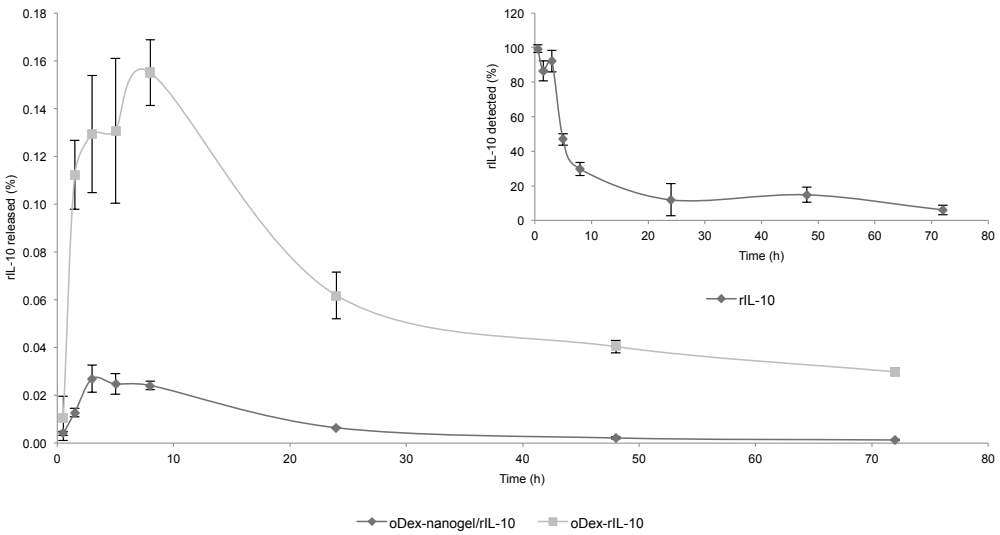

Figure 5.13 – rIL-10 release from oDex-rIL-10 and oDex-nanogel/rIL-10 hydrogels. Inset shows the percentage of the initial soluble rIL-10 remaining detectable using the ELISA in the same conditions as in the release assays. Shown are mean ± SD values (n=3).

The general goal of this experiment was compromised by the low stability of rIL-10. rIL-10 is a rather unstable protein as can be seen on the inset of Figure 5.13, where it is observed that the amount of solubilised (non-encapsulated) rIL-10 detectable with the ELISA decreases significantly and quickly, probably due to denaturation and aggregation. The stability of rIL-10 was accessed at 37ºC, by recording the CD spectra over time. rIL-10, at time 0, presented a typical CD spectrum of a helical protein, as expected [52-54]. The analysis of the mean residual ellipticity (θ) variation, at 222 nm, allowed the prediction of the rIL-10 half-life and this sample showed a half-life of 4.4 ± 0.7 days corroborating the high instability demonstrated by the protein in this release assay.

Although the cytokine have improved stability when encapsulated in the nanogel (as it has been demonstrated previously [18]), its release from the hydrogels (oDex and oDex-nanogel) is observed in both cases only in the first 6-10 hours of the experiment. Actually, the amount detected in the supernatant decreased henceforward, due to faster aggregation as compared to fresh cytokine being released from the hydrogel.

Therefore, more stable proteins were selected to evaluate the performance of the hydrogel-nanogel as a controlled protein release system.

β-Galactosidase (β-Gal) is a hydrolase of about 120 kDa that catalyzes the hydrolysis of β-galactosides. The release of the enzyme from the oDex and oDex-nanogel hydrogels was followed by monitoring the enzymatic activity of the β-Gal that released to the supernatant. The β-Gal substrate, o-nitrophenyl-β-D-galactopyranoside, is small enough to penetrate in the dextrin nanogel so that the activity of the enzyme can be determined even when it is encapsulated by the nanogel. Figure 5.14 depicts the activity of the β-Gal released from the hydrogels relatively to the β-Gal activity of the total β-Gal incorporated in the hydrogel in the beginning of the experiment.

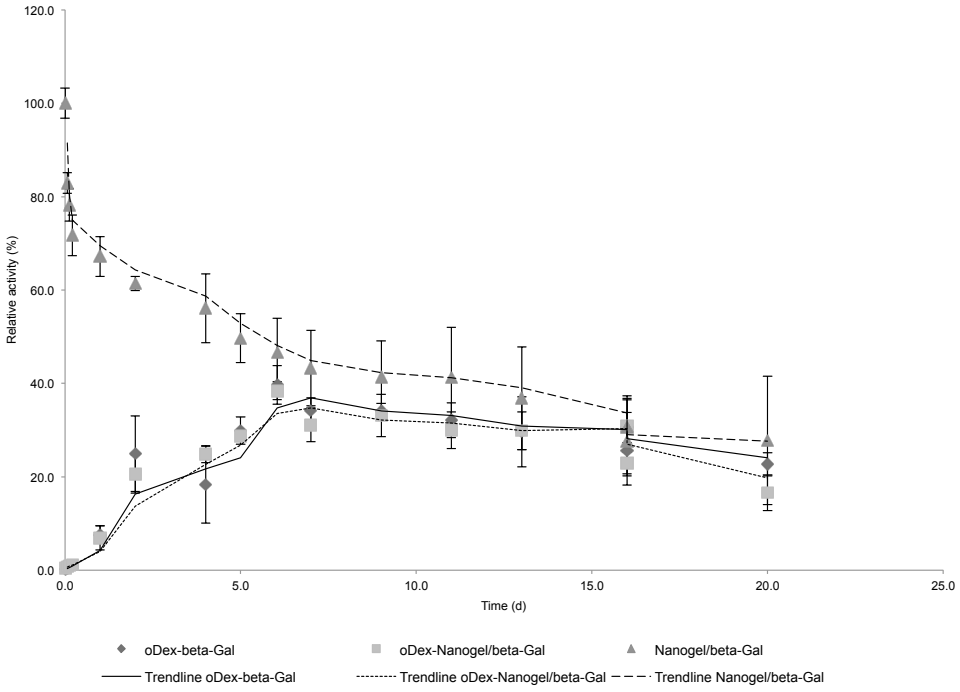

Figure 5.14 – Relative activity of the β-Gal released from the oDex hydrogels as a function of time. Shown are mean ± SD values (n=3).

The enzyme activity in solution (Nanogel/beta-Gal) decreased over time reaching about 40% of the initial activity in 6 days probably due to protein denaturation. The enzyme release from the oDex hydrogels did not exhibit a burst release profile, and it took at least 6 days until it reached 40% of the initial enzyme activity and remained fairly constant. Unexpectedly, the enzyme release profile was similar whether it was directly incorporated in the oDex or encapsulated in the dextrin nanogel incorporated in the oDex-

nanogel. As already stated, hydrogels usually present an initial protein burst release effect that is minimized by the incorporation of nanogels. With β-Gal this was not the case. β-Gal is a large protein and we suppose that it is mimicking the nanogel role in the composite system: the incorporation of a large protein in the oDex hydrogel acts like reinforced nodes. This hypothesis is also sustained by the slower degradation profile of the oDex-β-Gal hydrogels observed (similar to the degradation profile of the oDex-nanogel/β-Gal). On the other hand, being a galactosidase it is possible that β-Gal has some affinity to dextrin therefore slowing down its release from the oDex hydrogel.

Lynch and Dawson [9, 10] had already described a composite material, composed of poly(N-isopropylacrylamide) (NIPAM) based microgel particles entrapped in a hydrogel matrix. They called this composite material the "plum-pudding gel". The release of two compositionally different solutes from this composite hydrogel composed of two different populations of microgel particles embedded in a single bulk matrix was described [10], showing the potential of the "plum-pudding gel" as a multifunctional platform for controlled release. Later on, the same group studied the controlled release of fluvastatin from the "plum-pudding gel" [7].

These composite materials present themselves as an alternative approach to "simply" incorporate drugs into polymer nano or microgels. This strategy has some advantages comparatively to those of drug-loaded polymeric particles: by separating the functional role (of the polymeric particles) from the support matrix (polymeric hydrogel), it can simultaneously release several different drugs; additionally, elution of the polymeric particles does not degrade the polymer hydrogel, which leads to a more stable long-term elution profile. So, this composite oDex-nanogel hydrogel could be useful to overcome the initial burst release phenomenon often observed in nanogel and hydrogel drug delivery systems as it allows for the nanogel slow and controlled release. Overall, the effective incorporation of hydrophobic bioactive molecules and of proteins, associated to the stabilization of the later, allowing its controlled release, suggest that oDex-nanogel offer interesting properties for

applications as an injectable controlled delivery system. A more comprehensive study will be carried out in forthcoming work.

Conclusions

The oDex hydrogels presented acceptable mechanical properties and revealed an overall good biocompatibility. The oDex and oDex-nanogel hydrogels were biodegradable and allowed for the nanogel release over time. The presence of a dispersed hydrophobic phase in the hydrogel may represent an important advantage of the newly developed material. The dextrin nanogel permitted the efficient incorporation of CM, rIL-10 and β-Gal into the oDex hydrogel and their release from the composite hydrogel overtime.

The degradability and macroporous structure of DexOx hydrogels makes them attractive for the design of injectable protein delivery systems. The longer sustained release of the protein is advantageous in these kinds of applications as it may provide a continuous delivery of protein and prevent problems of cyclic variations in the protein concentration in blood with time and offer a maximum pharmacological efficiency at a minimum drug dose, reducing administration frequency and improving patient compliance to the therapy.

The straightforward preparation and the nanogel release properties, makes this system, composed of oDex hydrogels with incorporated dextrin nanogel, promising as a protein delivery system.

References

(1) Hoare, T. R.; Kohane, D. S., *Polymer* **2008,** 49, (8), 1993-2007.

(2) Bennett, S. L.; Melanson, D. A.; Torchiana, D. F.; Wiseman, D. M.; Sawhney, A. S., *J Cardiac Surg* **2003,** 18, (6), 494-499.

(3) Jen, A. C.; Wake, M. C.; Mikos, A. G., *Biotechnol Bioeng* **1996,** 50, (4), 357-364.

(4) Lee, K. Y.; Mooney, D. J., *Chem Rev* **2001,** 101, (7), 1869-1879.

(5) van der Linden, H. J.; Herber, S.; Olthuis, W.; Bergveld, P., *Analyst* **2003,** 128, (4), 325-331.

(6) Angelova, N.; Hunkeler, D., *Trends Biotechnol* **1999,** 17, (10), 409-21.

(7) McGillicuddy, F. C.; Lynch, I.; Rochev, Y. A.; Burke, M.; Dawson, K. A.; Gallagher, W. M.; Keenan, A. K., *J Biomed Mater Res A* **2006,** 79A, (4), 923-933.

(8) Salvati, A.; Soderman, O.; Lynch, I., *J Phys Chem B* **2007,** 111, (25), 7367-7376.

(9) Lynch, I.; Dawson, K. A., *J Phys Chem B* **2003,** 107, (36), 9629-9637.

(10) Lynch, I.; de Gregorio, P.; Dawson, K. A., *J Phys Chem B* **2005,** 109, (13), 6257-6261.

(11) Carvalho, J.; Goncalves, C.; Gil, A. M.; Gama, F. M., *Eur Polym J* **2007,** 43, (7), 3050-3059.

(12) Carvalho, J.; Moreira, S.; Maia, J.; Gama, F. M., *J Biomed Mater Res A* **2010,** 93, (1), 389-99.

(13) Hosie, K. B.; Kerr, D. J.; Gilbert, J. A.; Downes, M.; Lakin, G.; Pemberton, G.; Timms, K.; Young, A.; Stanley, A., *Eur J Surg Oncol* **2003,** 29, (3), 254-60.

(14) Frampton, J. E.; Plosker, G. L., *Drugs* **2003,** 63, (19), 2079-105.

(15) Hreczuk-Hirst, D.; Chicco, D.; German, L.; Duncan, R., *Int J Pharm* **2001,** 230, (1-2), 57-66.

(16) Gonçalves, C.; Gama, F. M., *European Polymer Journal* **2008,** 44.

(17) Goncalves, C.; Martins, J. A.; Gama, F. M., *Biomacromolecules* **2007,** 8, (2), 392-8.

(18) Carvalho, V.; Castanheira, P.; Faria, T. Q.; Goncalves, C.; Madureira, P.; Faro, C.; Domingues, L.; Brito, R. M. M.; Vilanova, M.; Gama, F. M., *Int J Pharm* **2010,** 400, 234-242.

(19) Bouhadir, K. H.; Hausman, D. S.; Mooney, D. J., *Polymer* **1999,** 40, (12), 3575-3584.

(20) Kunnumakkara, A. B.; Anand, P.; Aggarwal, B. B., *Cancer Lett* **2008,** 269, (2), 199-225.

(21) Aggarwal, B. B.; Harikumar, K. B., *Int J Biochem Cell Biol* **2009,** 41, (1), 40-59.

(22) Miquel, J.; Bernd, A.; Sempere, J. M.; Diaz-Alperi, J.; Ramirez, A., *Arch Gerontol Geriatr* **2002,** 34, (1), 37-46.

(23) Araujo, C. C.; Leon, L. L., *Mem Inst Oswaldo Cruz* **2001,** 96, (5), 723-8.

(24) de Waal Malefyt, R.; Abrams, J.; Bennett, B.; Figdor, C. G.; de Vries, J. E., *J Exp Med* **1991,** 174, (5), 1209-20.

(25) Fiorentino, D. F.; Zlotnik, A.; Mosmann, T. R.; Howard, M.; O'Garra, A., *J Immunol* **1991,** 147, (11), 3815-22.

(26) Gazzinelli, R. T.; Oswald, I. P.; James, S. L.; Sher, A., *J Immunol* **1992,** 148, (6), 1792-6.

(27) Bogdan, C.; Vodovotz, Y.; Nathan, C., *J Exp Med* **1991,** 174, (6), 1549-55.

(28) MacNeil, I. A.; Suda, T.; Moore, K. W.; Mosmann, T. R.; Zlotnik, A., *J Immunol* **1990,** 145, (12), 4167-73.

(29) Defrance, T.; Vanbervliet, B.; Briere, F.; Durand, I.; Rousset, F.; Banchereau, J., *J Exp Med* **1992,** 175, (3), 671-82.

(30) Jia, X. Q.; Burdick, J. A.; Kobler, J.; Clifton, R. J.; Rosowski, J. J.; Zeitels, S. M.; Langer, R., *Macromolecules* **2004,** 37, (9), 3239-3248.

(31) Goncalves, C.; Gama, F. M., *Eur Polym J* **2008,** 44, (11), 3529-3534.

(32) Goncalves, C.; Torrado, E.; Martins, T.; Pereira, P.; Pedrosa, J.; Gama, M., *Colloid Surface B* **2010,** 75, (2), 483-489.

(33) Goncalves, C.; Martins, J. A.; Gama, F. M., *Biomacromolecules* **2007,** 8, (2), 392-398.

(34) Kristiansen, K. A.; Potthast, A.; Christensen, B. E., *Carbohydr Res* **2010,** 345, (10), 1264-71.

(35) Aalmo, K. M.; Painter, T. J., *Carbohyd Res* **1981,** 89, (1), 73-82.

(36) Li, J.; Wan, Y. Z.; Li, L. F.; Liang, H.; Wang, J. H., *Mat Sci Eng C-Bio S* **2009,** 29, (5), 1635-1642.

(37) Anseth, K. S.; Bowman, C. N.; BrannonPeppas, L., *Biomaterials* **1996,** 17, (17), 1647-1657.

(38) Maia, J.; Ferreira, L.; Carvalho, R.; Ramos, M. A.; Gil, M. H., *Polymer* **2005,** 46, (23), 9604-9614.

(39) Chiellini, E. E.; Chiellini, F.; Solaro, R., *J Nanosci Nanotechnol* **2006,** 6, (9-10), 3040-7.

(40) Massia, S. P.; Stark, J., *J Biomed Mater Res* **2001,** 56, (3), 390-399.

(41) Ferreira, L.; Rafael, A.; Lamghari, M.; Barbosa, M. A.; Gil, M. H.; Cabrita, A. M. S.; Dordick, J. S., *J Biomed Mater Res A* **2004,** 68A, (3), 584-596.

(42) Moreira, S.; da Costa, R. M. G.; Guardao, L.; Gartner, F.; Vilanova, M.; Gama, M., *J Bioact Compat Pol* **2010,** 25, (2), 141-153.

(43) Maia, J.; Ribeiro, M. P.; Ventura, C.; Carvalho, R. A.; Correia, I. J.; Gil, M. H., *Acta Biomater* **2009,** 5, (6), 1948-1955.

(44) Chen, Y. M.; Shiraishi, N.; Satokawa, H.; Kakugo, A.; Narita, T.; Gong, J. P.; Osada, Y.; Yamamoto, K.; Ando, J., *Biomaterials* **2005,** 26, (22), 4588-96.

(45) Schneider, G. B.; English, A.; Abraham, M.; Zaharias, R.; Stanford, C.; Keller, J., *Biomaterials* **2004,** 25, (15), 3023-8.

(46) Zhang, X. Z.; Lewis, P. J.; Chu, C. C., *Biomaterials* **2005,** 26, (16), 3299-3309.

(47) Nuño-Donlucas, S. M.; Sanches-Diaz, J. C.; Rabelero, M.; Cortes-Ortega, J.; Luhrs-Olmos, C. C.; Fernandez-Escamilla, V. V.; Mendizabal, E.; Puig, J. E., *J Colloid Interf Sci* **2004,** 270, (1), 94-98.

(48) Puig, L. J.; Sanchez-Diaz, J. C.; Villacampa, M.; Mendizabal, E.; Puig, J. E.; Aguiar, A.; Katime, I., *J Colloid Interf Sci* **2001,** 235, (2), 278-282.

(49) Pillai, O.; Panchagnula, R., *Curr Opin Chem Biol* **2001,** 5, (4), 447-451.

(50) Peppas, N. A.; Bures, P.; Leobandung, W.; Ichikawa, H., *European Journal of Pharmaceutics and Biopharmaceutics* **2000,** 50, (1), 27-46.

(51) Bisht, S.; Feldmann, G.; Soni, S.; Ravi, R.; Karikar, C.; Maitra, A., *J Nanobiotechnology* **2007,** 5, 3.

(52) Josephson, K.; DiGiacomo, R.; Indelicato, S. R.; Ayo, A. H.; Nagabhushan, T. L.; Parker, M. H.; Walter, M. R., *Journal of Biological Chemistry* **2000,** 275, (18), 13552-13557.

(53) Zdanov, A.; Schalk-Hihi, C.; Gustchina, A.; Tsang, M.; Weatherbee, J.; Wlodawer, A., *Structure* **1995,** 3, (6), 591-601.

(54) Zdanov, A.; Schalk-Hihi, C.; Wlodawer, A., *Protein Sci* **1996,** 5, (10), 1955-62.

Chapter 6 | Conclusions and future perspectives

As an immunoregulatory cytokine, IL-10 has great potential in various medical fields, mainly in the treatment of acute and chronic inflammatory diseases. Nevertheless, due to the IL-10 low stability and reduced half-life *in vivo*, a delivery system is essential.

In order to functionalize chitin-based biomaterials two recombinant proteins, containing a human chitin-binding module, were successfully expressed soluble and active by *E. coli* (Chapter 2). The proteins were purified and their ability to improve fibroblast adhesion was tested. In the presence of the two proteins (ChBM and RGDChBM), surprisingly, cells did not attach to the surface of the biomaterial used (reacetylated chitosan films) or seem to stop growing. It was concluded that the human chitin-binding module (fused or not with the RGD peptide) interferes with the attachment of cells and thus it is not applicable as strategy to functionalize chitin-based biomaterials for IL-10 delivery.

Two IL-10 delivery systems were developed and/or tested (Chapter 3, 4 and 5):

First, a mutated form of murine IL-10 (rIL-10) was expressed in *E. coli* (Chapter 3). The recombinant protein was recovered and purified from inclusion bodies and it was demonstrated that its biological activity was similar to a commercially available one. This study demonstrated that dextrin self-assembled nanogel (developed previously) was biocompatible (Chapter 4) and efficiently incorporated rIL-10. It also protected rIL-10 from denaturation at 37ºC and enabled the rIL-10 release *in vitro* and *in vivo*. The biological activity of the rIL-10 released was confirmed *in vitro*, in endotoxin-activated bone marrow derived macrophage and, *in vivo*, in endotoxin challenged mice.

Despite the observed rIL-10 release, a significant amount of rIL-10 still remained trapped in the dextrin nanogels. This could be caused by the strong interaction of rIL-10 with the nanogel, most probably by the fast denaturation of rIL-10 (despite the stabilizing effect of the nanogel) verified in all *in vitro* assays. Thus, although the promising properties of the nanogel, which

effectively incorporates and stabilizes proteins, the quick denaturation of IL-10 does not allow a proper characterization of the release kinetics. The release time scale is still rather limited, apparently because IL-10 is a particularly challenging case study. Properties, like hydrophobicity, long-term stability and binding affinity, can influence the incorporation and release of proteins from nanogels; so, in light of these results, a different bioactive protein – not as unstable as IL-10 - should be tested to see if a different release profile could be achieved.

A composite system where dextrin nanogels were incorporated in oxidized dextrin hydrogels, was also studied (Chapter 5). These hydrogels presented acceptable mechanical properties and were biocompatible and biodegradable. It was also observed the controlled release of the incorporated dextrin nanogel. The inclusion of nanogel allowed the incorporation of rIL-10, curcumin and β-galactosidase in oxidized dextrin hydrogels further improving the nanogel and the hydrogel formulation, allowing their release over time. These encouraging results, make necessary additional tests with other bioactive molecules.

Dextrin is a very promising and relatively unexploited biomaterial, available in medical grade and accepted by the United States Food and Drug Administration for human application. Here dextrin was used for the preparation of both the nanogel and the hydrogel.

Taking into consideration 1) the interesting properties of dextrin; 2) the simplicity of the preparation of both nanogel and hydrogel; 3) the high incorporation efficiency associated with the nanogel; 4) the stabilization of rIL-10 encapsulated in the nanogel; and 5) the controlled release profile obtained with the hydrogel-nanogel composite; this system presents great potential as a protein controlled delivery system.